Title:

Techno - economical literature study of an offshore floating wind turbine CSC-semi.

THE AUTHOR:

LASSE JOHANNESSEN BACKHOFF TOLLEFSEN

SUPERVISOR

Zhiyu Jiang

University of Agder, [2023]

Faculty of [Technology and science]

Department of [Engineering]

Lasse J. Backhoff Tollefsen

Techno – economic analysis of the life cycle cost (LCC) of a floating offshore wind turbine, CSC-semi with a shared mooring system in the region of South North Sea II

A review of the technical economical study of the life cycle cost (LLC) for a OFWTs and prototype simulation with a chosen mooring system.

Master thesis spring

19. May 2023

UiA Handelshøyskolen

University of Agder, [2023]
Faculty of [Technology and science]]
Department of [Engineering]]

Abstract

The objective with this thesis was to investigate two subjects' the life cycle cost (LCC) and a dynamic response simulation of two prototype model I and II. Firstly, the economical part includes the main cost drivers, Capex (1), Opex (2), and Decom (3) for a Floating wind turbine (FWT). Furthermore, the dynamic response analysis of a prototype I based on catenary mooring configuration and prototype II with a shared arrangement and a mooring buoy as tension reliver. The prototype II concept are based of two horizontal platform oriented 180 degrees towards each other in the oriental plane and defined in a software program (Orcaflex). The response analysis includes several materials and dimension of mooring lines to be investigated. This for the maximum tension for several cycles of significant wave heights. The investigation has therefore been to evaluate the top tension (maximum) in each mooring lines based on two individual prototypes for comparing a single OFWT Vs. a shared mooring of two OFWTs. The simulation test has been tested for over 3800 seconds for each prototype I and II, of a total duration of 26600 seconds. The main purpose was to compare numerical mooring result based on the maximum tension in each mooing lines based for various sea state. In a sense, the shared mooring arrangement could possibly reduce the top tension in each line by including a mooring buoy in the mooring arrangement, in contrast to a single OFWT. The first prototype I was configurated with three mooring lines in a catenary plane with three chain lines. Prototype II was based on a mixture of taut mooring arrangement with material of polyester ropes and catenary chains defined in each end of the platform's (OFWTs) fairleads. In the process of modeling (designing) prototype II in the software (Orcaflex) the placement of design of parameters was also carried out. The cost cycle is the most important phase of a OFWTs project. This for evaluating the concept of a possible windfarm location for making a clear statement of the total cost estimates. The study will, therefore, investigate six cost drivers including: development and consenting (1), manufacturing (2), installation (3), transportation (4), exploration (5), and decommissioning (6). Based on this, a chosen type of platform structure which includs UMain volunternus 15MW and a turbine RWT-15 MW as reference for both subjects, meaning economical and simulation subjects' part. The proposed methods and assumption will therefore identify the cost cycle in relation to the six cost drivers as mentioned. The region at South North Sea II (SNII) is the reference location for both part subjects and meant for shallow waters of 70m and 168Km distance to the shoreline. The economical (part 1) and dynamical response

simulation (Part 2) will provide the cost expense, limit state of mooring tension, with these chosen methods will be considered for the thesis.

Key words: Cost life cycle (LCC); Capex; Opex; Decom; Dynamic response; prototype model; time domain; catenary mooring; shared taut mooring; buoy; RWT-15MW; Umain volunternus.

Preface

This thesis represents my final master's degree over a two-year period of 120 credit points (CPT) in industrial economies and technology management (INDØK) at the University of Agder (UIA). The master thesis started in the mid of January 2023 and ended in the spring of May 2023. The thesis represents 30 credit point (CPT) and is written at the department of engineering and technology of science.

The objective with this thesis was to analyze the economic cost drivers in the life cycle (LCC) of an offshore floating wind turbine. For the thesis, a reference platform and a turbine were used as reference to the South North Sea II. The cost model in this thesis was based on an international standard IEC 60300-3-3:2004 cost life cycle (LLC) and by (L. Castro-Santos et al, 2013) form the University of Spain.

The challenge with this thesis from my perspective was to combine the cost model with the aspect with the simulation software. This for the purpose of combining the subject and to create a meaningful thesis, all in all. However, the total amount of work that was done in this assignment for one person was difficult in some periods. This in relations to all the responsibility based on every decision and direction of the project's outcome. However, the motivation provided by associate professor Zhiyu Jiang for the project was with great help when subjects was discussed. I would therefore first like to thank my internal supervisor who followed up on a weekly basis, associate professor Zhiyu Jiang, Guodong Liang and finally Finn- Christian Wickmann Hansen at Semar AS.

Agder, Grimstad Norway

19. May 2023

Lasse Johannessen Backhoff Tollefsen

Nomenclature

1.	*AEP*	*Annual energy production*
2.	*ATB*	*Annual technology baseline*
3.	*Capex*	*Capital expenditures*
2	*OPEX*	*Operation and maintenance*
3	*DECOM*	*Decommissioning*
4	*LLC*	*Life cycle cost*
5.	*CBS*	*Cost brake down structure*
6.	*FCR*	*Fixed charge rate*
7.	*GW*	*Gigawatt*
8.	*KW*	*Kilowatt*
9.	*MW*	*Megawatt*
10.	*KWh*	*Kilowatt timer*
11.	*M*	*Meter*
12.	*MW*	*Megawatt*
13.	*MWH*	*Megawatt-hour*
14.	*O&M*	*Operational and maintenance*
13.	*OpEx*	*Operational expenditures*
14.	*USD*	*U.S. dollars*
15.	*Yr*	*Year*
16.	*ORCA*	*Offshore wind regional cost analyzer*
17.	*BOS*	*Balance of system*
18.	*WACC*	*Weighted average cost of capital*
19.	*NREL*	*National renewable energy laboratory*
20.	DNV	*Det Norske Veritas*
21.	COG	*Centre of gravity*
22.	COV	*Coefficient of variation*
23.	COB	*Center of buoyancy*
24.	FOWT	*Floating offshore Wind Turbine*
25.	TD	*Time domain*
26.	WF	*Wave Frequency*
27.	WTG	*Wind turbine Generator*
28.	LF	*Low frequency*
29.	PDF	*Probability Density Function*
30.	FLS	*Fatigue Limit state*
31	ALS	
32	ULS	*Ultimate limit state*

33.	MBL	*Minimum Breaking Load*
34.	MBS	*Minimum Breaking Strength*
35.	MPM	*Most probable Maximum*
36.	NOK	*Norsk krone*
37	Euro	*Euro*
38.	Lp	*Numbers of mooring lines*
39.	Lb	*Turbine blade length*
40.	PE	*Price per unit energy*
41.	SSP	*Semi-submersible platform*
42.	TLP	*Tension Leg Platform*
43.	SP	Spare buoy
41.	TLB	Vertical leg platform
44.	m	Meters
45.	SNII	South North Sea II
46	LJBT	Lasse Johannessen Backhoff Tollefsen
47	OFWT	Offshore floating wind turbines
48	FWT	Floating wind turbines
	CSC	

Table of Contents

Figure list:

Table list:

Graphs

Equations

1. Introduction

Global warming is changing rapidly, and the world needs alternative renewable energy to accommodate the negative CO2 emissions that's effecting the climate change. Therefore, new renewable solutions are therefore required to create a more sustainable and sustainable environment. The Norwegian ministry of Energy decided therefore in 2023 to open up new waters for windfarm development in the South North Sea II. The measured capacity of energy for these two areas combined corresponds to 4500MW. Based on the high energy potential, the marked growth of the offshore technology is therefore evolving rapidly with large scale turbines, innovative mooring configurations, and diverse platform designs for complex environment. Since large scale turbines produces more electricity than smaller ones, a further up-scaling for such turbines also requires large scale platforms and more materials to be used for such installations (Liu Jinsong et al, 2018, s. 1). Therefore, the cost expenses increase thereafter. However, some of the problem for such design configurations and installations is that the technology of offshore floating wind turbines is moving into harsher-, deeper waters with further distance to site locations. The process, therefore, makes the installations and operation very expensive and cost sustainable. In order for offshore floating wind turbines to be cost effective is to take a further look at the cost life cycle (LCC) defined by the cost six cost drivers. The fig. 1 illustrates some of the cost drivers and were they influences the most. As seen wind turbines represent 43% of the LCC and foundation 18%, and installation with 5% therefore to investigate the alternative for cheaper innovative solutions.

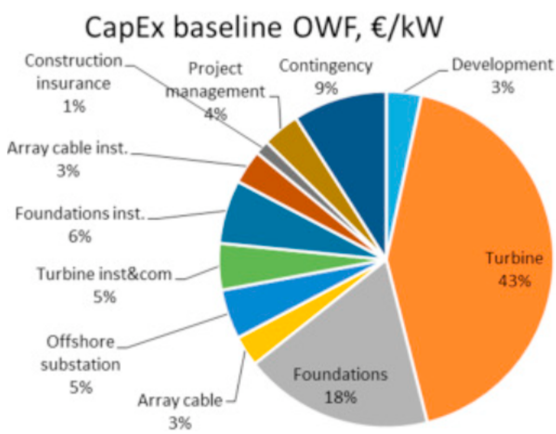

Figure 1 *(A. Martinez et al, 2021)*

The cost drivers are therefore largely affected by the installation- and operational cost. A key aspect of this report is to take use of a standardized cost breakdown structure (CBS) for the purpose of investigating more.

2.1 Methods and tools used for the thesis.

Introduction

This chapter describes the method and tools used to solve the thesis research question. The purpose for this is to provide a clear understanding to how the thesis has been solved. The thesis is divided between two subjects' methods, one economical part and a dynamic response simulation of a prototype model I and II. The chapters are described in chronological order for the purpose of providing a clear overview for both methods which are provided in the models.

The first part is the economical part where the cost model is presented over the total chain of the life cycle cost (LCC) with a description of each phase in the model and defined from 1-6 (see chap. 2.3). The purpose with this is to identify each cost components in the cost life cycle (LLC) of the offshore floating wind turbines (OFWT). The other part considers a clear and proper description of the setup simulation of the software program Orcaflex. The setup model is presented in (chap. 12). However, the simulation prototypes that is to be tested is based on two individual models I and II. A single OFWT with a chain catenary mooring line, and the other part is with two shared mooring line with two OFWT in the same setup model based with a calm base buoy.

2.2 Part 1, the economical method for the cost model.

Introduction to the economical method used in the thesis, this part describes the economical way-map based on the six main cost drivers. The cost drivers represent the total life cycle cost (LCC) defined over the work brake down structure (WBS) (see fig.3).

The methodology of the cost model is based on the international standard IEC 60300-3-3:2004 cost life cycle (LLC) ((Ingo Jermin et al, 2009, s. 1). The cost model could therefore be divided into to six main costs drivers and includes concept and definitions (1), design/

development (2), manufacturing (3), installation (4), operation & maintenance (5), and dismantling (6) (Ingo Jermin et al, 2009, s. 1). These cost drivers represent the capital expenditures (CAPEX), operation and maintenance (OPEX), and decommissioning (DECOM). Based on this, the developed way-map over the work brake down structure (WBS) provided in fig. 3 is the main cost elements and is divided in four levels from 1-4.

Firstly, level 1 provides an explanation of the reference location, life cycle cost (LCC). Secondly, level 2 represents the economical terminology with the main cost components with a clear description of the net average energy produced (AEP) followed by the main cost drivers Capex, Opex, and Decom. Furthermore, level 3 is the under-cost post that represent the main three cost drivers of the six under cost. Finally, level 4 provides the total value of Capex, Opex and Decom.

Economical map of the cost model (CBS)

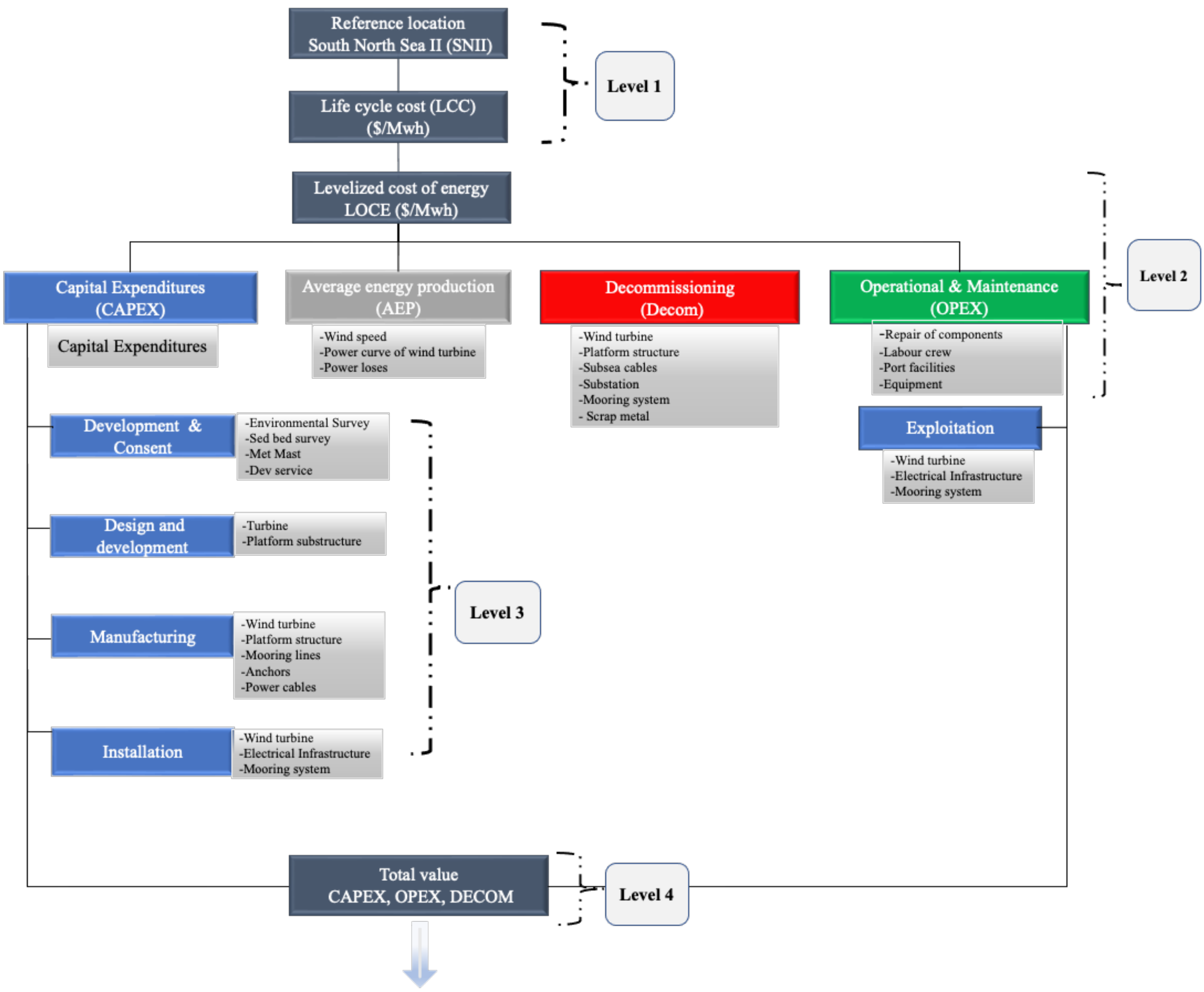

Figure 2 illustrates the work brakedown structure (WBS) of the financial cost model over the overall CAPEX, OPEX and DECOM of the LCC.. The model is designed In Power point and the consept of idea is added from (L. Castro-Santos et al, 2013) (Martinez, 2021, s. 7) The illustrated map figure of the work breakdown structure (WBS) is based on the international standard IEC 60300-3-3:2004 of the cost life cycle (LLC).

The illustrated WBS model in figure 3 identifies the main cost drivers in the Work breakdown structure (WBS). The six cost drivers and is followed in fig.4 and is the way map for solving the LCC and to solve the research question in relation to this thesis and is linked to (L. Castro-Santos et al, 2013) and (Martinez, 2021, s. 7).

***Figure 3** illustrates the way in the cost model based on each stage form 1-6 of the Life cycle cost (LCC) and is added form (L. Castro-Santos et al, 2013)*

2.3 Part 2, the simulation software Ocarina Ltd. Orcaflex

The simulation program used in this thesis is Orcaflex and the software is developed by the UK company (Ocarina Ltd., 2023, ss. 1-14). The software is an expensive license server borrowed for this thesis. The software provides a fully dynamic simulation analysis in 2D and 3D dimensional view of the OFWT in x-, y-, and z- axial positions. According to the Ocarina Ltd. the software uses the Morison approach for calculating the wave loads on the structure and is also mentioned by (Ibbrahim Engine Taze, 2022, s. 21). Moreover, the second order wave for Jonswap sea state conditions is also provided in the simulation software. The semi-submersible platform the UMain Volturnus 15 MW is as example file borrowed from Ocarina. Ltd and the link to the file is given here (Ocarina Ltd., 2023, ss. 1-14). For the software simulation to work, another software is needed, such as Pyhton.org 3.11.3 (Python.org, 2023). This is a separately downloaded file form another source. The function of Python is numerical coding software for scripting data from numerical output values from the simulation in Orcaflex. The presented figures below provide an overview of the 3D dimensional structure placed in waters in six degrees of freedom, also described in chapter 3 theory.

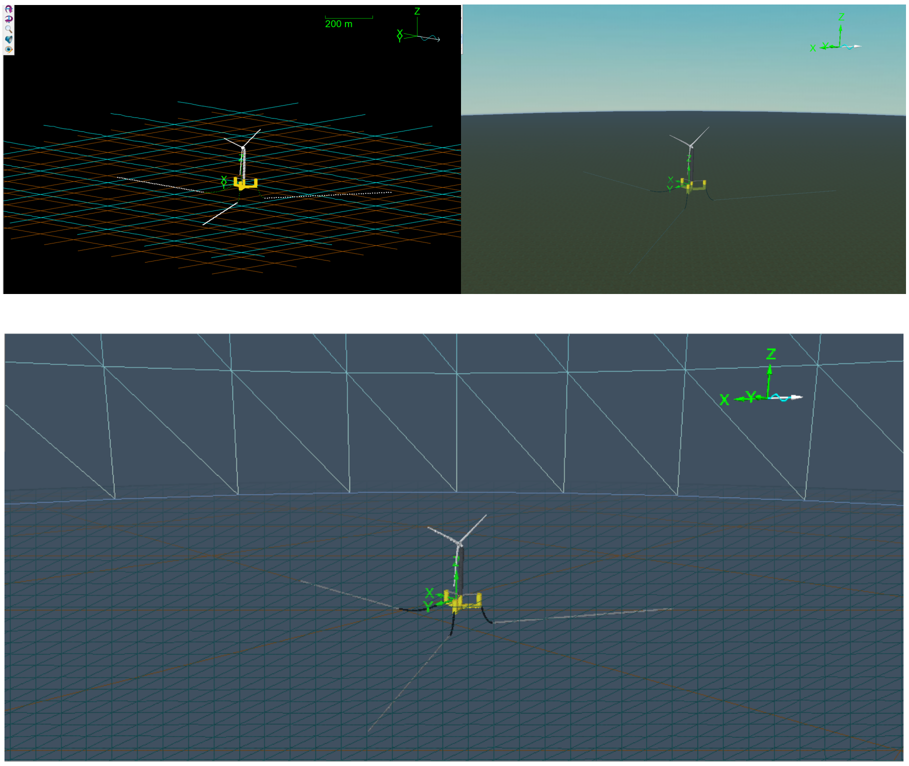

Figure 4 *Illustrates the tree various visons to see the screen shade and mash.*

The software therefore makes it possible to simulate several scenarios based on several aerodynamic and hydrodynamic conditions. The software could also be used for re- designing various components, such as platforms and turbine's structure.

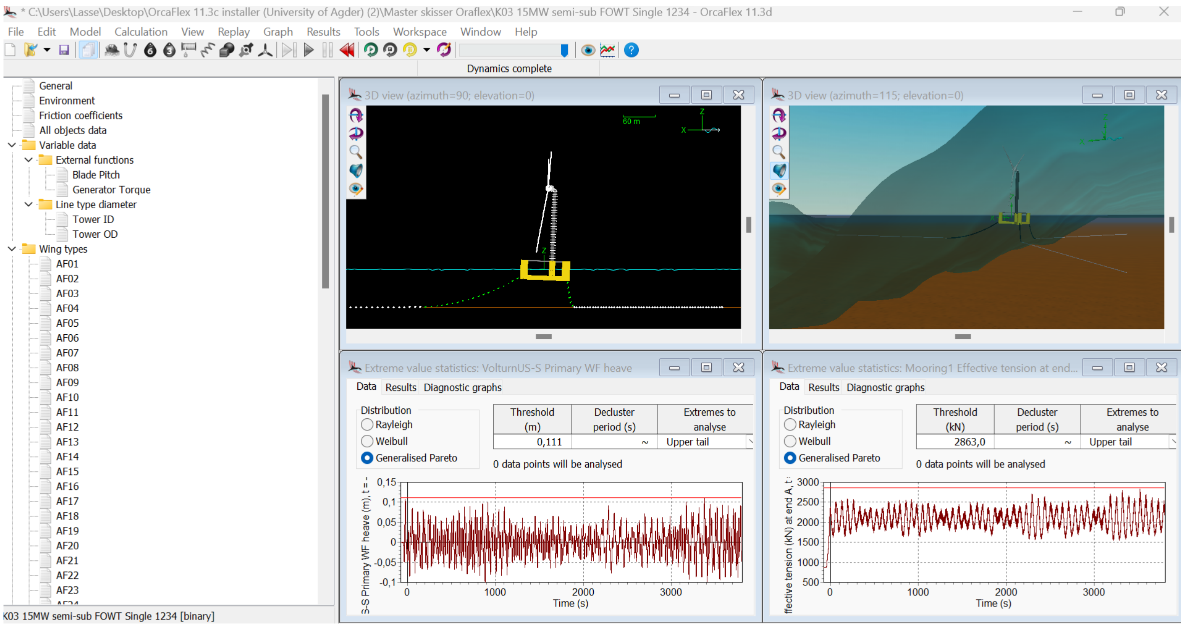

Figure 5 *Illustrates a screen overview of the Ocarina Ltd. Oraflex in the simulation test for a single OFWT prototypes.*

As could be seen in the fig. 6 to the left are all the main components of each file. Secondly, the time domain series after the simulation has been run provides the numerical graphs. The software has also been used for creating several figures of sketches in this thesis for the purpose of providing own illustrations along with the description.

2.4 Purpose and scope

The scope of the thesis is based on the state-of-the-art- technology and is a fairly challenge in relation to the high-cost expenses in this industry. This technology, however, is expanding rapidly for the purpose of reducing the global climate challenge and decreasing the fossil fuel into a more renewable energy and creating a new marked. Since the offshore wind industries today is very expensive new innovative solutions needs to be developed in order to gain global interest. This based on shareholders, governments, and private investors to see new profits in the OFWTs and state-of-the-art- technology. Therefore, new innovative solutions based on smarter, cheaper, and innovative solutions would possibly decrease the cost expense and make it more dynamic and cost effective.

The economical part of this project includes the total life cycle cost (LLC) for every six cost drivers in relation to installation, manufacturing, transportation, decommissioning, operation & maintenance service. The other experimental part is the simulation test of a scale prototype models I and II for different mooring configurations arrangements. The purpose with this is to measure the maximum peak tension for each individual mooring lines for the two prototypes tested by comparing the mooring configurations response effect. The test will also be performed with several mooring materials in relation to chain, steel wires and synthetic fiber ropes, also for comparing. Addition to the reasons analysis the test would also be measured along with the cost expense for one individual and multiple OFWTs for look at the cost.

2.5 Motivation

The technology of offshore wind installation has had a great success so far, to name a few Hywind Tampen, Dodger banks, Gamesa and several other wind projects globally. The concept with this OFWTs started back in 1991 in Denmark as a concept idea and has since then been a huge part of the renewable marked. The government in Norway opened therefore up new area for development for bottom fixed and FWT in the region of South North Sea II. This in 2023 by the Norwegian government. The South North Sea has significant potential for wind recourse of reusable energy to be utilized. The farm area according to NVE has a good wind and wave potential.

The motivation with the thesis subjects is to develop further knowledge with the cost chain of this type of renewable technology. Moreover, since it has become the green gold of renewable technology. The main cost components that makes up the total cost for an OFWT is an interesting subject. Moreover, the dynamic response in the mooring system is an important part which are related to the to the stabilizer of the platforms and is very linked to the cost expense.

In relation to capital expenses this type of technology it is still very expensive as mentioned. Since the effect are based on the manufacturing, installation, and maintenance service in these industries. Therefore, an optimizing of these cost drivers is needed to find cheaper and more sustainable alternatives in this manner. Nevertheless, an investigation of the several components would also provide some further knowledge and possible to identify a cost reduction with this technology.

The dynamic response of a simulation test would provide comparison with single Vs a shared mooring design to identify the response effect caused by the wave conditions. However, the concept of shared mooring lines with a buoy will therefore be investing to investigate. For this reason, possible findings could therefore provide more knowledge in relation to the cost of the life cycle and the response effect.

2.6 Problem definition of the research question

In relation to the LCC the capital and operational expenditures is largely affected by the mooring system, distance, and depth of wind location. For this reason, (L. Castro-Santos et al, 2013) investigated the cost lifetime cycle (LLC) of several types of offshore platform for comparing the cost for various mooring configurations in combination to a farm location. As a result, Semar AS has therefore investigated a technical solution that would offshore reduce the installation- and maintenance costs for a floating wind turbine. The technical solution consists of shared anchoring with a buoy and fiber mooring lines. The problem with such offshore installation in deep and shallow waters is due to high installation cost and environmental impact loads caused by wind and waves. The focus is therefore the technical solutions in combination with a 15MW model of a semi-submersible offshore wind construction. The main research for this project is to understand the physical behavior and carry out cost estimate for a prototype wind farm model. Simulations in Oraflex under various wind and waves circumstances namely hydrodynamics forces will be carried out. The main purpose is to develop a «Cost brake down structure» for the installation costs CAPEX, operating costs OPEX and decommissioning cost Decom. Today, huge amount of money is invested in the offshore industry and the demand continues to increase. Therefore, installation cost for such technical solutions will be an important part of further development.

Questions to be investigated and to be solved:

I. *How will different innovative mooring alternatives affect the system dynamic response and the life cycle cost costs (LLC) related to CAPEX, OPEX and DECOM of a 15MWsemi-submersible floating wind farm?*

2.7 Limitations

Since the master thesis is divided between two parts methods, one for each subject, meaning one economical part and one simulation part. The simulation part includes two individual scale prototypes I and II to be simulated, the fist model is based on a basic catenary mooring design configuration. The prototypes I and II are only meant for investigating the mooring line tension. The limitation of the thesis, based on the given timeframe and resources are very large subjects for one person to create deep knowledge for all the components and their configurations in relation to the research question. Therefore, the subject will be divided into simpler investigation subjects. The main goal for this thesis is to create a model of a prototype of a shared mooring arrangement between two 15MW platform with a buoy in the center in the software. This for comparing the mooring tension with several variables of sea state conditions for comparing the numerical data. The other part is to investigate the cost life cycle in relation to the mooring hardware, Installation, manufacturing, dismantling and operation and maintenance service fully described in chapter. 15 results. The outcome of the result in relation to the two investigated subjects will hopefully create a meaningful comparison with one and multiple OFWTs.

2.8 The main goal of the thesis.

The main goal with this research project is to estimate the total cost of a prototype model and a test simulation for comparing one single catenary mooring configuration Vs. shared mooring configuration to overlook the comparison over the response effect in the mooring lines. This for evaluating the cost and the dynamic responds effects. Therefore, in this thesis the main goals will therefore be:

1. To develop a cost breakdown structure of the total LLC of a wind farm in relation to Capital expenditure (Capex) along with operational & maintenance service (Opex) and decommissioning (Decom). This with cases 1 and 2 for assumed windfarm at South North Sea II with one 15MW and a 100MW wind farm also related to the prototype I and II models which are to be developed.
2. The other part is to create two shared OFWTs of a chosen prototype with a calm base marine buoy in the software program Ocarins Ltd. This with proper mooring configurations and properties.
3. Investigate the primary numerical collected data form the simulation test form Orcaflex and the economic cost which are collected through numerous articles and master thesis of other investigated work.

4. Finally, to compare the cost in each stage of the cost model and the mooring response system of mooring tension loads related to the15MW turbines with one, two shared etc.

2.8 The thesis overviews.

- **Chapter. 1**

The introduction to the thesis.

- **Chapter. 2**

The economical and simulation methods used for solving the thesis research question. A clear description of the methods and tools used for making a complete project in relation to both subjects economical and simulation software test.

- **Chapter .3**

Describes the theoretical theory of the mooring lines of single catenary and shared mooring lines configuration arrangement. Moreover, the drift motion caused on a platform structure in free water surface, the second order wave load along with wave and wind terminology, and finally monte Carlo simulation for describing the Weibull's probability paper for random variable number of numbers.

- **Chapter. 4**

The state- of- the- art technology based on various OFWTs configuration dependent on the platform structure. Followed by the various traditional mooring configuration based on catenary mooring, tut leg mooring, vertical tension leg, and shared mooring lines.

- **Chapter. 5**

The hardware components used in the mooring design. Firstly, the mooring lines based on chain, steel wire, synthetic fiber ropes. Followed by several anchors such as, drag embedded anchors, suction pile, pile anchor, gravitational anchor.

- **Chapter. 6**

This chapter provides the cost brake down structure (CBS) with clear description of six main cost drivers. The development and consenting, manufacturing, installation, transportation, operation and maintenance, and dismantling cost.

- **Chapter. 7**

The technical specification of the state- of -the -art technology.

- **Chapter. 8**

A clear description of the reference turbine RWT-15MW and the reference platform UMain Volturnus 15 CSC-Semi.

- **Chapter. 9**

The main mooring configuration arrangement is described and consist of catenary, taut line mooring, vertical tension leg, hexagonal shared mooring and two share mooring line.

- **Chapter 10**

The main mooring hardware components are described and includes chain, steel wire, synthetic fiber rope, anchors, shackles, and dynamic power cables.

- **Chapter 11**

The various vessel is presented with cost estimates.

- **Chapter 12**

The prototype models I and II are clearly defined with deep description aligned with the software of coordination's. The prototype I is a single OFWT and prototype II is a two shared OFWTs in the same setup. Moreover, the calm base buoy is properly described.

- **Chapter 13**

The case study is presented with the chosen reference location South North Sea II (SNII).

- **Chapter 14**

A collection of numerical cost data is presented with the authors.

- **Chapter 15**

The assumed possible windfarm in the south North Sea II for estimating the net average energy produced (AEP) for the two case 1 and 2.

- **Chapter 16**

The result is provided for the part 1 of the economical subject.

- **Chapter 17**

The result of the simulation test for both prototype I and II part 2 of the subject.

- **Chapter 18**

The discussion of the result both economical and simulations to founding's.

- **Chapter 19**

The discussion of the result mooring tension.

- **Chapter 20**

The

Theoretical backgrounds

This chapter considers the theoretical terminology of the several equations for the purpose of providing the general theory of wave, wind, and mooring lines in combination to the drift forces. The first part of the chapter provides the environmental wind and wave conditions. Secondly, a description of the mooring lines based on catenary and shared mooring design is developed. Moreover, the platform responding effect caused on the body in free motion based on the second order wave load principles. Moreover, a deeply description of a single and shared mooring line. Last the chapter of state-of-the-art technology.

3 Theory

3.1 Wind energy

Wind energy is developed when moving air pushes the rotor blade of the turbine to rotate. The rotating turbine blades utilizing the kinetic energy form the wind and developing a rotation and converts the kinetic energy into mechanical energy. The power in the wind is dependent on the wind speed which are a proportional factor to the rotor area. The equation of wind energy is therefore given as half the mass of air (m), multiplied by the square of the velocity (V^2). For a representation of the total power energy produced is given by these two eq. 1 and 2.

The equation for kinetic energy is given by:

$$Kinetic\ energy = \frac{1}{2} m V^2 \tag{1}$$

(Gofrey Boyle et al, 2012, s. 356)

Moreover, by substituting equation (2) into equation (1) for (m).

$$m = \rho A V \tag{2}$$

(Gofrey Boyle et al, 2012, s. 356)

$$P_{power} = \frac{1}{2} \rho A V^3 \tag{3}$$

(Gofrey Boyle et al, 2012, s. 356)

The final by combination of equation by 1 and 2 gives the energy power of the wind turbine and is also a description of the net average energy produced (AEP)

P = is the density of the air.

A= Area of the turbine blade

V^2= The wind speed

4 Mooring design theory.

Mooring and platform- configurations shared mooring lines.

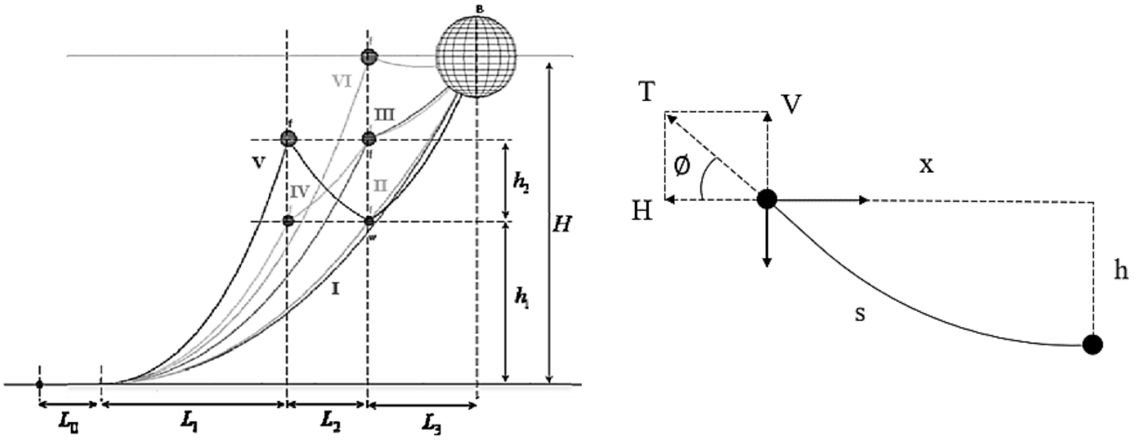

***Figure 6** illustrates the different mooring configurations profile such as Slack.* (H Munir, MC Ong, 2021)

Calculation of the mooring rope(wire) between two individual given point A and B

In order to designing the mooring lines between two equal symmetrical points, defined as (A and B) at the same level of height. The catenary equation is therefore useful for designing the mooring line in the right shape between two equal given points. The equation must therefore define one of the given points as the origin (A or B) between the shared mooring line (A-fairlead) and defined in a catenary plane (H Munir, MC Ong, 2021)For this, the mooring design are based on two equation and needs to be measured according to (H Munir, MC Ong, 2021)

$$X = \frac{H}{W} log\left(\frac{\sqrt{H^2+V^2+V}}{H}\right) + \frac{H}{EA}S \tag{4}$$

(H Munir, MC Ong, 2021)

$$h = \frac{1}{2}\frac{WS^2}{EA} + \frac{H}{W}\left[\frac{1}{cosø} - 1\right] = \tag{5}$$

(H Munir, MC Ong, 2021)

Description of the equation is x and h are defined as the vertical and horizontal distance of the measured point at the origin (A). The following H and V represents the vertical and horizontal mooring line tension defined as T based at the origan A, the total length of the shared mooring line (s), the weight per unit length is (w) defined in water. Finally, EA is the extensional stiffness(E) and elastic modulus(A)of the cross-sectional area. In relation to this the total length can be solved with iteration (H Munir, MC Ong, 2021). ***(Addition to this, when designing the mooring length of the vertical and horizontal mooring line in the software. The measured shape of mooring line is provided when calculating the total distance between two points from A to B, the shape of the line will therefore be provided.)***

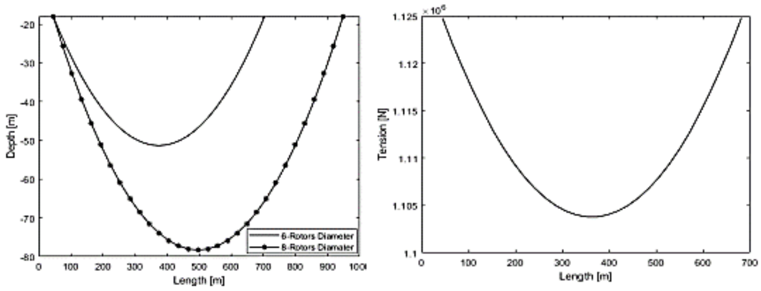

***Figure** 7 seen from left to right Catenary plane and Shared line* (H Munir, MC Ong, 2021)

Figure 8 (AMARAL, 2020, s. 48)

4.1 The calculation of the circle radius of the buoy

Addition to estimating the circle radius length of the vertical mooring line from the ground to the marine buoy. The calculation from the anchor point could be estimated by using the stretch factor bungee (L_b) in combination to Pythagorean theorem (CDIP mobile, 2023, ss. 1-2) .

$$Mooring\ length = 2xD = (S-1) * L_b + 2D \text{ =bungee stretch factor} \quad (6)$$

(CDIP mobile, 2023, ss. 1-2) .

By using the mooring length and substituting in the equation of Protagoras, the equation becomes.

$$R_c = \left|\sqrt{(S-1) * L_b + 2D^2}\right| \text{= The circle distances to the buoy} \quad (7)$$

(CDIP mobile, 2023, ss. 1-2) .

4.2 Morrison equation for the drag forces in the mooring lines.

Drag force in the mooring line on the marine buoy.

The drag force caused by wave loads on the mooring line could be calculated by using the Morison equation, since the lines are defined as slender lines (Zhi-Ming Yuan et al, 2019, s. 5)and therefore could be estimated for chain, wire, and synthetic fiber ropes. The respective drag forces per unit length of mooring lines is given by the equation (1)

$$F^D = \frac{1}{2}\rho\pi D C_{dt} v_t |v_t| + \frac{1}{2}\rho D C_{dn} v_n^2 \quad (8)$$

(Zhi-Ming Yuan et al, 2019, s. 5)

The equation of Morrison could also be used for calculating the drag force caused from the wave loads on a marine buoy. The equation of drag force in X-, Y-, and Z-directions is therefore given by:

$$F_x^D = \frac{1}{2}\rho\pi D C_{dx} v_x |v_x| = \text{X-direction} \quad (9)$$

(Zhi-Ming Yuan et al, 2019, s. 5)

$$F_Y^D = \frac{1}{2}\rho\pi D C_{dY} v_Y |v_Y| = \text{Y-direction} \quad (10)$$

(Zhi-Ming Yuan et al, 2019, s. 5)

$$F_Z^D = \frac{1}{2}\rho\pi D C_{dz} v_z |v_z| = \text{Z-direction} \quad (11)$$

(Zhi-Ming Yuan et al, 2019, s. 5)

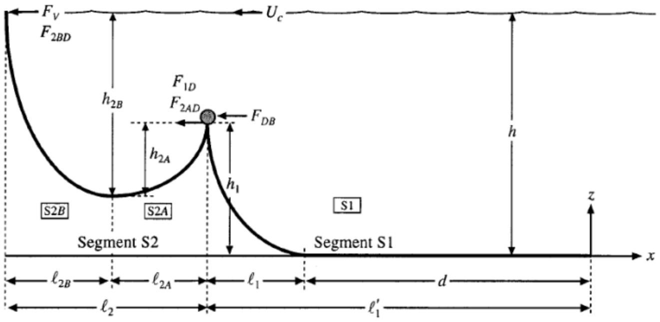

Figure 9 (AMARAL, 2020, s. 49)

The definition of the equation, the diameter of the line is given by (D), (ρ) is the water density (1000), nondimensional quadric tangential drag forces(C_{dt}) , and the lateral(V_t) and the flow velocity (V_n^2) (Zhi-Ming Yuan et al, 2019, s. 5)

The tension load in single catenary mooring line

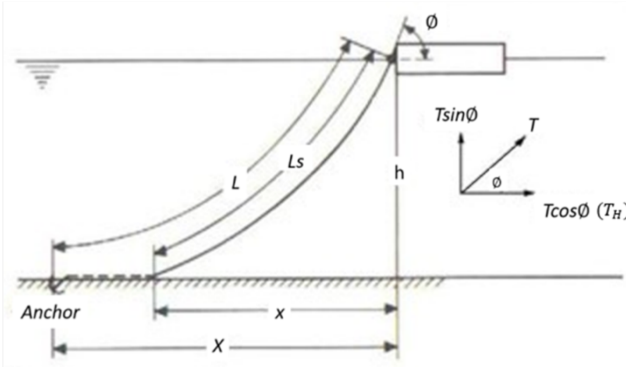

Figure 10 *Illustrates the radius (m) to the anchor point and based on (6-8) the water depth, this in relation to 70m. The resulting radius length is 610 m.* (Yang, 2021, s. 2)

To estimating the static catenary shape of a single mooring line in relation to the given water depth (h). The unit (h) represent (h) in the equation, (ω) is the weight of the unit length of mooring line in wet water (ton/m). (T_{max}) is the horizontal load between the responding point (ωh) is the total weight of mooring line (Yang, 2021, s. 2). The equation therefore becomes.

$$l_i = h\sqrt{2\frac{T_{max}}{\omega h} - 1} \tag{12}$$

(Yang, 2021, s. 2).

The horizontal distance between two points is defined as the distance (x) between the fairlead and to the anchor point, the equation is expressed by:

$$x = \frac{T_{max-\omega h}}{\omega} cosh^{-1}\left[1 + h\left(\frac{\omega}{T_{max} - \omega h}\right)\right] \tag{13}$$

(Yang, 2021, s. 2)

By combining these two equations the restraining line forces becomes

$$= h\sqrt{2\frac{T_{max}}{\omega h} - 1} + x = \frac{T_{max-\omega h}}{\omega} cosh^{-1}\left[1 + h\left(\frac{\omega}{T_{max}-\omega h}\right)\right] \tag{14}$$

(Yang, 2021, s. 2)

4.3 The drift motion caused by wave loads on a floating structure.

The six degrees of freedom.

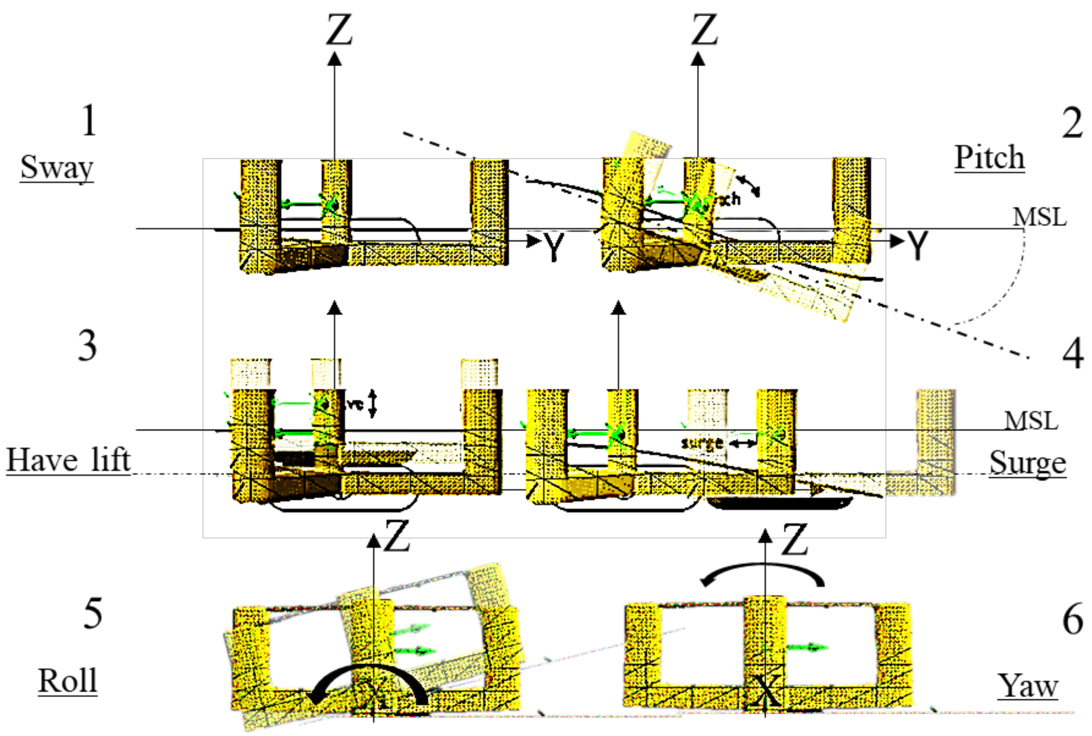

Figure 11 *Illustrates the drift motion caused by the wave drifts on the floating body (Platform). The fig.12 is redesigned model based on (Godfrey Boyle et al, 2018, s. 455). The motion drift **(1)** steady state position, **(2)** pitch, **(3)** have lift, and **(4)** surge. The Z-axial position shows the direction in the geometrical plane. The illustrative figure is designed by the author.*

For a single floating body in free waters there are six drift motions the body (platform) could encounter in relation to wave, wind, and current loads. Firstly, the translational is described as sway (1), pitch (2), have lift (3), surge (4), roll (5) and yaw (6), also defined as the six degrees of freedom. The drift motion is divided between two categories translations in longitudinal (X)-, lateral (Y)- and vertical (Z)-axis. The other motion is rotation in the longitude (X)-, lateral (Y)- and vertical (Z)-axis (Marcin Gradowski et al, 2017). Further explanations are given below.

Definitions of free motions

- **(1)** Sway is a transverse motion where the body shifts from one side to the other and back again, this in the same linear direction in lateral axis (DNV, 2021, s. 15)
- **(2**) Pitch is defined when rotation encounter about the lateral axis and causing rotation on the body (Godfrey Boyle et al, 2012, ss. 455-456).

- **(3)** Have lift is when the body going up and down in a vertical linear direction and along the vertical axis (Godfrey Boyle et al, 2012, ss. 455-456).
- (**4**) Surge is when the body going back and forth in a horizontal x-axial direction, meaning along the longitudinal axis (Godfrey Boyle et al, 2012, ss. 455-456). (DNV, 2021, s. 15)
- (**5**) Roll is a rotational motion defined around its longitudinal axial direction. (DNV, 2021, s. 15)
- **(6)** Yaw is a rotation caused on the body defined in the vertical axis Rotation about vertical axis (DNV, 2021, s. 15)

4.4 The motion of a floating body (platform) in a frequency domain.

In relation to six degrees of freedom of a flotation body in free motion based on have lift, sway, pitch, and roll. The definition of free motion could be determined by using the dynamic equation of equilibrium in a frequency domain (Yang, 2021, s. 5). The equilibrium is based on Newton second law of motion, meaning the total mass of the system (M) with a given acceleration (m/s) in defined direction. The principle could therefore be expressed with d'Alembert's principle. The principle could be defined for a platform structure and mooring lines in water in a time domain (Yang, 2021, s. 5).

$$[M + \mu_\infty] + \ddot{X} + \int_0^\infty R(t-\tau)\dot{x}d\tau + Cx = F^{fk} + F^{d} + F^{sd} + F^{w} + F^{c} + F^{m} \tag{15}$$

(Yang, 2021, s. 2).

The unit in the equation seen from left to right could be described as, (1) M is the mass of the platform structure, (2) infinite added mass($\mu_{\infty)}$, (3) the retardation function $(R(t-\tau))$, and the (4) hydrostatic restoring coefficient (C). additional for solving the integral the Froude-Krylov force and diffraction forces could be solved. The Froude -Krylov (F^{fk}), the diffraction force(F^{d}) , the second order wave load(F^{sd}) , the wind load (F^{w}), current load (F^{c}) and finally (F^{m}) the mooring transmitted forces (Yang, 2021, s. 2). The initial retardation function is solved by the integral over $R(t-\tau)\dot{x}d\tau + Cx$ and is an inverse function in relation to Fourier transformation) (Yang, 2021, s. 2).

4.5 Time domain in relation to wave response.

The sea state condition Jonswap wave loads could be defined with Pierson-Moskowitz spectrum equation. The equation estimates the drift forces acting towards the OFWT in relation to have lift (3), surge (4), and pitch (2) (see figure). The equation below referred to (ω) is the wave frequency (Hz/s), (H_S) is the significant wave height and(T_P) is the significant wave periods (zero-crossing period in in seconds. The sea state could be defined as the highest significant wave heights (H_S) and the responding wave period (T_P). Significant wave height is defined as 1/3 of the largest wave and provides of the highest average of all the measured wave (J.M.J. Journee et al, 2001, s. 183) Based on this, the second order wave loads could be used …. frequency higher but also lower than the frequency in the wave. This means that the force square is a proportional factor of the wave amplitude (J.M.J. Journee et al, 2001, s. 369) Since the wave forces has significant impact on the platform structure (body) the responding expansion of the moored OFWT could be calculated using the second order term of the mean Jonswap. **The simulation software Orcaflex is estimating this in the response to second order wave load.**

$$S(\omega H_{s,T_P}) = \frac{320 H_{1/3}^2}{T_P^4} exp\left[\frac{-1950}{T_P^4} * \omega^4\right] * \gamma^A \quad (16)$$

(J.M.J. Journee et al, 2001, s. 194)

H_s = Significant wave heights (m)

T_p = Significant time periods (rad/s) or (Hz/s)

(Hyungjun Kim et al, 2014)

4.7 Design of mooring lines.

For designing mooring lines based on requirement of standards of mooring lines there are a specified consequence class in relation to the loading factor for mooring lines limited state. The table below provides the limited state of ULS and ALS in relations to the consequence class defined in. (DNVGL AS, 2018, s. 75) When the possibility if the mean tension exceeds 2/3 of the characteristics of the dynamic tension, the value 1,3 must be should be applied instead of the safety factor. The class are related to safety factor class and could be found in DNVGL-OS-E301

ULS-Ultimate limit state is to calculation for the individual mooring line to have adequate strength to withstand the load effect caused in extreme conditions dynamic tension is combined with a safety factor (S_c) (DNVGL AS, 2018, ss. 50-57)

The equation is therefore given by:

Ultimate limit state (ULS)

$$T_d = \gamma_{mean} * T_{c,mean} + \gamma_{dyn} * T_{c,dyn} \tag{17}$$

(Yang, 2021, s. 2).

$$T_{mean} = Mean\ tension$$

$$T_{dn} = Dynamic\ tension$$

$$\gamma_{mean} = \gamma_{dyn} = Loading\ factors$$

$$S_c = 0.95 * S_{mbs} \tag{18}$$

(Yang, 2021, s. 2).

$$S_c > T_d \tag{19}$$

(Yang, 2021, s. 2).

Selection of mooring system

$$\text{Performance index} = \frac{\mathrm{T_d}}{\mathrm{S_c}} * (\mathrm{D_c} * \mathrm{S_f}) \tag{20}$$

(Yang, 2021, s. 2).

ALS- Accidental Limit state meaning to ensure that the mooring line adequate capacity to withstand the failure of one mooring line, trust failure for unknown reason (DNVGL AS, 2018, ss. 50-57).

FLS- the fatigue limit state is to ensure the individual mooring line to withstand the cycling load (DNVGL AS, 2018, ss. 50-57).

Table 1 *Illustrates the coefficient of the ULS, ALS* (DNVGL AS, 2018, s. 75).

Limit state	**Load factor**	**Consequence class**	
		1	2
		Safety class	
ULS	γ_{mean}	1.35	1.55
ULS (Normal wind load) DNVGL-ST-0437	γ_{dyn}	1.1	1.25
ALS	γ_{mean}	1.0	1.15
ALS	γ_{dyn}	1.0	1.15

For calculating the required proof load, maximum breaking load, and minimum breaking load for studdles steel chains these equations are used Eq.22, Eq.23, Eq.25. Moreover, the evaluation of chain design is referred to the gradings of steel R4 chain links and is further described in chapter (17.2 chains). The relation is to find the right test strength of chains in relation to the maximum restraining tension the chains are dimensioned for.

Proof load

$$\textit{Studdles R4}{=}00192d^2(44-0.08d){=}N \textit{ in mm} \tag{21}$$

(American Bureau of Shipping (ABS), 2017, s. 29)

Maximum breaking load

$$\textit{Studdles R4}{=}0.0274d^2(44-0.08d){=}N \textit{ in mmm} \tag{22}$$

(American Bureau of Shipping (ABS), 2017, s. 29)

Minimum breaking load

$$\textit{Studdles R4}{=}00192d^2(44-0.08d){=}N \textit{ in mm} \tag{23}$$

(American Bureau of Shipping (ABS), 2017, s. 29)

5 Net annual energy produced - AEP

The (Cp) capacity factor needs to be estimated. The factor is measurement by taking the annual energy produced (APE) and divided it by the turbines rated power for a one-year period. Since the total days in a year is 365 days and 24 hours in a day the total is 8760s. The calculation is therefore presented in the equation below.

$$C_p = \left(\frac{Annual\ Energy\ Production}{(Rated\ pwer)x\ 8760s}\right)X\ 100 = \text{Capacity factor} \tag{24}$$

Authors notes for earlier lecture

$$P_m = \frac{1}{2} \cdot \rho \cdot A \cdot C_p(u_i^3) = KW \tag{25}$$

Authors notes form earlier lecture

6 Economic methodology and definitions

6.1 Cost model of the (brake down structure)

Introduction

Addition to the cost breakdown structure, this thesis has reused the cost model by (L. Castro-Santos et al, 2013) and 2016. as an assumption in the cost model. For every phase in the cost model the source for the authors will be clearly identified. The purpose with the cost model is to make a proper decision for dividing the cost components down to it specific drivers, defined from 1-6. See figure. The cost model will define each cost components to be evaluation in the Life cycle cost (LCC). This will be calculated in result (chap. 16)

Phase 0. life cycle cost (LLC)

Phase 1. Conception and definition

Phase 2. Design and development

Phase 3. Manufacturing

Phase 4. Installation

Phase 5. Exploitation

Phase 6. Dismantling

Figure 12 *illustrates the way in the cost model based on each stage form 1-6 of the levelized cost cycle (LCC) by (L. Castro-Santos et al, 2013)*

6.2 The total life cycle cost (LLC) of the OFWT.

The tool accounts for every cost component in the development of a finalized and complete project from each individual cost components. The convenient output estimated could therefore be used for comparing each technology with other power plant and comparing their competitiveness in the technology marked. Nevertheless, it could be used for evaluating the overall project if its compatible () Addition to (L. Castro-Santos et al, 2013) and (Ala' K. Abu-Rumman et al, 2017, s. 186) the total life cycle cost (LCC) is found by taking each cost component in the right order and multiple all cost components Eq 22.

$$\text{LCC}=({C^1}_{Concenting/\,Development}) + ({C^2}_{Design\ and\ deveopment}) + ({C^3}_{Manufactoring\ cost}) + ({C^4}_{installation\ cost}) + ({C^5}_{Decomisoning}) + ({C^6}_{Operation\ \&\ maintence}) \quad (26$$

(L. Castro-Santos et al, 2013)

(Ala' K. Abu-Rumman et al, 2017, s. 186)

***Table 2** Provides the nomenclature of the total life cycle LCC components (L. Castro-Santos et al, 2013) (Ala' K. Abu-Rumman et al, 2017, s. 186)*

Nomenclature	Description
$C^1_{Development})$	The development cost.
$C^2_{Turbine\ \&\ platform}$	The manufacturing cost Wind turbine
$C^3_{Transportation})$	Transportation cost.
$C^4_{Installation})$	Installation cost.
$C^5_{Operation\ \&\ maintenace})$	Operation and maintenance cost.
$C^6_{Decommissonig)})$	Decommissioning cost.

6.3 The conception and definition (1)

Phase 2, The conception, and definition are related to the viability of the total project. The cost is divided into three stages such as marked survey (1), legislative factors (2), and design of windfarm (3). The market survey is feasibility research of the overall project for a possible investment. The survey is a research study and evaluation if the overall project could be investible and deliver revenue of investment. Legislation is the cost which are related to tax, governance, and a scope of possible impact the project may cause on the environment (L. Castro-Santos et al, 2013). The conceptual design is the survey for estimating the total cost of every turbine (C_{NT}), resources needed, development cost, and the power output from each individual turbine(C_{ED}). The equation for estimation the total development $(C^1_{Development})$ cost is given by:

$$(C^1_{Development}) = C_{Resourse\,\&\,development} + C_{Numbers\ of\ turbines} + C_{The\ power\ of\ each\ turbines} \quad (27)$$

(L. Castro-Santos et al, 2013)

Table 3 Provides the nomenclature of the conception and definitions. *(L. Castro-Santos et al, 2013)*

Nomenclature	Description
$C_{Resourse\,\&\,development}$	*Development*
$C_{Numbers\ of\ turbines}$	*Numbers of turbines*
$C_{The\ power\ of\ each\ turbines}$	*The power of the turbines*
$C^1_{Development})$	*Total cost*

6.4 Manufacturing cost (2)

The fabrication is the cost related to each component of a complete assembly of the floating wind turbines. The cost is divided into multiple fabrication post and includes turbines (1), platform (2), mooring lines (3), anchors (4), and electrical power cables (5). For the turbine cost $C_{Turbine}$ is based on the tower, nacelle, and rotor, and is defined for each individual turbine (L. Castro-Santos et al, 2013). Furthermore, the fabrication of platform, mooring lines, anchors are defined as a sub-cost with many variable activity-based-cost performed at the harbor dock, according to (L. Castro-Santos et al, 2013). Generally, the cost also includes labor cost, material cost and the variable activity-cost as mentioned. Addition to the total amount of materials that are used in each cost components is a factor and is provided in Eq. 29. The is the total mass (m_{steel}) of each material, and C_{steel} is the density of materials. Finally, for each material is multiplied by their cost price in the marked. Addition to this the equation is therefore given. The electrical power station is based on the total amount of electrical cables needed for every substation per turbine. *The equations is therefore given by:*

$$C^2_{T\&P} = C_{Turbine}+C_{Platform}+C_{Moooring}+C_{Anchoring}+C_{Electricity} \tag{28}$$

(L. Castro-Santos et al, 2013)

***Table 4** Provides the nomenclature of the manufacturing components (L. Castro-Santos et al, 2013)*

Nomenclature	Description
$C_{Turbine}$	*Transportation*
$C_{Platform}$	*Mooring*
$C_{Moooring}$	*Anchors*
$C_{Anchors}$	*Cables*
$C_{Electricity}$	*Total installation*

$$C_{matrial\ cost} = m_{steel} * C_{steel\ price} + m_{concrete} + C_{price\ of\ concrete} + m_{ballast} * C_{Price\ ballast} = \tag{29}$$

(Alberto Ghigo et al, 2020, s. 14)

Table 5 Provides the nomenclature of the material cost *(Alberto Ghigo et al, 2020, s. 14)*

Nomenclature	Description
m_{steel}	*Total mass*
$C_{steel\ price}$	*Steel price*

6.5 Installation-, transportation- cost (3)

The installation cost is the where the OFWT is to be installed in the farm location. This cost represents the installation of wind turbines **(1)**, platform structure **(2)**, mooring (3), anchors (4), and electrical power cables (5) and start- cost (6). () Nevertheless, the transportation cost from the harbor dock to the farm site, by towing a complete set assembly of the OFWTs. The transportation cost is very effected by the total distance between the harbor dock to farm sites. Since long duration hours are very expensive in relation to vessel of day rates, direct labor cost and renting of equipment. The installation of mooring line and anchors are pre- installed before the complete set assembly of the WT is to be installed at farm site. Therefore, the total installation cost ($C^4_{Installation}$) is based on several sub-cost drivers for a complete assembled OFWT. The fists one is the traveling cost back and forth to the location (C_{travel}), the installation of mooring equipment ($C_{mooring}$), installation of anchors ($C_{Anchors}$), installation of electrical (C_{Cables}), and finally the (C_{Cables}). The equation below is the total calculation of installation ($C^4_{Installation}$).

The equation is therefore given by:

$$C^4_{Installation} = C_{Transport} + C_{mooring} + C_{Anchors} + C_{Cables} + \cancel{C_{start\ up}} \tag{30}$$

(L. Castro-Santos et al, 2013)

Table 6 *Provides the nomenclature of the installation and transportation components (L. Castro-Santos et al, 2013)*

Nomenclature	**Description**
$C_{transport}$	*Transportation*
$C_{mooring}$	*Mooring*
$C_{Anchors}$	*Anchors*
C_{Cables}	*Cables*
$C^4_{Installation}$	*Total installation*

6.6 Dismantling cost (4)

The dismantling of the OFWT is when the turbine is in its final stage of operation after 25 years of lifetime (). The process of dismantling each component in the OFWT is based on turbine, generator, platform, mooring lines, anchors, shackles, and marine buoy. Theas individual components are to be recycled and transported from the farm location and to sold for scrap price in the marked. The power generator $C_{Power\ generator}$ consist of valuable materials such as, cobber, aluminum, and steel. The construction steel in the platform structure ($C_{Platform}$) is the scrap value of recycling. The mooring cables, wire, and chains ($C_{Mooring)}$ + and anchors ($C_{Anchors}$), and the cost of recycling of materials is the array cables ($C_{electisity)}$. The final stage is transportation of the scarp material from the farm location (L. Castro-Santos et al, 2013). However, since no OFWT has been dismantled regarding the 25 years the technology is new. According to (Martinez, 2021, s. 7) *the dismenteling cost is the reverse process of the installtion cost, therfore,*

The equation is therefore given by:

$$(C^{6}_{Decommissonig\ of\ arrengment}) = C_{Power\ generator} + C_{Platform} + C_{Mooring} + C_{Anchors} + C_{transport} \tag{31}$$

(L. Castro-Santos et al, 2013)

***Table** 7 Provides the nomenclature of dismantling components (L. Castro-Santos et al, 2013)*

Nomenclature	**Description**
$C_{Power\ generator}$	*Generator*
$C_{Platform}$	*Platform*
$C_{Mooring}$	*Mooring*
$C_{Anchors}$	*Anchors*
$C_{transport}$	*Transportation*
$C^{6}_{Decommissonig\ of\ arrengment)}$	***Total value***

6.7 Exploitation cost (5)

The exploration is a cost divided between administration cost, assurance cost, business cost over the OFWTs lifetime. The process of operation & maintenance (O&M) is divided into preventive- and corrective-maintenance. This service includes inspection of turbines, platforms, mooring lines, anchors, sensors, and removals of parts. For both O&M the cost expenses that impacts the most are the material cost, labor cost and transportation cost of vessels. The prevention could therefore be divided into a schedule or condition-service (Costro-Santos, 2016, s. 32).

The preventive (PM) is the service that is already established in the strategy of plane in the project schedule. The other part is conditional based, which includes inspection and history monitoring of the various components in the farm site (Puglia, 2013, s. 17). The service is meant for comparing present with future possible cost (Puglia, 2013, s. 17).

The corrective is the potential of failure for the components and these are either repaired or totally removed form site (Puglia, 2013, s. 17).The corrective (CM), is the maintenance service which includes miner repair, or the component is left with some issue (Puglia, 2013, s. 17).

In this thises, the cost of O&M will only account for transportation cost ($C^1_{O\&M}$), materials cost ($C^2_{O\&M}$) and finaly labour cost ($C^3_{O\&M}$). Based on this, the Eq.(29) for estimatimatig operation & maintenance becomes.

$$C^5_{Operation\,\&\,maintenace} = C^1_{O\&M} + C^2_{O\&M} + C^3_{O\&M} \qquad (32)$$

(Costro-Santos, 2016, s. 32)

Table 8 *Provides the nomenclature of the Operation and Maintenance (Costro-Santos, 2016, s. 32)*

Nomenclature	Description of units
$C^1_{O\&M}$	*Transportation*
$C^2_{O\&M}$	*Cost of materials*
$C^3_{O\&M}$	*Crew labor*
$C^5_{Operation\,\&\,maintenace}$	**Total value**

In response to the installation, operation & maintenance, and decommissioning they are all dependent on transportation. This means fuel price and labor cost for renting vessels needs to be accounted for based on daily rent per day.

7 Technical terminologies

7.1 State- of -the- art technology

In this chapter, the terminology of the Semi-submersible platform will be described in detail for the purpose of developing a reference case in addition to the mooring configuration systems. Since the CSC-semi structure, UMain Volturnus 15 is chosen as the reference platform for this thesis. The other platform design and configurations will only be described briefly in response to Barge, Spar buoy (SP) and Tensile leg platform (TLP).

There are many types of OFWTs described by their design of configuration. The main design is **Barge (a),** semi-submersible (SSP) **(b),** spar- buoy (SP) **(c)** and tension leg platform (TLP) **(d).** These types of configurations are defined as a state-of-the-art technology. The main purpose for these floating structures is when bottom fixed platform (Jackets) no longer is possible and economical viable (Karsten M et al, 2020, s. 1), (Xinkuan Yan et al, 2023, s. 1). Hence, the water depth exceeds above > 40 meters (Taze, 2022) Normally, the platforms' structure is categorized into their specific water levels depending on their optimal spacing. The spar-buoy design is normally used for deep water>1000m, semi and barge >50 m water depth. However, since the semi-submersible structures has a low buoyancy in waters, the SSP could also be used for shallow waters.

A) **Barge buoyancy stabilized** is a design where the platform creates stability by distributed buoyancy, meaning the design uses the large surface area of the platform on water. The shape of platform is formed as a rectangular shape. The inner center of the structure is a moon pool that absorbers the wave energy (Mohammad Barooni et al, 2022, s. 5).

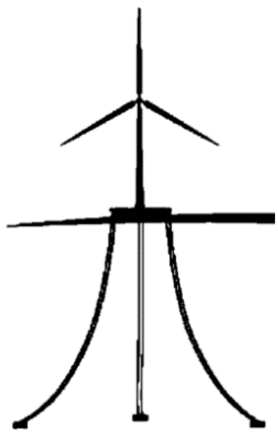

(a)

Figure 13 *Barge (Maximiano, 2021)*

B) **Semi-submersible platform (SSP)** is a design structure where the stability is created through the restoring mooring lines, normally three lines for anchoring. The structure is generally designed up with columns in various formations depending on the configuration design. The main purpose with the columns is for developing good stability in the ocean water, but also to create a connection between the submerged pontoons. The pontoons are meant for keeping the structure floating (). The turbines placement could be at the center of the platform or at one of the outer columns. Since the SSP has a very large mass compared to the other structures motion caused by have lift is very low. This means that the design is very stable in the ocean (Godfrey Boyle et al, 2012, s. 338).

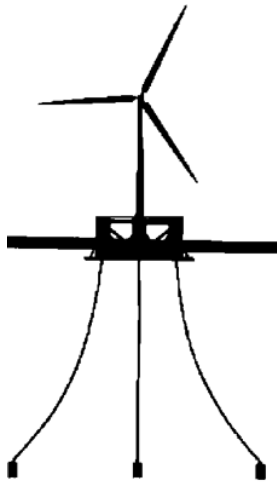

(b)

Figure 14 Semi-submersiblel SSP *(Maximiano, 2021)*

C) **Spear buoys (SP)** is a design as a cylindrical tube where the platform crates stability by using ballast seawater with a heavy weight hung below a buoyancy tank. The platforms stability is created with three mooring lines attached for restraining the structure. The design is constructed up by three parts; fist a cylindrical tube-shape that are divided into two sections. Firstly, the top section of the cylindrical tube is meant for keeping the structure floating. The lower part is the heavy ballast for the purpose of creating low buoyancy beneath the center of buoyancy. The turbine is vertical raised in the ocean.

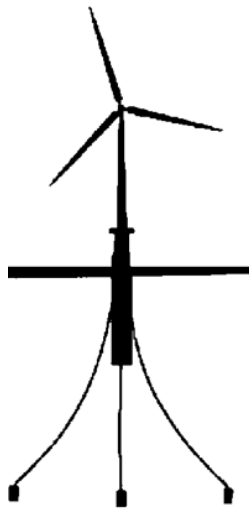

(c)

Figure 15 *Spar-buoy (Maximiano, 2021)*

D) Tension leg platform (TLP) is a design that is designed with a center column and raiser arms for developing stability. The meaning with the raiser arms is to create large tension between the arms and the mooring lines for strainment. Since the structure is highly buoyant the large tension in the mooring lines and raiser arms are pulling the floater downwards which causes a high tension between the structure and the seabed.

(d)

Figure 16 Tension leg platform *(Maximiano, 2021)*

The table below provides a cost comparison between various mooring configuration in relation to the mooring configurations with the various platform design. The collected date is added from. The cost estimations in this situation are converted to dollar and with today's inflation rate.

Table 9 *provides a cost comparison between the total for platform structures the collected data is added by and converted today's inflation rate and in dollar* (Sintef, 2019)

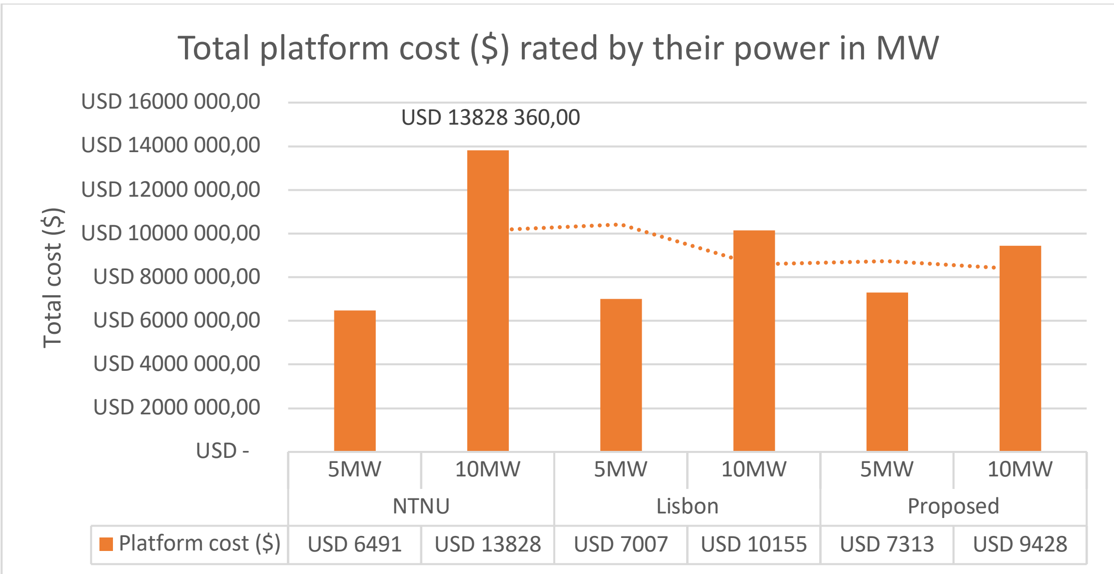

8 Semi-submersible platform (SSP)

Introduction

This chapter provides a deep description of the main reference platform and the wind turbine. The purpose is to gain knowledge of their configuration and properties for both designs. Moreover, the founding's will be added in the cost model and simulation test of a prototype.

Semi-submersal platform is a very known structure and is related to the earlier design from the oil industries. This type of SSP provides many advantages for deep and shallow water installations and are based on its robust quality and stability in harsh environments. The semi structure has many designs based on shapes and formations, but generally a triangular shape based on three or four columns. The vertical columns are meant for maintaining buoyancy but also holding the horizontal submerged pontoons connected (Kabir Sadeghi et al, 2019, s. 31). Nevertheless, the structures center point is configurated above the buoyancy and provides low gravity and good balance on the structure in water. The pontoons and columns are connected in a pattern of cross-section, which means that the structure is strengthened in each direction on the structural foundation. In relation, to the various designs it could include gangway/deck, heavy plates, and stiffeners in the arrangement of the platform.

The main advantage with a Semi-submersible platform (SSP) is the high mobility and balance for various environmental conditions. Nevertheless, the large surface area of structures creates high personal security for crew in the maintenance service (O&M). However, some disadvantage is related to the high manufacturing cost, material cost and fabrication based on its enormous size. Generally, the expected lifetime is 25 to 30 years.

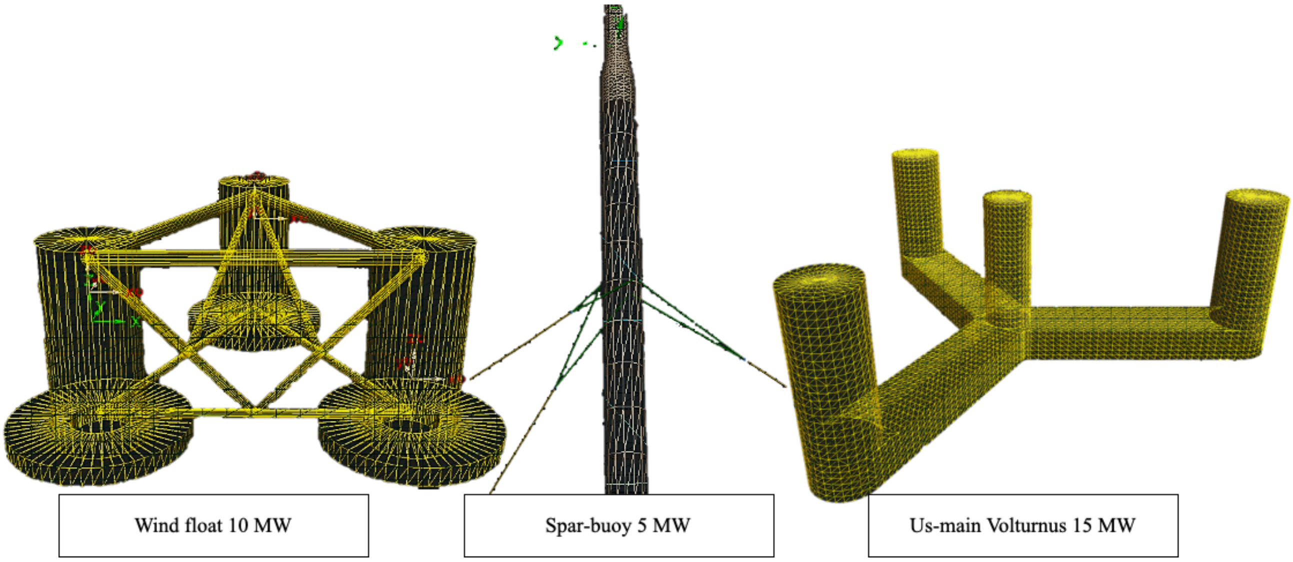

Figure 17 *Illustrates the wind float (10MW), Spar buoy (5MW) and the CSC-semi(15MW). The illustrative design to the left is purely designed by the author LJBT from Orcaflex and was in the beginning of the thesis meant to be used as a possible reference platform.*

Three individual OFWP

1) **Wind float (SSP)** is a structure developed with three columns formed in a triangular formation where the turbine tower is developed on one of the outer columns.
2) **Hywind O3** Spear-buoy (SP) is a structure design formed in a cylindrical tube. The configuration is constructed up with two parts (see chapter 14.1) with a heavy ballast in the lower end for creating balance to the structural shape defined in a vertical position in the ocean water (Mert kaptan et al, 2021)
3) **CSC-semi (SSP)** is a bracelets structure (Mert kaptan et al, 2021) and the formation is designed with 4 columns total, meaning one in the center meant for the turbine tower and three outers. The CSC- semi is the chosen platform structure used as a reference for both cases in this thesis; economical and prototype simulation (see chapter 12). In relation to the CSC-semi the first design was developed according to (Mert kaptan et al, 2021) by Norwegian research center.

The illustrated fig. 18 present various marine structures such as, Wind float 10MW 5 MW OC3-Hywind, and 15MW CSC-semi. Additionally, the estimated cost for such structures is dependent on the total weight of materials. In relation to this, its assumed only the weight of materials in relation to steel and concrete. The table below indicates the total cost of materials defined in ton.

8.1 Reference offshore floating wind platform; CSC-Semi

The UMain-Volturnus 15MW.

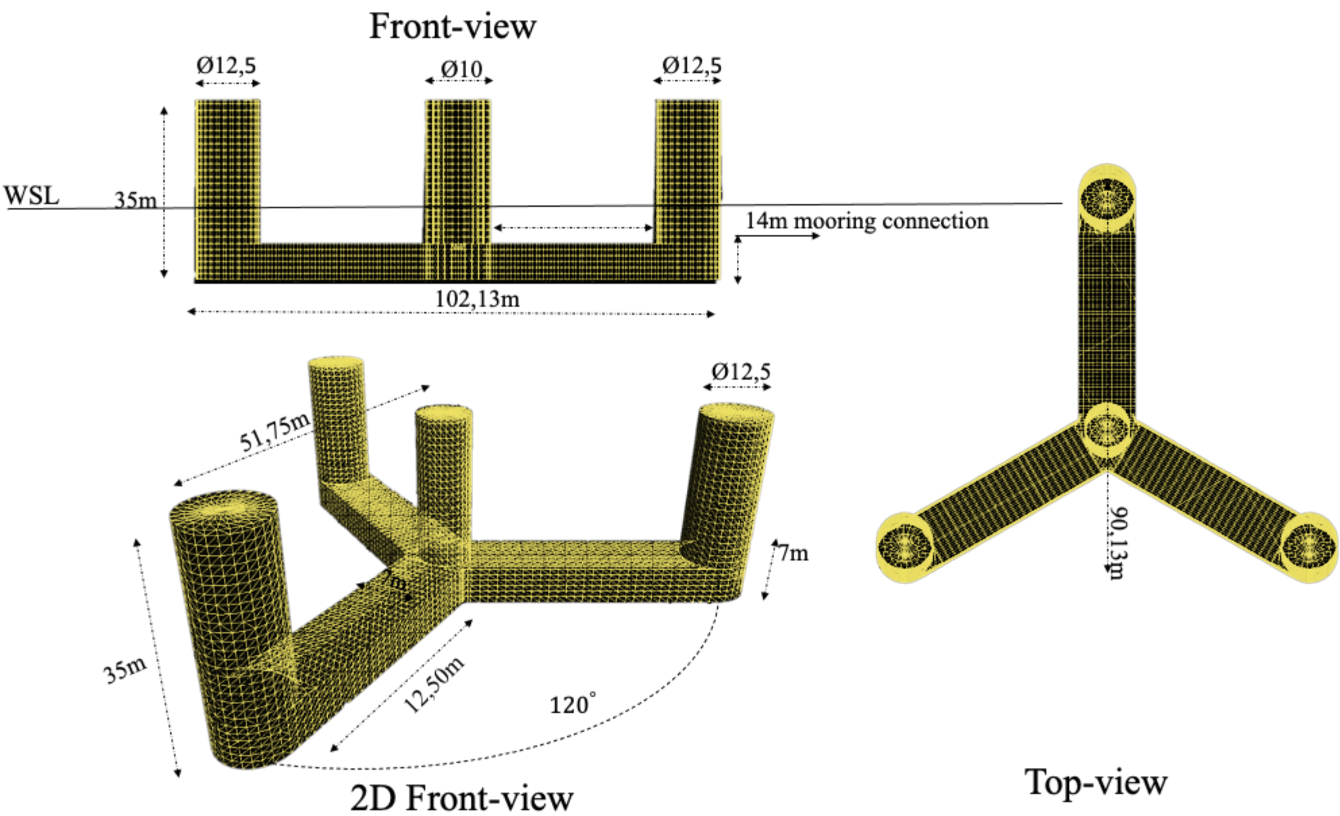

Figure 18 *illustrates the platform structure CSC-semi;* UMain Volturnus *15MW and the is constructed up by four columns. The mooring attachment are at the lowest bottom on each column angled at 120 degrees. The illustrated sketch is redesigned from Orcaflex and is designed by the author LJBT. The measure of dimensions is done with traditional power-point.*

The chosen reference structure in this thesis is the CSC-semi; Umain Volturnus 15- MW. The platform design is developed in a collaboration between University of Main and NREL. The model is a design meant for academical reason. The formation of structure is based on four columns, three outer and one in the center (seen in fig. 19). The other columns are oriented 120 degrees around the center column where the tower interface is constructed. The total weight of the platform is respectively 20206 ton according to NREL (Christopher Allen et al, 2020, s. 6). The ballast seawater corresponds to 56%, construction steel 19,37%, concrete 12,44%, tower interface 0,5% and 11,7% of other materials. In relation to other materials, its unfortunately not defined by the author (Christopher Allen et al, 2020, s. 6) Moreover. the exact specific steel is not defined either, but its assumed construction steel possible S430 or S 355. The table. 1 provides the properties of total weight of the CSC-semi platform.

Table 1 *is the dimension of the semi-submersible platform based on NREL report* (Christopher Allen et al, 2020, s. 6).

Input properties of the US main:	**Values**	**Units**
Hull displacement (total weight)	20206	Ton
Hull construction steel mass	3914	Ton
Tower interface mass (concrete or steel)	100	Ton
Ballast mass (Fixed/Fluid)	2541/11300	ton

8.2 Reference turbine IEA RWT- 15 MW.

IEA- RTW-15MW Turbine.

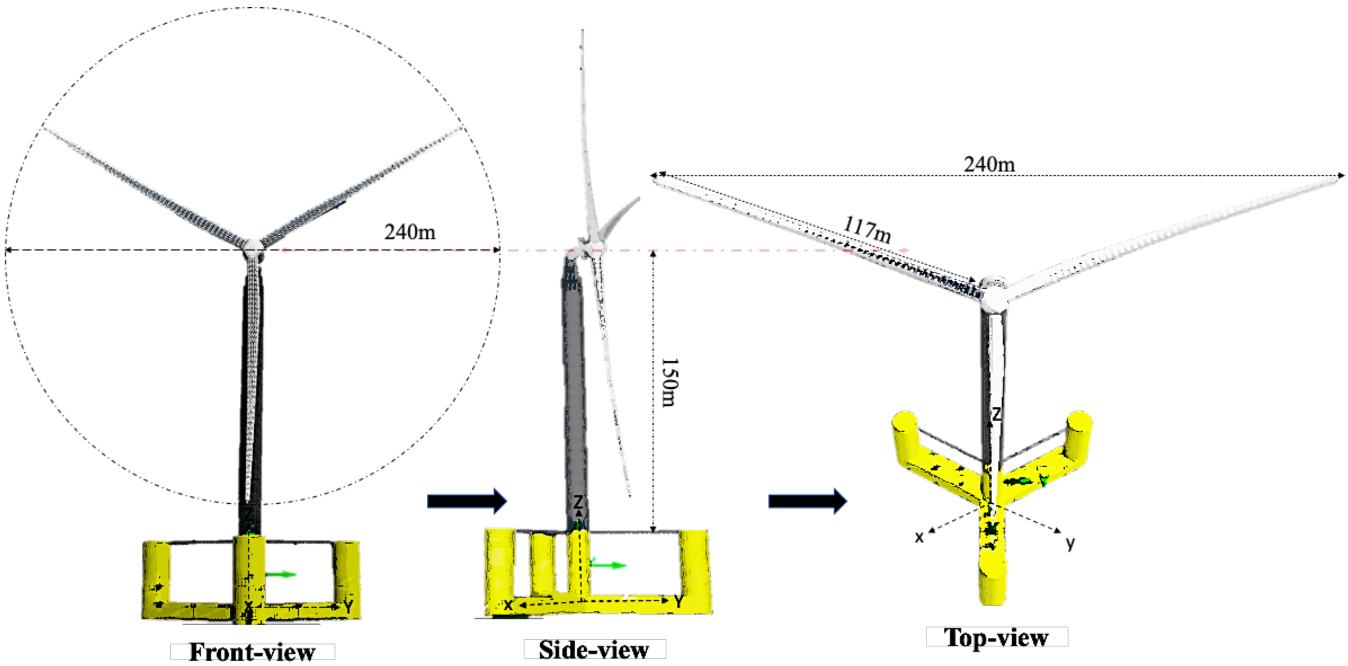

Figure 19 *Illustrates the turbine seen form front- view, side- view and top- view. The illustrative design is developed by the author from Orcaflex. The turbine has a roto diameter of 240m and hub height of 150m. The blade is measured to 117m.*

The reference turbine used in this thesis is the IEA RWT-15MW with a rotor diameter of 240 meters. The turbine, however, is not a real scale model but is purely meant as a research model for investigation of the next generations. The shape and design is developed as an collaboration between University of Denmark, National renewable energy of laboratory, the international energy agency (IEA) and finally the U.S. Department of Energy (Evan Gaertner et al, 2020, s. 19) The upscale of this turbine is meant for the next generation turbines due to its enormous size. The power coefficient (cp) for this model is evaluated at 0.489 and defined by the report (Evan Gaertner et al, 2020, s. 19). Generally, for real turbines the average wind capacity is between 30-40% measured over one year period (Luvside, 2020) However, the expected lifetime for traditional turbines is 20-25-years without any damage or any issues regards to operation and maintenance (Tyler stehly et al, 2019, s. 20)

8.3 Hub, generator, and nacelle.

The illustrated fig.21 presents the hub shall (1), generator (2), and the nacelle/ shaft (3) in the following order form left to right. The design is a 3-dimensional CAD- model and is an academic concept according to IEA report (Evan Gaertner et al, 2020, s. 19). The hub is configurated as a hollow steel shell meant for three turbine blades oriented in a 120° angle. The generator is designed as a combination including turbine rotor, stator, generator rotor and the shaft. The generator rotor and shaft are connected into one unit and has tilt upwards of 6° angle. The total defined generator weight is 317.57 ton according to (Evan Gaertner et al, 2020, s. 31).

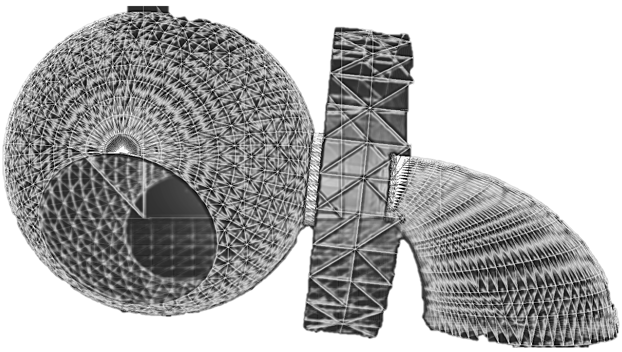

Figure 20 *shows the hollow hub steel structure (1), generator (rotor, stator) (2), nacelle (shaft) (3) with a upward 6° angle.. The design is added form Orcaflex by the author LJBT.*

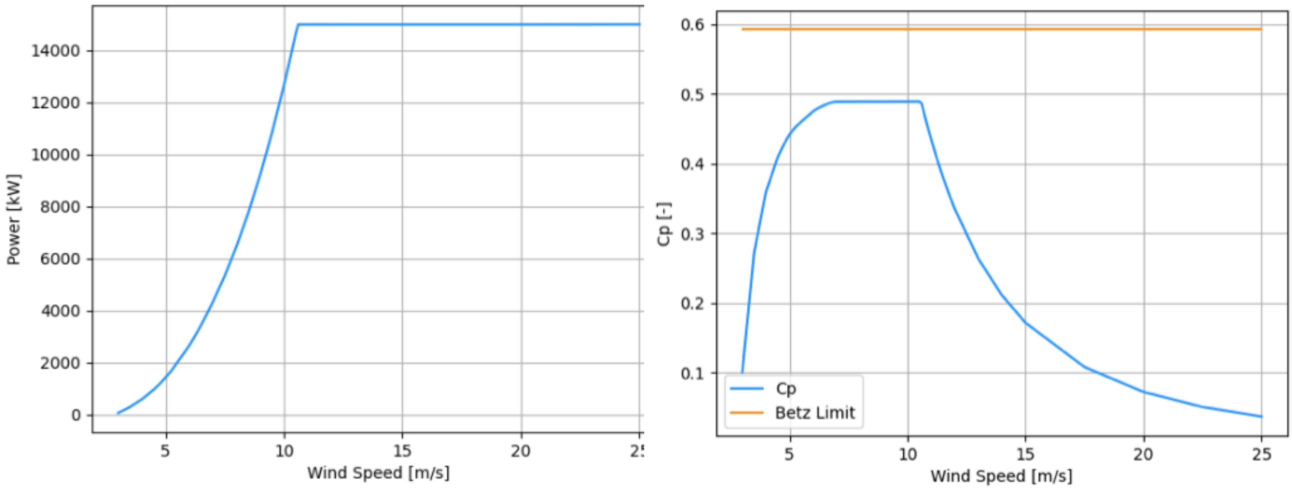

Figure 21 *illustrates the power rate curve and capacity power and both fig.22 is collected from (nrel.github, 2020)*

Table 10 represents the parameters of the RWT 15 MW turbine and provides the parameters and dimensions of total weight of structure.

Table 10 *provides the parameters for the 15 MW RWT turbine. (Evan Gaertner et al, 2020, s. 31).*

Turbine properties RWT-15 MW

Type	**Value**	**Units**	
Turbine class	IEC Class 1B		
Airfoil series	FFA-W3		
Rotor orientated	upwind		
Power coefficient	0.489		
Numbers of blades	**3**	**-**	
Power rate	**15**	**MW**	
Rotor diameter	**240**	**m**	
Hub height	**150**	**m**	
Rated speed	**10,59**	**m/s**	
Operational wind speed			
Generator type			
Rotor mass	385	t	20.5%
Nacelle mass	632	t	33.6%
Tower mass	860	t	45.8%
Total	1877	t	100%

8.4 Comparison of material cost between various turbines.

There are many turbines with various rated power defined by the cut- in and cut- out wind speed. The fig. 23 provides an overview of their power curves compared between 6-, 10-, and 15-MW. The power curves are a measure with the turbine’s full capacity power.

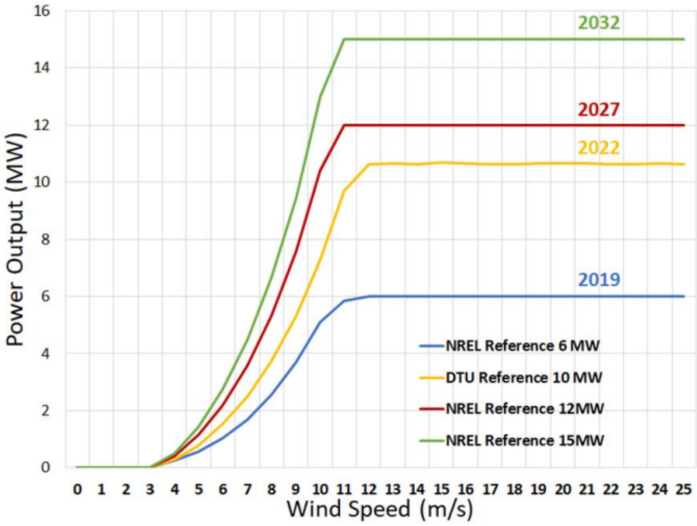

***Figure 22** (Walter Musial et al, 2020, s. 17)*

Table 12 illustrates a comparison between turbines with their various parameters and is compared between 5MW, 10MW and 15MW. The collections of data are form (Tyler stehly et al, 2019, s. Vi)

***Table 11** provides a comparison between turbines fNational renewable energy laboratory, 2020, s. vi) (Tyler stehly et al, 2019, s. Vi)*

Properties	**Comparison between turbines**		
Types	***NREL 5MW***	**DTU-10MW**	**NREL RWT- 15MW**
Power rate	*5MW*	10MW	15MW
Hub height	*90m*	119m	150m
Rotor mass	*115m*	230.7t	1017t
Nacelle mass	*110t*	446t	
Tower mass	*240t*	628.4t	860t
Total mass	*347.5t*	1305.1t	1877t
	Ref.	**Ref.**	**Ref.** (Even Geertner et al, 2020, s. 5)

Therefore, it has been made a cost comparison based on the materials cost and evaluated between three individual turbines rated by their power, such as 5MW, 10MW and 15MW. The graphs show the weight of rotor, nacelle, and tower. The evaluation is based on the weight of construction steel. The marked price of steel today is 1084 $/per metric tons (Focus-economics, 2023). The estimation is given in $/kg

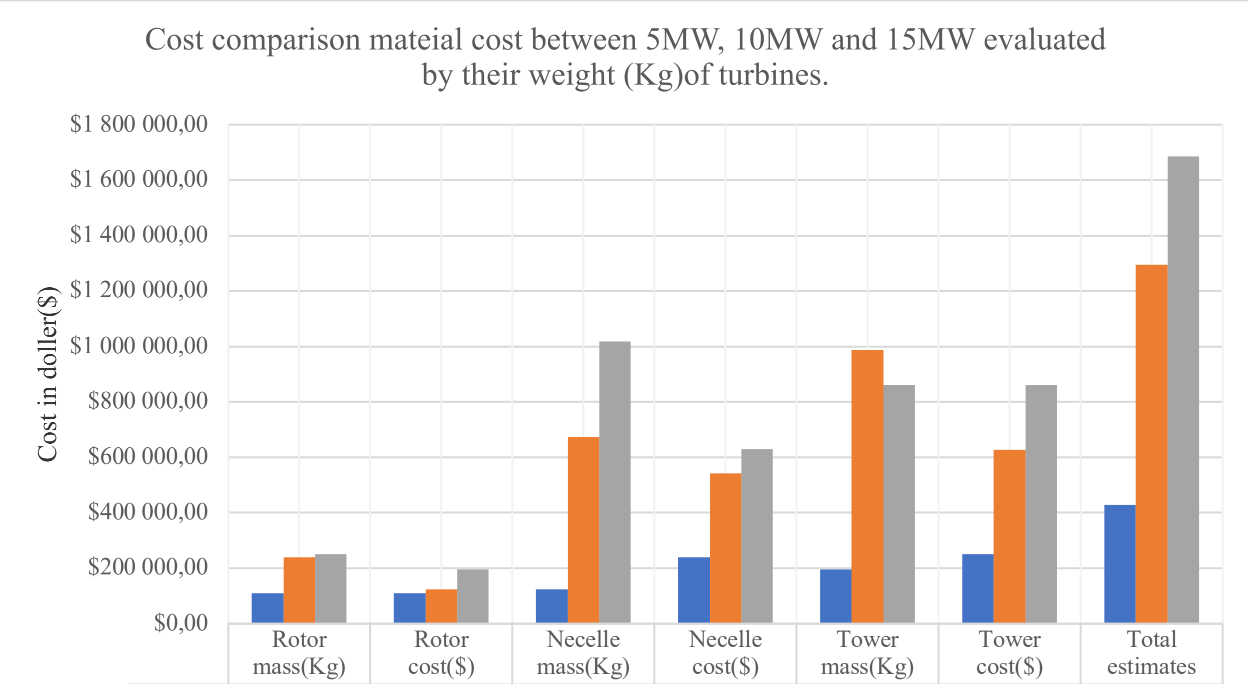

	Rotor mass(Kg)	Rotor cost($)	Necelle mass(Kg)	Necelle cost($)	Tower mass(Kg)	Tower cost($)	Total estimates
5MW	110000	USD 110 00	123000	USD 240 00	195000	USD 250 00	428000
10MW	240000	USD 123 00	674000	USD 542 60	987000	USD 628 49	USD 1294 0
15MW	250000	USD 195 00	1017000	USD 630 88	860000	USD 860 00	USD 1685 8

Graphs 1 *shows a cost comparison between 5MW, 10MW and 15MW only based on their cost of materials of construction steel. The total weight is in ($/Kg)*

9 The main mooring configuration system.

9.1 Introduction of the terminology mooring system and mooring hardware.

Introduction

In this chapter, the main mooring system will be described and categorized in relations to each mooring configuration systems. The purpose is to gain further knowledge based on their various configurations and will be deeply described in this chapter.

9.2 Catenary mooring system – Slack.

Catenary mooring is a configuration design where the mooring lines are designed with a slack (curvatures) and spread like arrays onto the seabed floor. The large curvature lines are quite common for this catenary configuration and are commonly designed with drag embedded anchors (see chapt.17.5). In relation to catenary configuration, the design is suitable for horizontal loads but not for vertical loads (J.M.J. Journee et al, 2001, s. 412) The configuration system is very dependent on the weight of the chain lines for developing a high restoring downwards force meant stabilizing structure (Monfort, 2017, s. 4). However, the mooring lines could also be mixture of both chains and fiber ropes in the same line. However, since the chain links uses its total weight as a restoring force, the height of sea depth is very important for this mooring system. For this reason, the disadvantage of using this catenary system for shallow waters is that the capacity of chain lines would decreases according to (Xinkuan Yan et al, 2023, s. 1). This is because low levels of depth decrease the gravitational downward force and losses the anchors capability to withstand horizontal loads (Xinkuan Yan et al, 2023, s. 1). The illustrated figures. 24 illustrates the mooring system and shows the large slack and wide curvatures in the chain mooring lines. Therefore, various water depths and mooring length must be considered for this mooring configuration system.

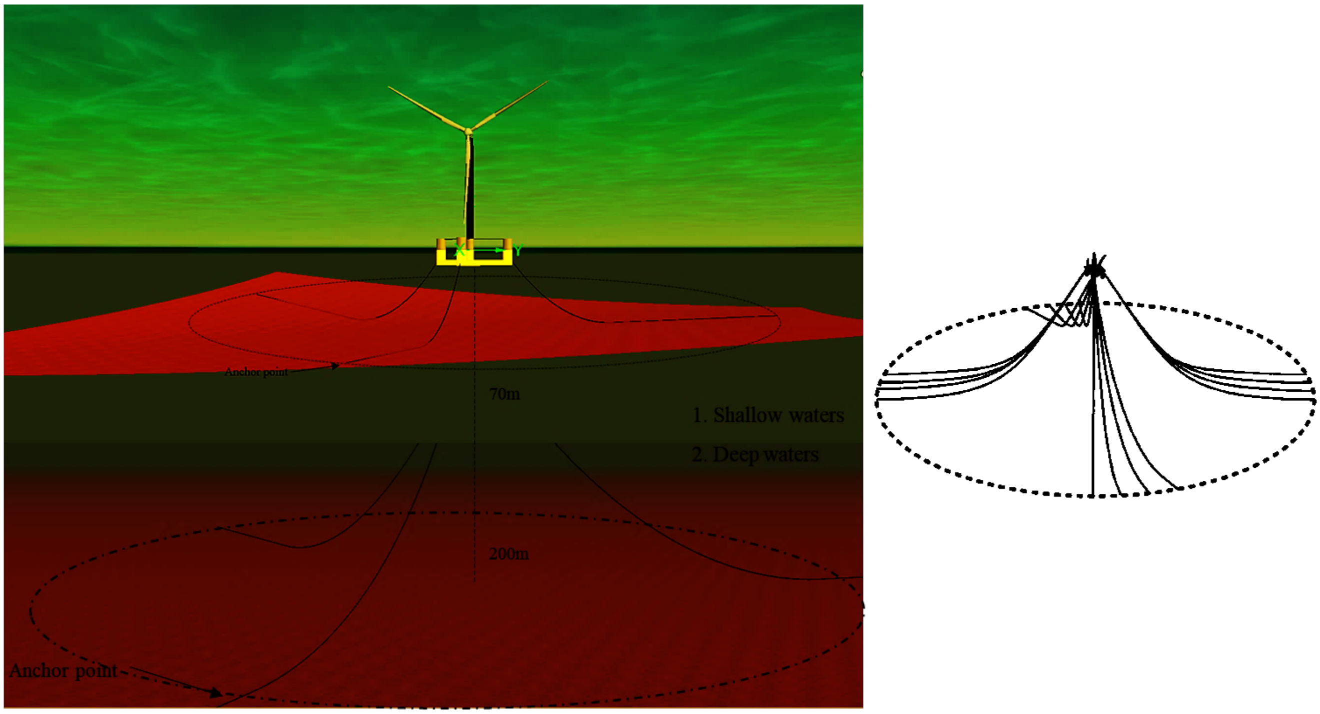

Figure 23 *illustrates the catenary mooring configuration system. As could be seen from the figures the mooring lines has large curvature of chain lines. The mooring lines could also be combined with fiber rope as a mix method. The first fig. is redesigned by the author LJBT form Orcaflex. The other illustration is added form* (abc-mooring.weebly, 2023).

9.3 Taut line mooring system- TLP

Taut line mooring (TLP) is based on a lightweight of taut/teel ropes and is also defined as pre-tension lines with no curvatures or spread tension lines. Therefore, the configuration would be defined as the opposite of catenary configuration design. The mooring system is suitable for both horizontal loads as to vertical force and is based on the elasticity in the lines (J.M.J. Journee et al, 2001, s. 412) Morover, the high restoring tension in the mooring lines is poportianall to youngs modulus and needs to have low material factor becouse the ropes would be damage (Monfort, 2017, s. 4). This based on and the tensioned lines the mooring lines are (Abc-moorings, 2023). The angled between the tension lines onto the seabed floor are angled at 30-40 degrees (Abc-moorings, 2023). For this kind of configuration, the tensioned mooring lines could be based of several lines as many as six lines. The lines are stretched to the anchor points as showed in the illustrated fig. 25.

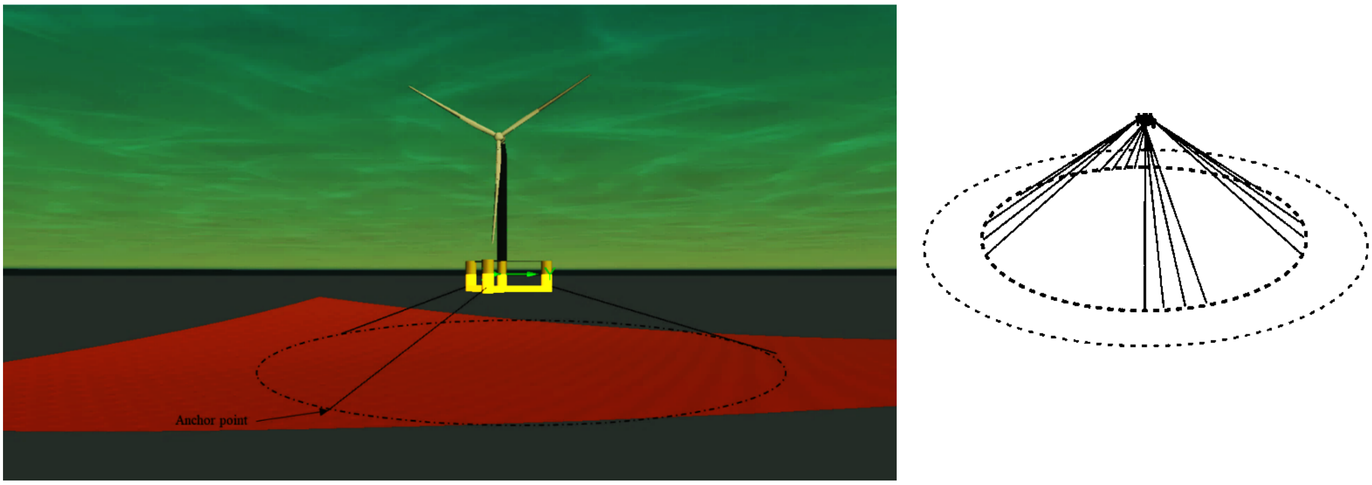

Figure 24 Illustrates the taut mooring configuration system as could be seen from both fig. the mooring has no slack but strait lines in each direction. The first fig. is designed by the author the other one is added form (abc-mooring.weebly, 2023)

9.4 Vertical Tension leg mooring system – TLP

The vertical tension leg (TLP) mooring is based on vertical heavy steel wires or cables with large braces on the seabed. The mooring configurations is defined for deep water installations (Weiwei Zhou et al, 2023, s. 1). The importance with this mooring configuration is that the wires needs be starched (Tensioned) for the purpose of creating large tension between the platform and the anchors. The vertical mooring lines is also designed with some angle for the purpose of obtaining both vertical as to horizontal offset forces caused by the wave loads acts on the stabilizing platform (Abc-moorings, 2023). The TLP is illustrated in the fig. 26.

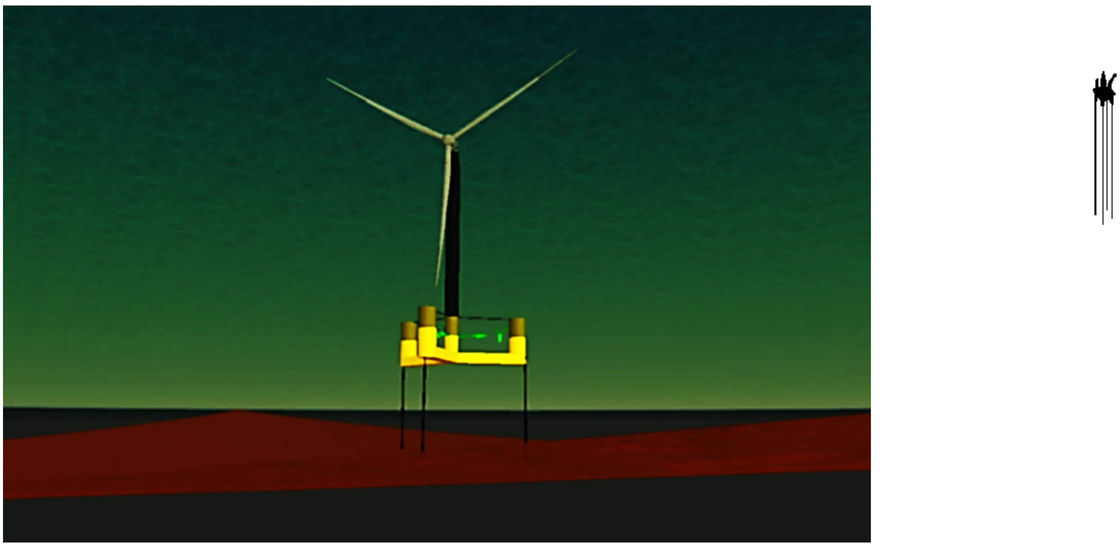

Figure 25 Illustrates the vertical tensile leg mooring lines between the structure and seabed floor. The first fig.26 is designed by the author LJBT from Orcaflex. The other illustration is added from (Iñigo Mendikoa Alonso, 2021, s. slide 5).

9.5 Hexagonal farm layout arrangement

The concept with shared anchoring and mooring lines is based on an arrangement where the mooring lines is formed in various formations or arrays between OFWTs. The idea of the concept is that one anchor is shared equal between a multiple set of FWT in contrast to many separate single ones (Rahul Chitteth Ramachandran et al, 2021). For this reason, there are many formations and variety of farm layouts, however, some layouts is investigated by (Matthew Hall & Patrick connolly, 2018) and (Fontana, 2019) as possible arrangments. These shapes are defined as triangles, squares, and hexagonal formation. The many advantages with the concept are mainly to reduce the material cost by reducing the total amount of anchors in the mooring arrangements. Since the anchor is very expensive in relation to fabrication and in the installations process. Therefore, the concepts potential to make cheaper and more sustainable mooring arrangement and more sustainable solution. Secondly, the re-connection in the (O&M) for repair, failure, and removal with the heavy chains between the anchors and lines could also be reduced according to (Rahul Chitteth Ramachandran et al, 2021, s. 19)

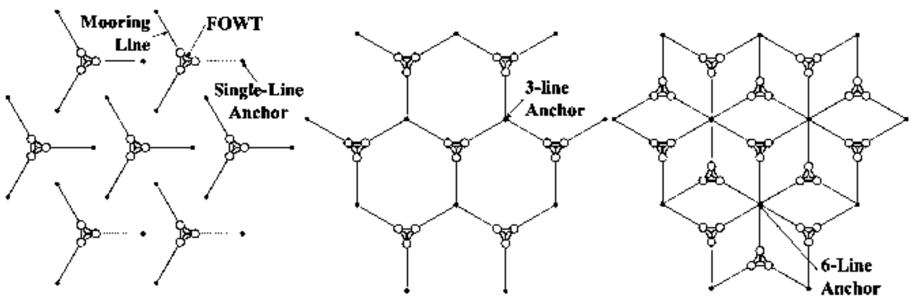

Figure 26 *seen form left single line, hexagonal 3 lines and finally 6 lines (Fontana, 2019)*

Nevertheless, the shared anchoring arrangement in contrast to many separate OFWT is that the total amount of lines, mooring length, anchors, and spacing in the mooring arrangement between turbines is minimized according to (Matthew Hall et al, 2018). However, a further reduction of weight and cost would also be done by changing the mooring material to alternative fiber ropes instead of chains or steel wires according to (Samuel Wilson et al, 2021, s. 11) Since a single OFWT normally has three anchors per turbines. Therefore, also mentioned by (Matthew Hall & Patrick connolly, 2018, s. 8) the total reduction percentage of anchors with this concept would be decreased to 36% (Matthew Hall & Patrick connolly, 2018, s. 8) in contrast to many single OFWT. Based on the advantages, the concept, the mooring tension could optimize the dynamic performance for sharing the tension between a multiple set of OFWTs. Since the many lines in contrast to one will reduces the tension and creates less tension in the mooring lines.

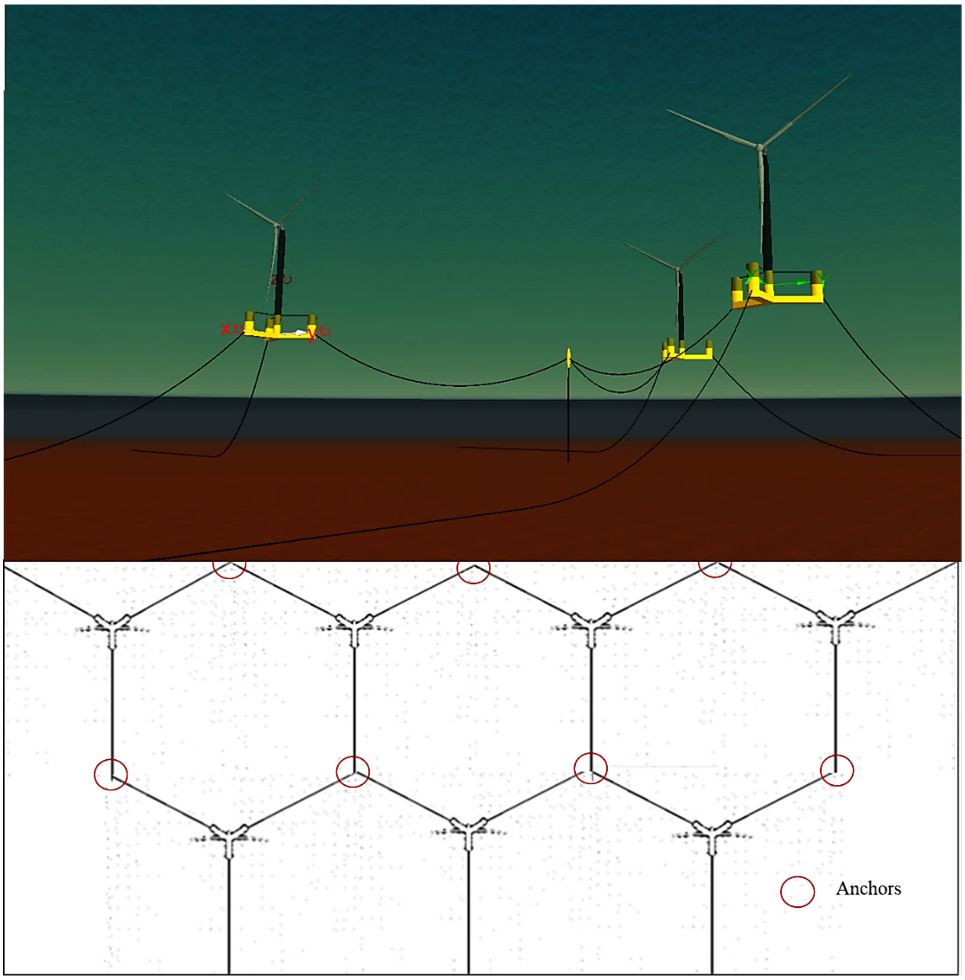

Figure 27 *Illustrates the shared mooring arrangement with a combination with mooring buoy and shared anchor in the center between the three OFWT. The mooring buoy acts as a connecting point and tension reliver. Each illustration is design from Orcaflex by the author LJBT. The figure below represents an overview of the hexagonal farm layout.*

The illustrated fig. 28 above shows the total hexagonal farm layout and the mooring arrangement Semar AS and (Matthew Hall & Patrick connolly, 2018) have investigated as a possible innovative solution for further cost reduction of innovative solutions. For this reason, by estimating the shared anchor efficiency in the farm layout, according to (Evgeniy Dimkin at DNVGL noble Denton, 2019, s. slide 17) is found by the equation:

$$\left(1 - \frac{Number\ of\ anchors\ in\ shared\ anchore}{Numbers\ of\ anchore\ in\ standard\ windfarm}\right) = \eta^{`} \tag{33}$$

(Evgeniy Dimkin at DNVGL noble Denton, 2019, s. slide 17)

9.6 Shared taut mooring buoy arrangement with two turbines.

The taut mooring surface buoy with vertical lines is an arrangement where the buoy is the connection point and holds the platform in position. The arrangement is developed with horizontal vertical load anchor (Smith, 2009). As mooring materials rope or steel wires are use as lines. The concept with this arrangement of sharing mooring line has in some degree been tested as a pilot project. This for evaluating the performance in the dynamic response of the mooring lines and as a total system. The concept is tested by (H Munir et al, 2021, s. 5) at University of Stavanger and (Samuel Wilson et al, 2021, s. 11). However, these tests were only performed with shared wire lines between two FWTs and no mooring buoy. In this connection the concept will therefore further be investigated in this thesis, but with a submerged mooring buoy lowered beneath sea level. The buoy is lowed beneath water level for eliminating the large shift forces and for decreasing the tension in the mooring lines (Torbjørn Herberg Roksvaag et al, 2021, s. 25) and are further described in see chapter 12.

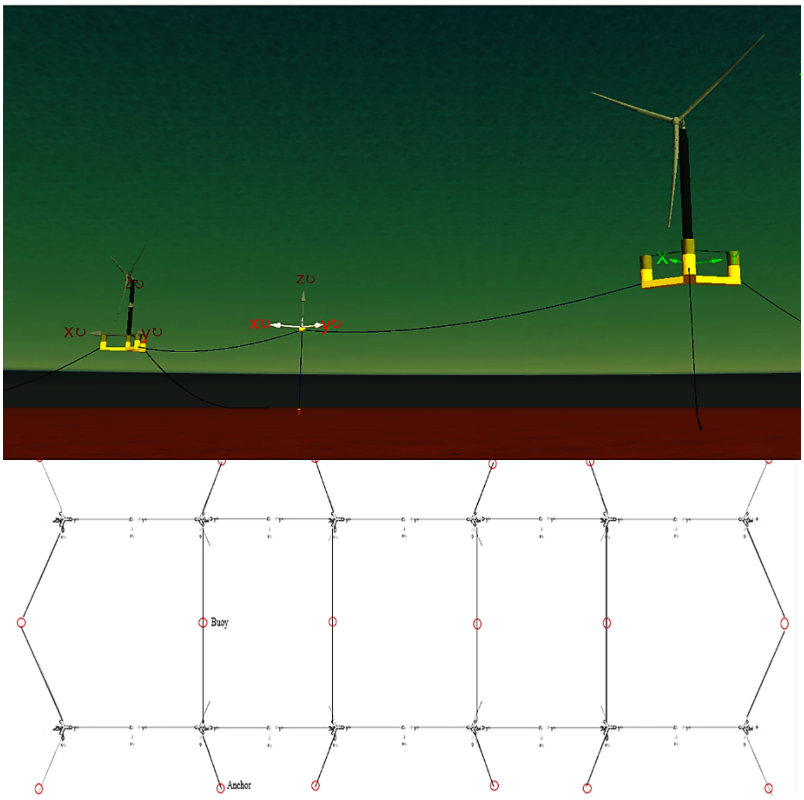

Figure 28 *Illustrates the shared taut mooring line of farm layout (row) based of steel wire or fiber rope also known as taut mooring lines with marine float (buoy). This mooring configuration system will be used in the response analysis in the case study for SNII. The figures are designed by the author.*

The illustrated fig.29 provides the two platform with a mooring buoy in the center with a vertical tensioned line connected to a vertical anchor (VLP) in six degrees of freedom.

10 Mooring hardware components and dynamic power cables.

Introduction

In this chapter, several mooring hardware will be deeply described for the purpose of developing further knowledge based on the several components in the mooring installations. This in order to find the cost for each component. This chapter will include the cost price for every mooring hardware with a deep description of their configurations. Since some of the cost components are provided in pound or euro it will be converted to a common currency, namely dollar ($) and with today's inflation rate.

10.1 Mooring hardware cost.

In relation to the cost of mooring hardware and configuration, it has been developed a cost comparison added from another investigated work based on their founding's herby (Ågortnes, 2013, s. 67) The cost comparison shows TLP, TLB, Hywind and Wind float. The added numerical data is based on their estimations of various mooring configurations. The estimates are converted to today's currency in dollar ($) and with today's inflation rate.

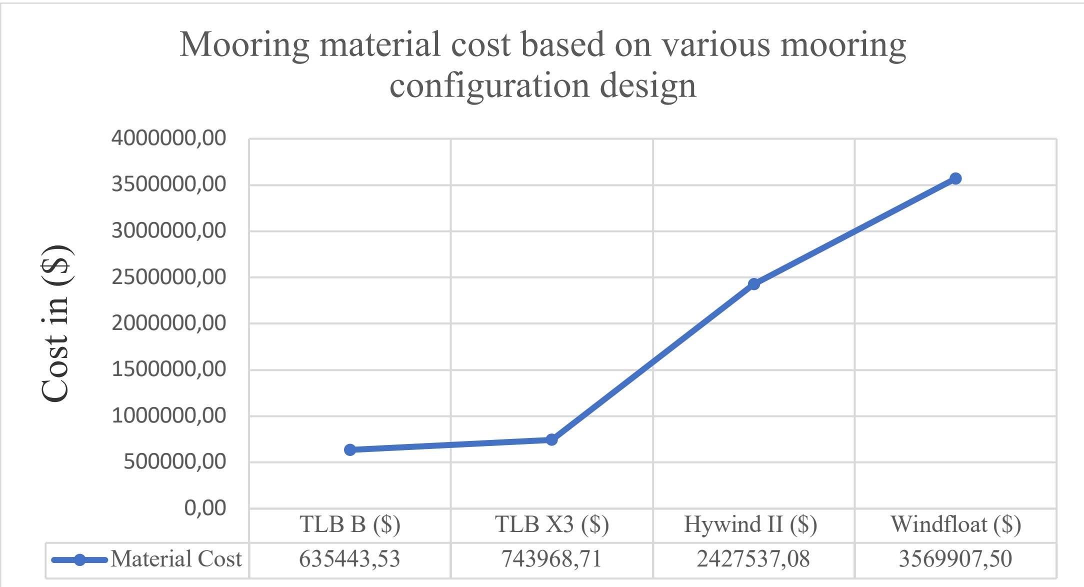

***Graph 1** illustrates the cost comparison between several mooring configuration weighted by the mooring cost* (Ågortnes, 2013, s. 67)

10.2 Chain

Chain moorings lines is widely used for deep and shallow water-installations. The relation is due to its good quality for obtaining large tension loads, shared toughness, and resilience for abrasion on the seabed floor (Wei-Hua Huang et al, 2021, s. 4). The tension strength in the chain links is factor which are based on the gradings of steel. For this reason, each grad can be divided into six class grades based on R3, R4, R4s, R5 and R6 and could be referred to DNVGL-ST-0437() and DNV-OS-E302 (Det Norske Veritas, 2013, s. 22) Moreover, chains links is divided into studded link and studdles link (seen in fig. 30) with different configurations in the coils. Nevertheless, other parameters that has an impact in the choice is the tensile strength, diameters, and coil (opening size) (Reardon, 2023). The cost of chains is dependent on the weight of steel, length, and formation/shapes (coils) of the chain links. The advantages with using chain in shallow waters is based on the chains high stiffness, low elasticity, and maximum breaking load (MLB) (Det Norske Veritas, 2013, s. 22) However, studded link is not much used as mooring lines, but typical used as mooring lines for permanent uses (). Nevertheless, since is heavier than studdles chains the weight of mooring lines would increasing (Jump, 2021, s. 21)The cost price for chain is dependent on the steel wight per ton, but the price for 100mm is between 700$/ton-800 $/ton (Made-in-China, 2022). Moreover, the cost for studdles link is relatively cheaper than studded link because of less material. According to the steel price of R5 180mm is 649kg/m in table 12 it has been used the marked value of steel 1084 $/ton (Steelbenchmarker, 2023, s. 2)

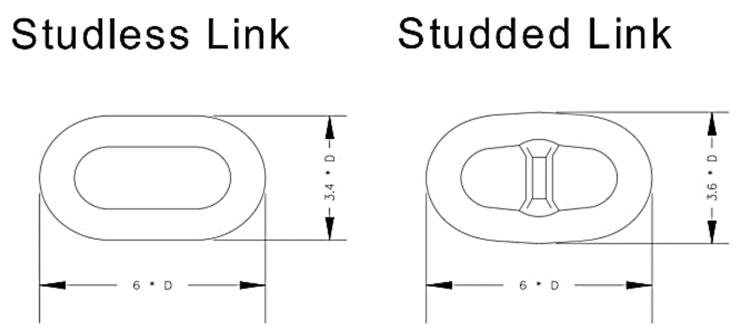

Figure 29 *Illustrates the different shape of studdles link and studded link.*

The mooring chain has two different shapes and configurations such as studdles and studded links illustrated in the fig.30. The table below defines the grads R, maximum breaking load (MBL), and cost prices based on marked value of steel 1084$/ton.

Table 12 *shows the grade of chain links and the multiplication factor C. The MBL for the gradings and assumed price range between.*

Chain	Chains Grade	C-factor	Minimum braking load (KN)	$/ ton	Sources in relation to the steel price $
Studdles	*R3*	0.0223	14.8	1084	(Steelbenchmarker, 2023, s. 2)
Studdles	*R3S*	0.0249	18.0	1084	(Steelbenchmarker, 2023, s. 2)
Studdles	*R4*	0.0274	12.6	1084	(Steelbenchmarker, 2023, s. 2)
Studdles	*R4S*	0.0304	21.6	1084	(Steelbenchmarker, 2023, s. 2)
Studdles	*R5*	0.032	31.9	1084	(Steelbenchmarker, 2023, s. 2)

10.3 Steel wires

Steel wires is categorized into two different groups based on their revolved strands in the wire lines. There are many shapes of wires in relation to the many strands in the wire. The construction shape is (6x19)- or (6x36)-strands but could also be a mixture with fiber core as well (see fig. 34). The advantages with wire ropes are due to its light-wight and high tensile stiffness. The stiffness in the wires could be higher than chains and have the same breaking load (Nordvik, 2019, s. 6) In relation to the strands in the steel wire the tensile strength could restore up to 90% of the tensile strength according to DNV(). Moreover, its good resistance to corrosions (Ronson, 1980) However, the strength in the line is dependent on the number of strands in the wire. Since, wires are a good alternative in contrast to chains based on its low weight, equal strength, and cheaper price $/m. The illustrative fig. 31 and table 13 represents some chosen dimensions of steel wires with various dimensions and maximum test load. The steel wires follow a recruitment standard DNVGL-OS-E301and is related to the strength, braking loads, and DNVGL-OS-E304 related to corrosion. The price is based on the market value of steel 1084$/ton (Steelbenchmarker, 2023, s. 2)

Figure 30 *provides the design of side view of Six strands (left) and Spiral strands (right)* (Ronson, 1980)

Table 13 *illustrates some parameters of their nominal diameters of wires* (Vryhof manual, 2015, s. 17).

Types of steel wire Group	Nominal diameters (m)	Breaking load KN	$ per/ m	Ref. sources
Steel wire fiber core 6x 19	0.064	3360	1.084	(Vryhof manual, 2015, s. 17)
Stee wire 6x19	0.102	7799	1.084	(Vryhof manual, 2015, s. 17)
Steel wire 6x36	0.127	11134	1.084	(Vryhof manual, 2015, s. 17)
Steel wire 6x36	0.140	12925	1.084	(Vryhof manual, 2015, s. 17)

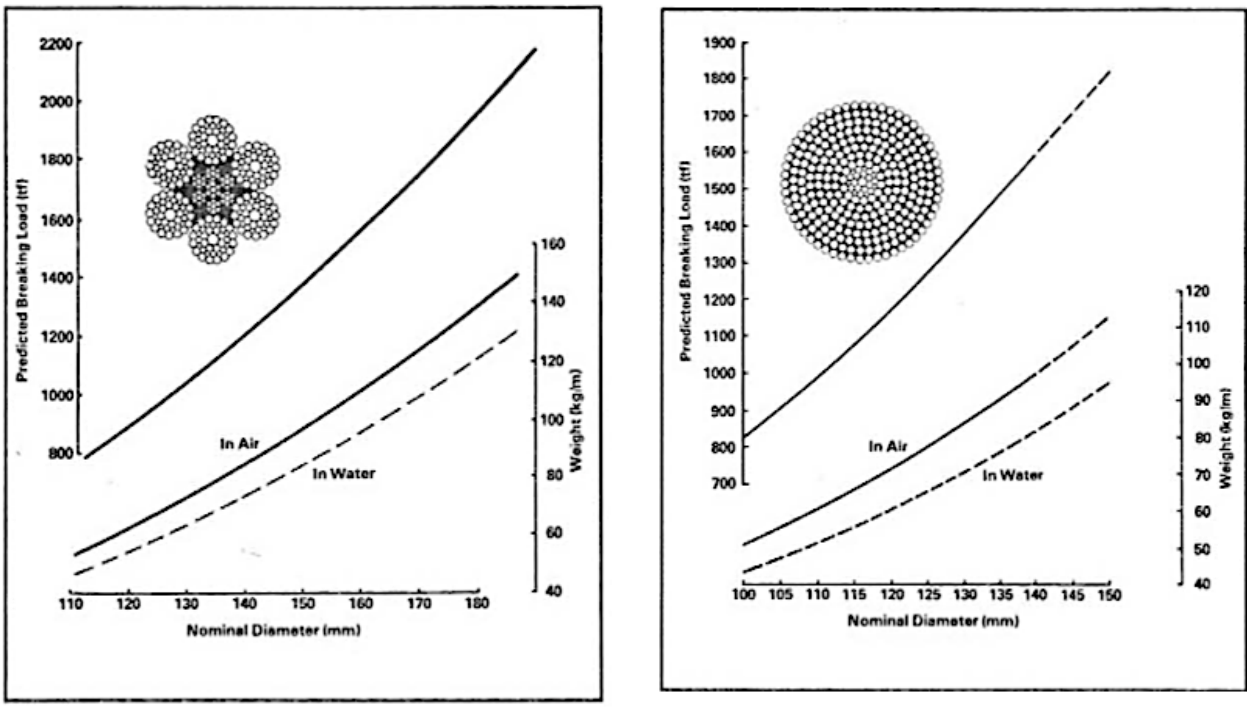

Figure 31 *Illustrates the relationship between the max. braking load of six strands and spiral in water and in air. The relation between the nominal diameter and weight (Ronson, 1980)*

10.4 Synthetic- fiber ropes

Synthetic fiber ropes are based of many layers of yarn and materials like aramid, HMPE, LCP, polyester in the rope (Espen Oland et al, 2017, s. 1) Nevertheless, the rope is configurated with core, strands, yam, and cores revolved to one unit of a rope. Thus, some of the common materials that is used as mooring materials are nylon, polyester, and polypropylene (Xu, 2015, s. 33) Generally, fiber ropes are seen as a comparable material because of its low weight, low price, and a maximum breaking strength (MBS) up to 70% of the rope (Espen Oland et al, 2017, s. 2) Fiber rope, such as polyester is seen as a preferable material, because it could operate with a constant tension of 15%, 30% and MBS up to 60% (john F. Flory et al, 2004, s. 4). Synthetic fiber ropes use standards DNV-GL-RP-E305/ (304) for the maximum tension load The Braking strength for fiber rope is between 1000-4000 N/mm^2 according to (Xu, 2015, s. 33) Additionally, the cost price defined by (Ågortnes, 2013, s. 73) is estimated to a price range of 602 - 617 £^{2013}/m (Ågortnes, 2013, s. 73) and in today's currency 962.74 - 991.84 \$^{2023} per/m. The fig. 33 and the table 14 represent some parameters of fiber ropes given by their dimensions.

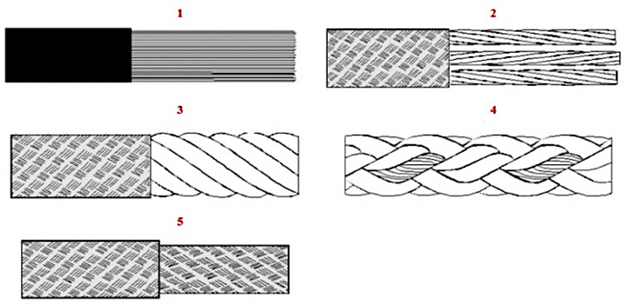

***Figure 32** provides the various configuration of fiber mooing lines baes on their revolved strands* (Pham, 2019, s. 32)

***Table 14** provides some properties of synthetic fiber ropes along with their breaking loads.*

Synthetic fiber Polyester	Nominal diameters (m)	Breaking load KN	$ per/m	Ref. sources
Polyester	0.113	3723	962.74 - 991.84 \$^{2023}	(Vryhof manual, 2015, s. 146)
Polyester	0.183	10830	962.74 - 991.84 \$^{2023}	(Vryhof manual, 2015, s. 146)
Polyester	0.227	17261	962.74 - 991.84 \$^{2023}	(Vryhof manual, 2015, s. 146)
Polyester	0.245	10307	962.74 - 991.84 \$^{2023}	(Vryhof manual, 2015, s. 146)

The fig. 34 illustrates the comparison of their maximum breaking load (MBL) based on various materials polyester, chains, and spiral strands of steel wires.

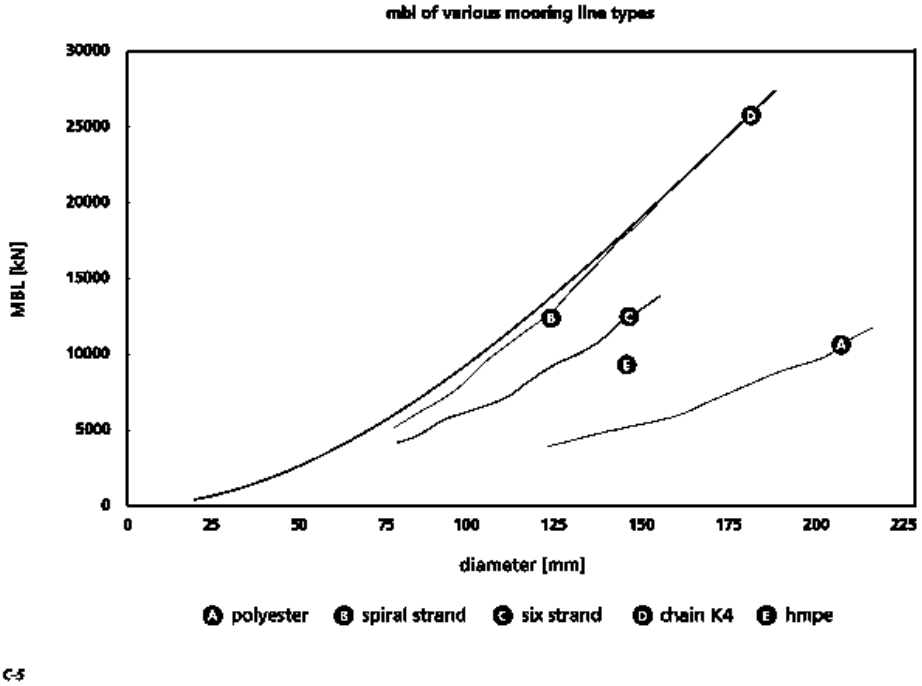

***Figure 33** illustrates the various mooring material and diameters of their maximum breaking loads (Vryhof manual, 2015, s. 146)*

10.5 Drag embedded anchors.

Drag embedment anchors is normally a very heavy design and are developed with a hook, as could be seen in fig. 35 and table.15. The installation process is that the anchor is dragged along the seabed for purpose of develop enough resistance until the anchor's stopes (Vryof anchors, 2005, s. 10). Moreover, it could penetrate the soil fully or partly according to (Vryof anchors, 2005, s. 10). For this reason, the soil conditions are a major factor when it comes to the capacity performance for this type of design. Nevertheless, the anchor is both meant for clay as to sandy soil according to (Aceton , 2023) However, the drag anchor is only suitable for obtaining horizontal loads and not vertical loads, which is clearly mentioned in the manual by (Vryof anchors, 2005, s. 10). They also identified that there are some drag embedded anchors that are configurated for obtaining vertical load as well (Vryof anchors, 2005, s. 10). These anchors ranging inn sizes and for some could weights up to 15kg to 60 ton (Vryhof manual, 2015, s. 115) The cost range for this type; Stevshark MK5 is between 25.000 - 223.886 $ and are provided in table 15.

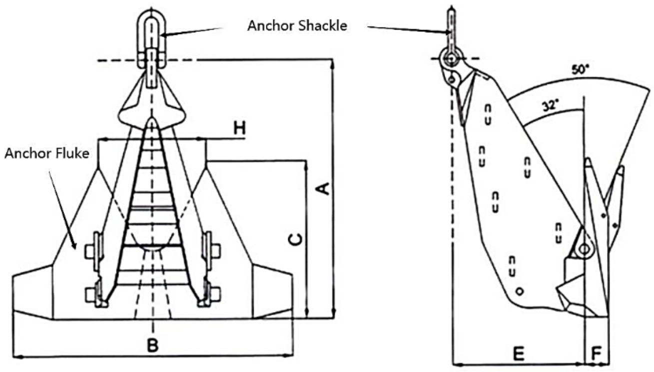

Figure 34 *Illustrated the drag anchor form top- and side -view* (solarpontoon.wixsite, 2023).

Table 15 *Various types of anchors and the following cost.*

Anchor types	Cost ($)	Ton	Source ref.
Drag-embedded	177.140.27USD	-	(Ågortnes, 2013, s. 73)
Stevshark MK5	207.488.5 USD	17	(Ågortnes, 2013, s. 73)
Stevshark MK5	223.886.1 USD	-	(Ågortnes, 2013, s. 73)
Stevshark MK5	25.000 USD	10	(Wentzell, 2023)

10.6 Suctions anchors - Vertical suction pile

Suction pile (Anchors) is based on a two-parts pile meaning the upper part are used as a connection between the lower part of the part section. The upper part is designed as a hollow pipe, seen in fig.36 The installation process is manly done in two stage processes. First, the self-weight penetration is done by the anchors own weight by penetrating trough the soil surface. Secondly, creating under pressure with a high-pressure pump on top of the pipe (T.T.Bakker et al, 2006, ss. 1-8) The suction anchors is capable to withstand both vertical and horizontal loads (Vryof anchors, 2005, s. 11). However, the configuration is very dependent on the resistance in the soil. This is becouse some clay and sand have different soil resistance. In this occasion, the soil increases the performance of the suction pile between the soils and the pile (Vryof anchors, 2005, s. 11). Therefore, the penetration depth and the resistance in the soil is therefore important (T.T.Bakker et al, 2006, ss. 1-8) However, the installation time of this design, and investigated by (Junho Lee et al, 2021, s. 2) could take up to 12 hours for a total completion (Junho Lee et al, 2021, s. 2) and is costly affair. In relation to the design and configuration, the anchor follows a required standard and instructions based on the process of installation. The vertical pile is defined in relation to DNVGL-RP-C212/(115), DNVGL-ST-E237, DNV-RP-C212, and for various soil conditions DNV-RP-E303 (Subseadesign, 2023). The cost range is between 676.826USD $-13.083.124USD$ defined in table. 16.

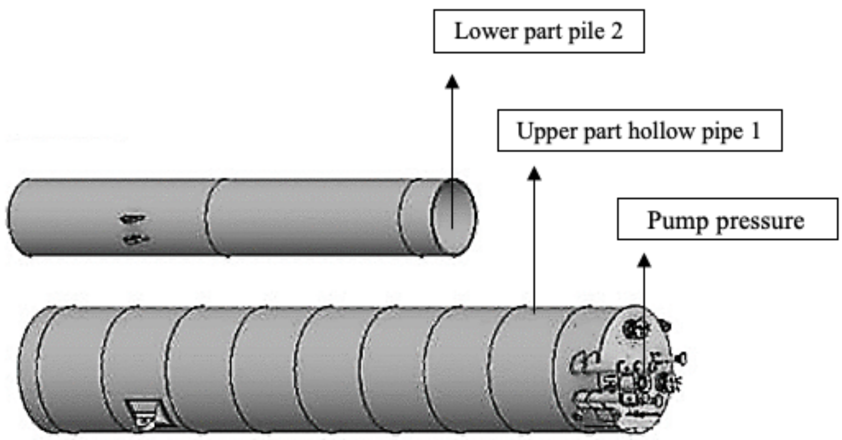

Figure 35 *Illustrates the pile and the hollow suctions (pile) anchor and is installed vertical in the soil (Acteon, 2022, s. 11)*

Table 16 *provides some cost estimates for some suction pile given by their weight. Reference is provided in the table.*

Suction anchors	Cost ($)	Ton	Units	Source ref.nr.
Suction pile	676.826.39 USD	50t	1	(Ågortnes, 2013, s. 73)
Suction pile	1.895.113.91 USD	140t	1	(Ågortnes, 2013, s. 73)
Suction pile	6.069.934.99 USD	-	1	(L. Castro-Santos et al, 2013, s. 43)
Suction pile	13.083.124.26 USD	-	1	(L. Castro-Santos et al, 2013, s. 43)

10.7 Vertical load anchor-VLA

The vertical load anchors (VLA) are similar to drag embedded anchors, but the main difference is that the configuration could obtain vertical loads and horizontal loads (Vryhof anchor , 2005, s. 11). Moreover, the penetration is deeper for this type of design in the seabed soil (Vryhof anchor , 2005, s. 11) The installation process is installed in a vertical position and rotated to obtain large resistance for fully restrain in the soil (L. Castro-Santos et al, 2013, s. 43) The configuration of the VLP is more sutible for clay than for sandy soil (Aceton , 2023) (Costra-Santos, 2013, s. 270). The other advantage with this type of anchor is that it's cheaper than drag embedded anchors, which are based on less weight of steel material that are used for this type (L. Castro-Santos et al, 2013, s. 43) (Costra-Santos, 2013, s. 270), The table. 17 provides some cost ranges.

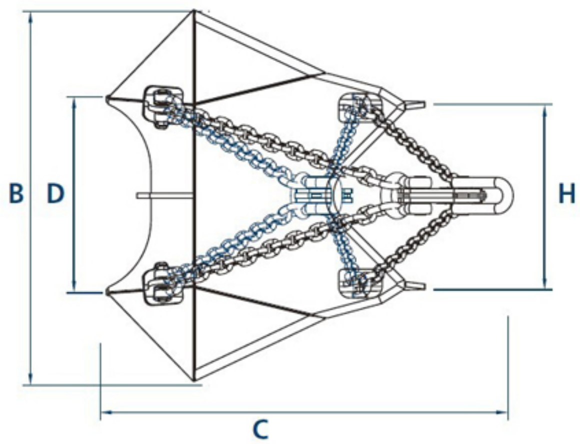

Figure 36*Vertical load anchor (VLA)* (jinbomarine, 2023)

Table 17 provides the cost price for vertical load anchor.

Vertical anchors	Units	Mass (ton)	Cost $(USD)	Source ref. nr.
Very small	1	-	186,54- 2810.62	(Fortress marine anchors, 2023)

10.8 Dead weight anchors

Gravity anchors is a designed that uses the deadweight of steel materials and could obtain vertical and horizontal loads purely based on the friction forces in the soil of its share strength (Vryhof manual, 2015, s. 17). The anchor obtains the resistance against the uplift forces caused by wave, wind, and current forces. However, this configuration design is not used for large installations or deep waters, but more of small installations (Vryhof manual, 2015, s. 17).

***Figure 37** seen from left to right, deadweight steel weights* (Vryhof manual, 2015, s. 17) and new type of dead weight design *(Offshore wind design AS, 2023)*

Table 18 provides the mass of anchors and some cost price.

Gravity anchors	Unit (s)	Mass (ton)	Cost $(USD)	Source ref. nr.
Steel shot	1	5.6t	77560	(Nick Cresswell et al, 2016, ss. 5-7)
Steel shot + frame	1	495t	59784.78	(Nick Cresswell et al, 2016, ss. 5-7)
High density concrete	1	18.1t	898.370	(Nick Cresswell et al, 2016, ss. 5-7)
High density Concrete	1	392t	1.070.800	(Nick Cresswell et al, 2016, ss. 5-7)
High density concrete	1	590t	67529.23	(Nick Cresswell et al, 2016, ss. 5-7)

10.9 Pile anchor and gravity torpedo pile

The vertical pile anchor is divided between driven pile and drilled pile designed as a hollow steel pipe which are installed either with a hammer or a vibrator drilled into the seabed soil (Vryhof anchor , 2005, s. 11) the pile penetrates deep beneath the slip surface (Dimitrios Loukidis et al, 2014) The vertical pile is designed for deep waters installations since the configuration could restrain vertical load as too lateral forces. Generally, the design could be used for clay and sandy soil conditions. However, the design is more suitable for deep water installation due to it large size for obtaining at a high performance, therefore not suitable for shallow waters (Vryhof anchor , 2005, s. 11). The gravity anchor is used as a hybrid anchor meaning as a combination of both vertical and horizontal loads. The installation process is totally based on its weight of the gravitational forces. The type is used for deep water installations (Vryhof anchor , 2005, s. 18).

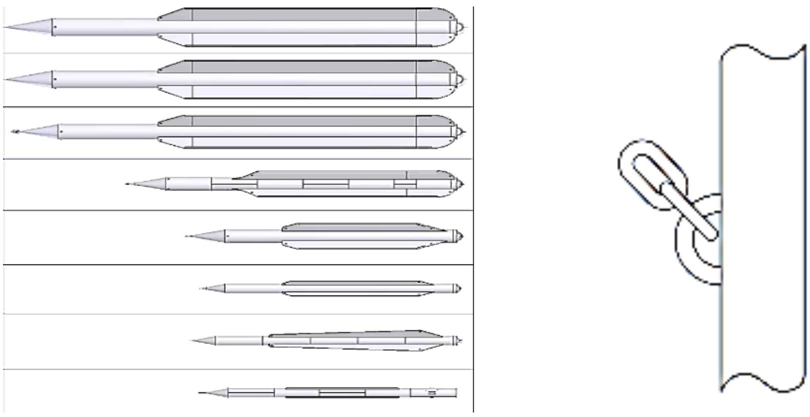

Figure 38 *seen from left to reight torpedo pile and pile* (Vryhof anchor , 2005, s. 11).

Table 19 provides the anchors mass and their cost.

Pile anchors and gravity torpedo pile	Units	Mass (ton)	Cost $(USD)	Source ref. nr.
Pile	1	5.6t	1291.212$	
		5,6t	77560$	
Torpedo anchor (2000$) rolled + scrap	1	9.8t	25086.45$	(C.D. O'Loughlin et al, 2015)

10.10 Diverse connection shackles

The several connection points for anchors, mooring lines, mooring buoy, platform structures are done with shackles **(1).** These connectors come in many shapes and formations as showed in fig. 40 (Vryhof anchor , 2005, s. 11). These types are link kenter type **(2),** link pear shaped **(3**), c-type **(4)** (Vryhof anchor , 2005, s. 11).

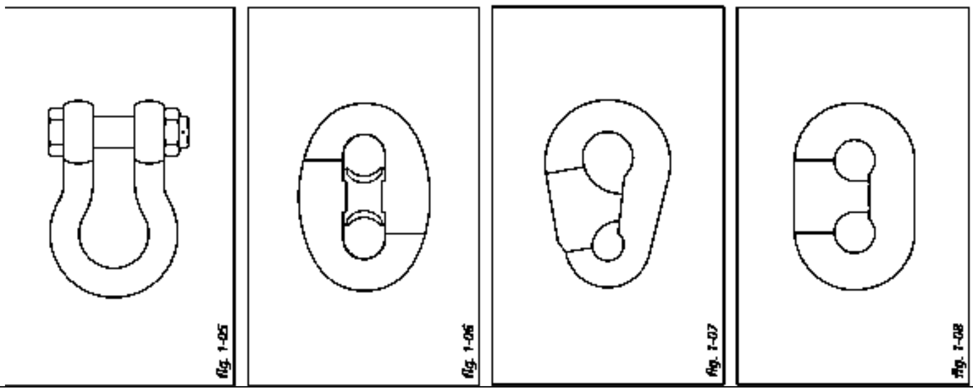

Figure 39 *seen form left, Shackles (1), link kenter (2), link pear shaped (3), c-type (4). (Vryhof anchor , 2005, s. 11).*

10.11 Marine buoy

There are several mooring buoys designed in various size and shapes. The large ones could range from 2,4-4 meters in height and ability to obtain a buoyancy up to 10kg- 100 tons (CRP subsea, 2023). From the illustrated fig.41are some of the design. The top of the buoy is the connection point where the mooring lines are connected. The table below provides some cost price for traditional steel buoy. The traditional mooring buoy is most sutible for shallow waters and with soil conditions such as mud, sand and gravel sefloor (PADI International Resort Association, 1996-2005). The morring buoy also reduces the tension in the mooring lines (Torbjørn Herberg Roksvaag et al, 2021, s. 25) and are used as tension relivers in the mooring lines.

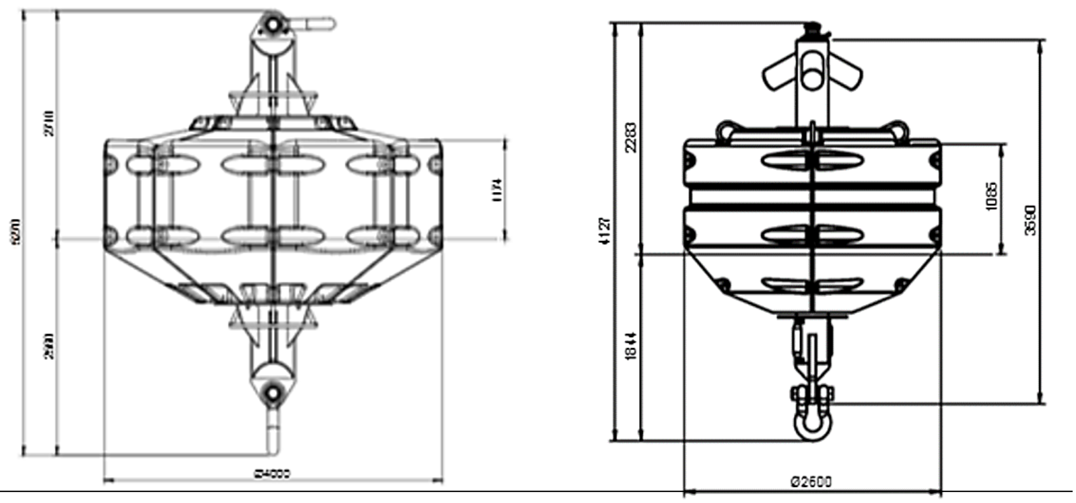

Figure 40 Illustrates two mooring buoys of AMR 7000 and AMR 7000 with different connection points of shape T *(hydrosphere.co.uk, 2014)*

Table 20 provides some types of mooring buoys and some cost price.

Marine buoys	Units	Mass (ton)	Cost $ (USD)	Source ref. nr.
PE/EVA cylindrical Foam filled buoys	2	Customized	100-3000	(Made-in-china, 2023)
Steel mooring buoys	1	1.2m	200-1000	(Alibaba.com, 2023)
Cylindrical steel buoy crucifix	1		100-5000	(Alibaba.com, 2023)
Subsea energy solutions	1	10ton		(Jump, 2021, s. 27)

10.12 Array electrical power cables

The power cables system also defined as dynamic cable system and defined as inter-array cables (Maria Ikhennicheu et al, 2020, s. 89). These cables are configurated between the turbines are defined in kilovolt (KV) and their volt-capacity ranges from 6.6-132 KV (Maria Ikhennicheu et al, 2020, s. 89) As illustrated in the figure a description to how the cables are configurated. The power cable used in the offshore wind turbines are between 33KV-66KV (Shayan, 2017)

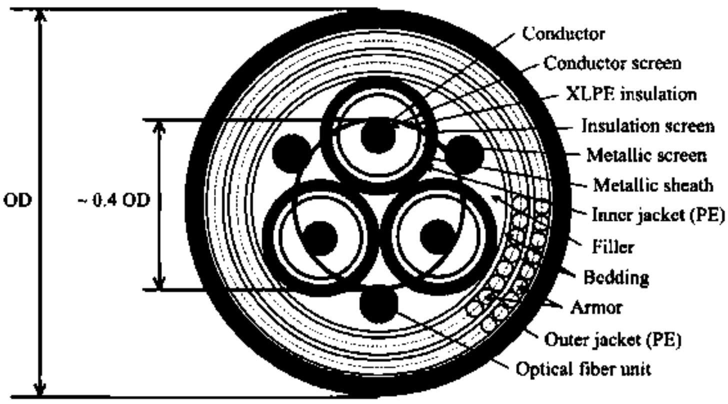

Figure 41 *illustrates the dynamic power cable and an overview of the inner part of the power cable (Twind offshore wind energy, 2021, s. 4)*

In relation to the cost estimates of dynamic power cable the equation. 36 needs to be calculated. The table below provides the units, which are needed in the estimation of cable costs. The table is added from Corewind (Maria Ikhennicheu et al, 2020, s. 89).

Table 21 *provides the coefficients needed for estimating the cable cost (Maria Ikhennicheu et al, 2020, s. 89)*

Dynamic cable	**Units**	**Cost coefficient**			**Range MVA**	**Keuro /Km**	**Ref. source**
Power rate	Max KV	**C1**	**C2**	**C3**		Keuro/ Km	(Maria Ikhennicheu et al, 2020, s. 89)
11MV	12	69.12	22.85	0.22	12.5	Keuro/ Km	(Maria Ikhennicheu et al, 2020, s. 89)
22MV	24	-1.27	70.92	0.07	27.5	Keuro/ Km	(Maria Ikhennicheu et al, 2020, s. 89)
33MV	33	-49.42	112.20	0.041	44	Keuro/ Km	(Maria Ikhennicheu et al, 2020, s. 89)

For calculating the total length of cable for the WT in the farm site Eq.1 is used. Moreover, for the cost coefficient Eq.2 is used and finally, Eq.3 for the total cable-cost estimates.

$$L_{ac} = 2 * Dw * 2{,}6 + Dwt = \text{Length of cable} \tag{34}$$

(Maria Ikhennicheu et al, 2020, s. 89)

$$CPC = C_1 + C_2 \exp{(C_3 * S)} \tag{35}$$

(Maria Ikhennicheu et al, 2020, s. 88)

$$Total\ cost\ cables = \sum_{t=1}^{n} Cpc * l_{pc} * N_{pc} \tag{36}$$

(Maria Ikhennicheu et al, 2020, s. 88)

Distribution of units.

- CPC = cost of single cable ($/m)
- L_{ac} = length of cable
- N_{pc} = Number of cables
- S= Cables rated power = MVA

11 Vessel types and their configuration for installation and maintenance process.

Introduction of vessels and configuration.

In this part, the traditional vessel will be explained for the purpose of identifying and categorize each vessel into their various operations. The operations include installation and maintenance service. Based on this, the total cost for operation could therefore be estimated for identifying each cost drivers in the brake down model. The estimation is provided in chapter 15 result.

There are many vessels used in the offshore industries and is based on the project task. Since each vessels have different configurations, they are used differently in the process of installation or in the maintenance service. The various types of vessels could be categorized into tug vessel, floating crane (barge), anchor handling tug supply (AHTS), and supply vessels (SUV). Moreover, CTV and OCV cable vessel layers. In the installation phase of FWT this could be done in two ways. The first is by towing a complete assembly of the FWT from the harbor dock to the farm location. The other solution is assembly at location, this by using a crane vessel (lifter). In relation to (Ågortnes, 2013, s. 88) for such operations, it is based on a strategical solution and is defined in an early stage of the project. Based on the process of mooring installation (L. Castro-Santos et al, 2013) found that anchoring handling vehicle (AHV) are also used for installation of anchors (L. Castro-Santos et al, 2013, s. 43)

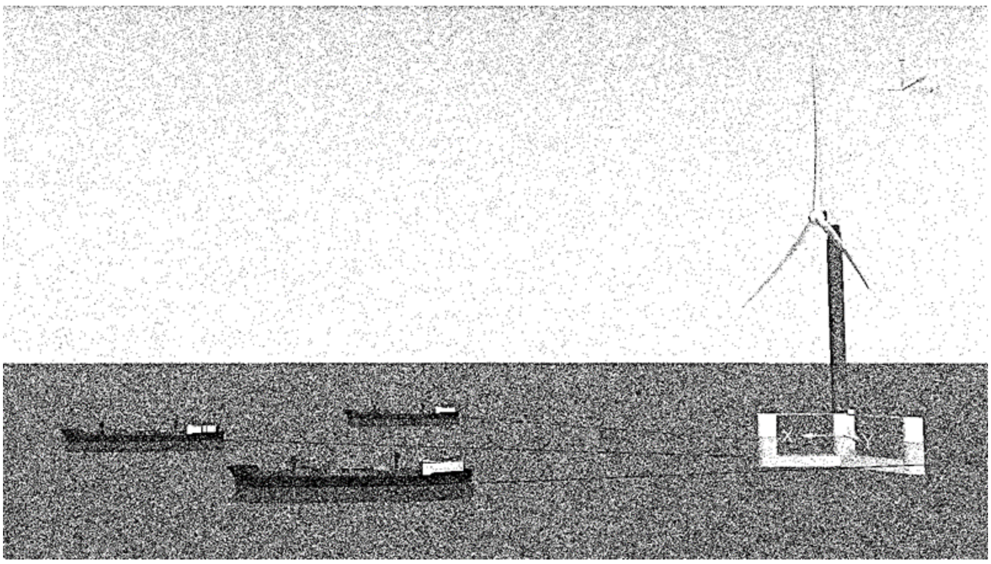

Figure 42 *Illustrates the towing process of a complete assembly by using towing vessels. The tug vessels illustrated in the figure are not the ordinary vessel but only meant as an illustration view over the 15MW US main towing. Designed by the author.*

Additional to the various vessels a further explanation will be described based on the vessels configuration and its purpose in the offshore industries. There are many vessels ranging in size, weight, and cost. In relation to cost expense these rates are normally given in daily rates. Nevertheless, in the process of installation and maintenance service various vessel could be used, but for O&M Crane bare, AHTS, SUV and CTR are normally used. The table below provides some of the traditional vessels.

Barge/ crane barge

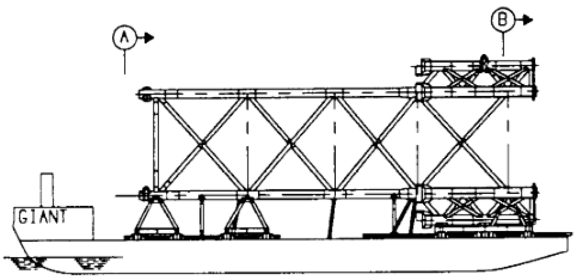

Figure 43 *crane barge/barge* (J.M.J. Journee et al, 2001, s. 38)

Barge crane vessel presented in (fig. 44) are used as crane lifters for installation of vertical turbines onto the platform structure in the farm site. This vessel could also be used in the maintenance service for miner repair or totally removal. The cost range per day is between 150.00-250.000$ according to (Ågortnes, 2013, s. 73)

Tug vessels

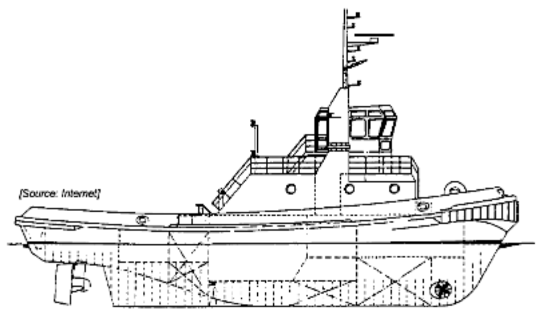

Figure 44 *Tug vessel* (J.M.J. Journee et al, 2001, s. 38)

The towing vessel presented in (fig. 45) is the vessel used for transportation of towing structures in the installation process. Generally, these vessels could be defined as the working horses on water in relation to their extreme pull power. In case of using three of these towing vessels has the capacity of pulling as much as 70 – 80 tons. The vessel ranging in size and has a daily cost price between 1000 - 5000 $ according to (L. Castro-Santos et al, 2013, s. 43) .

CTV-speed vessel

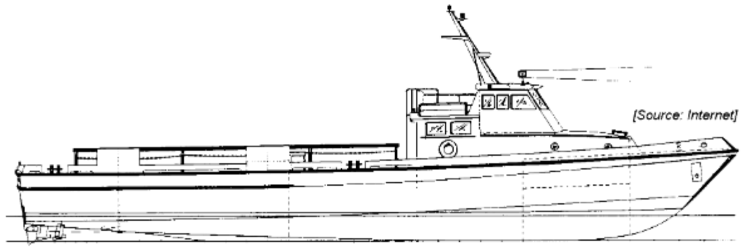

Figure 45 *crew transport CTV* (J.M.J. Journee et al, 2001, s. 38)

Crew vessel CTV presented (figure 46) are meant for transporting crew workers back and forth to farm location. These vessels could have maximum of 12 crew works and are much used for maintenance service with miner repair and inspection. The maximum speed limit is 20 knots, and estimated cost is respectively 2500 pounds.

Anchor handling tug supply (AHTS) and supply vessel SUV

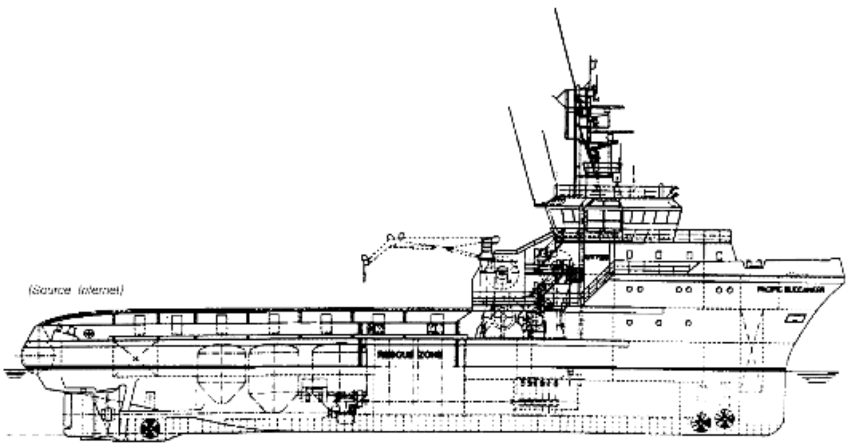

Figure 46 *AHTS, SUV supply vessel* (J.M.J. Journee et al, 2001, s. 38)

Anchor handling tug supply vessels (AHTS) presented in (figure 47) are used in operations for both installation and maintenance service. Normally, they are used in the installation for mooring-, anchors-installations, towing operations, shipping supply, and lifting operations. This vessel ranges in size and weight and could be 25-397 tons and speed limit 23 Km/h. Since these types of vessels could be used for lifting operations, they are configurated with crane (Ågotnes, 2013, s. 51). The estimated cost ranges for the AHTS per day is between 22175.99$ - 55439.98$. The other similar vessel type is the supply vessel (SUV) but are normally used as an assistant vessel meant for cargo supply, personal supply, and equipment supply meant for large operations. The estimated cost range for SUV is between 3.000-36.000$ (Ågotnes, 2013, s. 51) and could store up to maximum of 60 crew works.

Cable vessel

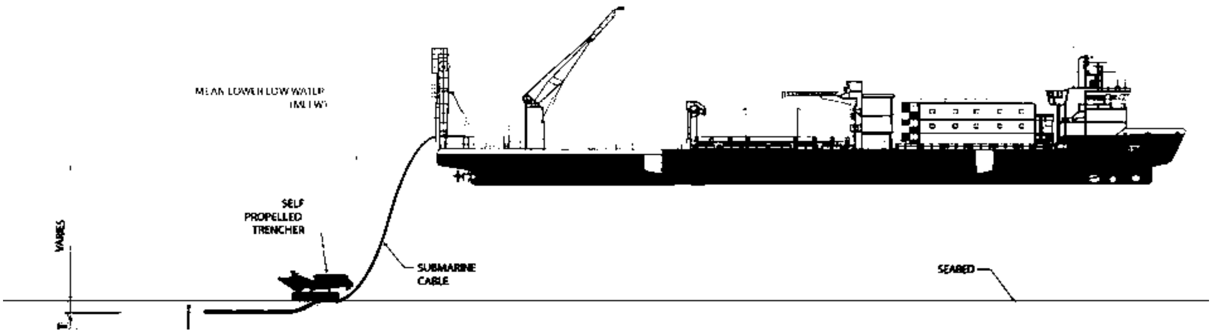

Figure 47 *(Bureau of ocean energy management, Boem, 2011, s. 1)*

The OCV-cable vessel is meant for installation of power cables and for such vessel the cost ranges per day is respectively 100.000 $ (Axelsson, 2008, s. 9) and converted today 140.191,27 $/per day.

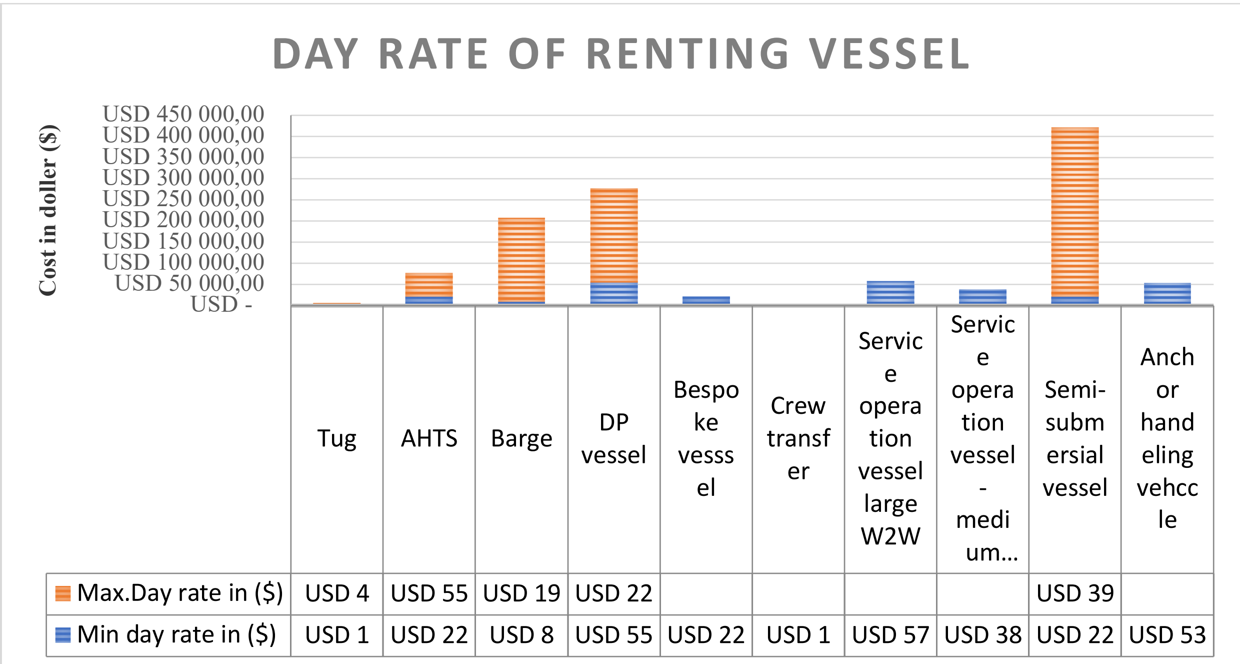

Graphs 2 *Comparison of different vessels cost per day rate.*

The table provides a cost comparison for several vessels based on their daily rates. The table above is collection of cost estimates for various vessels based on chapter 15. The table below represents some finding related to the rent cost per day.

12 Introduction to the simulation case of prototype 1 and 2.

A summary of the simulations and prototype design.

In the following case, a description of the simulation test will be performed for the two individual prototype models I and II. This summary will therefore provide a deep description of each prototype design and assumptions that has been done in these two models studies. The first prototype is a single CSC-semi of the Umain Volturnus 15- MW and the RWT-15MW turbine both defined in chapter 12.1 The first model is configurated in relation to the report by (Christopher Allen et al, 2020, s. 13) (NREL). The other prototype is a chosen designed with two single CSC-semi and a calm base buoy in the center. The mooring buoy is centered between the structures and has some similarities in the mooring arrangement identified in the report by (H Munir et al, 2021, s. 5) defined in chapter 9.6. The relation with this concept, is that two platforms is orientated 180 degrees with a shared wire line as a connection line as tension reliver in between. The calm- base buoy is used for binding the platform together. In the center between the platforms is a shard vertical anchor for obtaining the vertical tension. The response test which will be evaluate in both simulation is to find the maximum tension in each mooring lines for the purpose of comparing one single prototype Vs. the other prototype, of two shared mooring arrangement. The purpose with these prototype models I and II is to design them in the right dimensions and for comparing the mooring tension.

The test simulations for both prototypes are run three times for each design with various significant wave heights of 2, 4 and 6 meters. Moreover, a further explanation is provided in chapter 13.3 sea state conditions. In response to the test run (simulation), various mooring lines will be tested with different materials and dimensions. The mooring materials are used is studdles link chain grade R4 185 mm, steel wires with fiber core of 100mm, 150mm, and finally synthetic polyester rope of 268mm. The purpose with this is to evaluate the comparative comparison of the maximum tension in each mooring lines based on the wave loads condition at North Sea. Jonswap is the North Sea wave conditions based on variable wavelength and are defined in the software Orcaflex. (See chapter 2.3) The time duration of the simulation is run 3800 seconds x 3 per separate significant wave heights for 2, 4, and 6 meters. Moreover, the input value of significant wave periods is set to 4, 6 and 8 seconds (se fig.54 in chapter 13.3) the average wind speed is 10.5m/s at SNII. (See chapter 13.3 and fig. 54. The main purpose is to measure the maximum, minimum, mean, std dv, root means square tension measure for each mooring lines in KN. The dynamic response in this study is to estimate and observe the effect caused on the semi-submersal structure and the mooring lines in shallow waters of 70m defined in the region of **SNII.**

12.1 Prototype model I, catenary mooring arrangement.

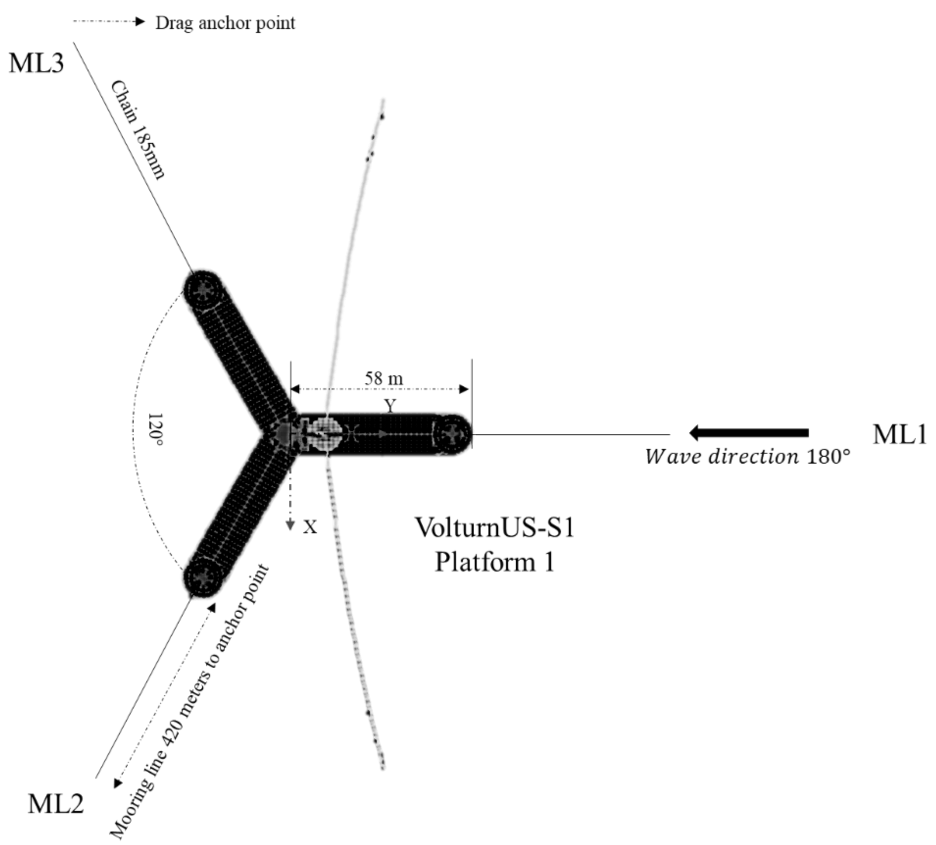

Figure 48 *Example of the single OWP in simulation model 1. File example designed by Ocarina Ldt. oraflex.*

In prototype 1, three chain mooring lines based on 185 mm studdles chain grade R4 as illustrated inn fig. 49. The chains are placed in 120 degrees in each direction out of the platforms fairlead and are given radius anchor point of 610 meters. The chosen mooring length is estimated to 420 m + safety length of 100meters in this case for ML1. The platforms stability is based on a chain catenary mooring system with drag embedded anchors for stability in horizontal directions. The definition of the platform is defined as VolunturnUS-S1 and each mooring lines as ML1, ML2 and ML3, see design prototype I fig.49. The chosen concept of the prototype I is to evaluate the response performance for the tensile force in KN for studdles chain 185mm mooring lines. The wave direction is given in chapter 13.3. In addition to the given input values, it's important to provide a symmetrical design of the mooring lines and with equal input values of the lengths. The table. 22 provides the parameters with the coordinates of placement of the platform, anchors and mooring lines defined in the oriental plane, x-, y-, and z-directions. The file of the prototype (Ocarina Ltd., 2023) and a description of file (Orcina Ltd., 2023, ss. 1-14).

***Table 22** Coordinate of placement of the single- OFP in Orcaflex*

NR.	**Prototype I coordinate**	**Coordination of placement**			**Total length (m)**	**Line types**
		X (m)	Y (m)	Z (m)	m	-
*	Platform 1 VolunturnUS-S1	0.0	0.0	0.0	-	-
1	Fairlead A (ML1)	55	0.0	-14	620	Studdles chain 185mm
2	Fairlead B (ML2)	-28	50	-14	620	Studdles chain 185mm
3	Fairlead C (ML3)	-28	50	-14	620	Studdles chain 185mm
4	Anchor radius (ML1)	740	0.0	0.30	710	Drag embedment 17t
5	Anchor radius (ML2)	-330	-560	0.30	620	Drag embedment 17t
6	Anchor radius (ML3)	-330	560	0.30	620	Drag embedment 17t

The estimated length for each mooring line is 610 meters in each direction to the anchor point. The mooring line ML1 is chosen an extra length of 100 meters because of the wave direction is set in this direction. The illustrated graph provides the total length in relation to the average water depth of 70 meters.

12.2 Prototype model II shared mooring arrangement.

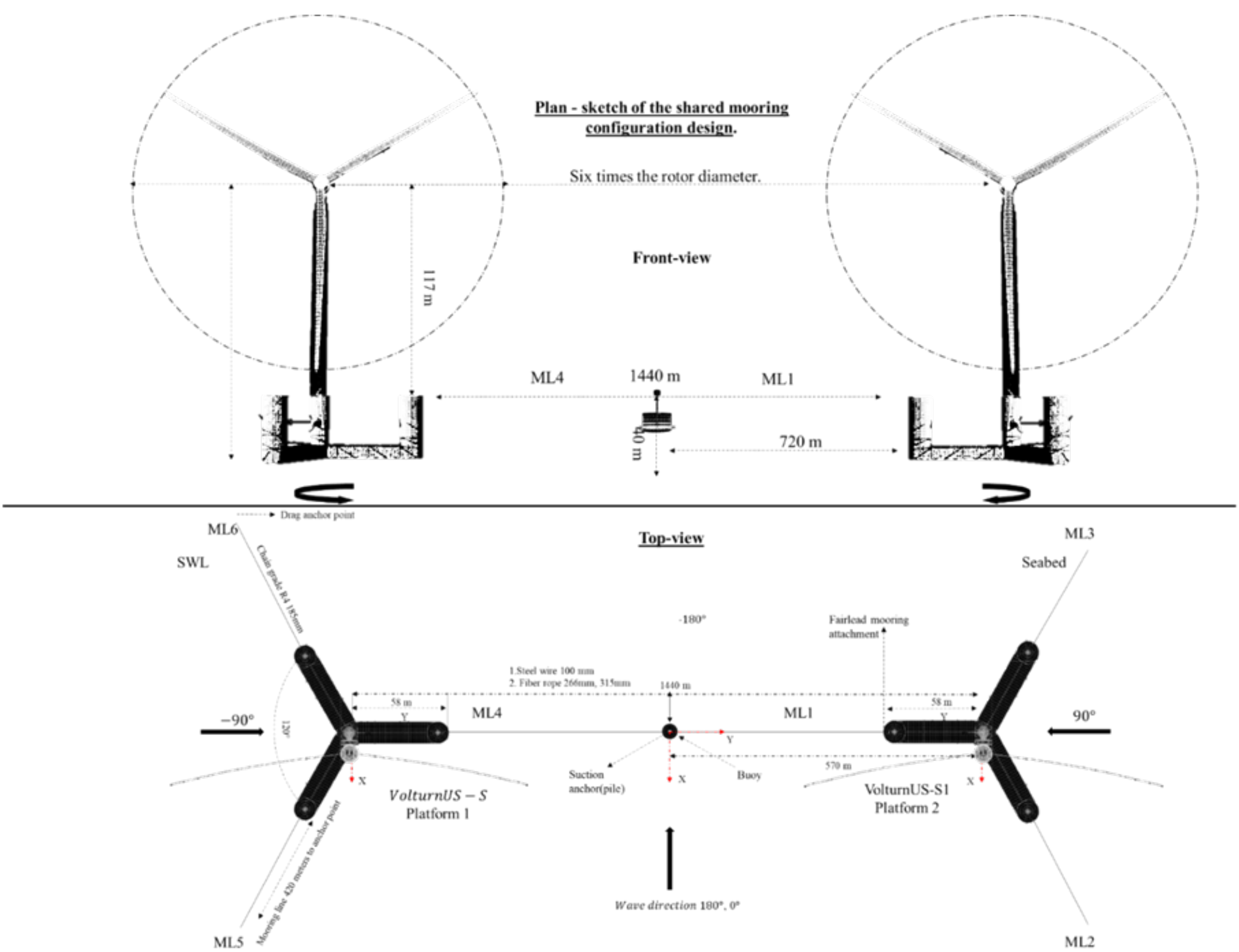

Figure 49 Illustrates plane sketch design of the two horizontal OFWT oriented 180 degrees. Plane-sketch designed by the author LJBT.

In prototype II, the two platforms defined as platform 1 (**VolunturnUS-S1**) and platform 2 (**VolturnUS-S**) are the two floaters orientated 180° degrees in horizontal positions as presented in fig. 50. The configuration spacing between the turbines is six times the rotor diameter with the total distance of 1440 m (6 x 240) according to (al, Jens N. Sørensen et, 2018, s. 2) this is due to the wake effect. The shared wire line between the platforms is centered equal to the connected calm- base buoy and is centered in the mid-section, respectively 720 m. In relation to the calm -base buoy the vertical anchor (VLP) (defined in chapter 10.7) is centered equally between each platform. The buoy is lowered 30 meters beneath the water surface (see table 23). The submerged vertical wire between the calm- base buoy and the vertical anchor (VLP) is estimated to 40 meters. The mooring lines in between the platform's fairleads is of material steel wires of 100 mm. The simulation is also tested with mooring line of polyester rope of 268 mm and are further described in in table. 26.

The four restrained chain lines (4 x chain lines) is defined in a catenary plane and is configured with drag embedded anchors for stabilizer. The origan is chosen at the platform's fairleads (defined in theory 4). The mooring materials used is chain 185 mm steel chains grade R4. The configuration model has its purpose of evaluating the tensile load and dynamic response based on the calm base buoy for random significant wave heights, see table 21. The importance with this design is when modeling the accuracy of input values in relations to length and coordinates is equal. This is because the symmetrical measure will eliminate possible errors that would occur in the simulation test. The coordinates of platforms and calm base buoy is defined in table 24. Before the test simulation in the model in the software needs to be set in **free motion**, meaning the mooring lines and anchors are fully tensioned stabilizer in an x-, y-, z-direction, defined in the oriental plane (Ocarina Ltd., 2023, ss. 1-14).

Table 23 *Placement of mooring configuration and two- horizontal OWPs.*

NR	Prototype II Coordinates	Coordinates of placement			Total length	Mooring line dimension
		X(m)	Y(m)	Z(m)	(m)	
*	**Platform 1 (A)** VolunturnUS-S1	0.0	0.0	0.0	-	-
1	Fairlead upstretched wire ML1	55	0.0	-14	720	100 mm steel wire
2	Anchor radius strained ML2	562	327	0,30	620	185 mm studdles chain (R4)
3	Anchor radius strained ML3	-562	327	0.30	620	185 mm studdles chain (R4)
*	**Platform 2 (B)** VolturnUS-S	0.0	-1440	0.0	-	-
4	Fairlead upstretched wire ML4	55	0.0	-14	720	100 mm steel wire
5	Anchor radius strained (ML5)	560	-1765	0.30	620	185 mm studdles chain (R4)
6	Anchor radius strained (ML6)	-560	-1765	0.30	620	185 mm studdles chain (R4)

The presented table. 29 is a representation of the workbench for the configuration model se figure 50. The definition of the mooring lines is as follows: *ML1* = ML4 Is the steel wires or fiber ropes to the calm base buoy. *ML2=ML3=ML5 = ML6* = Is the chain mooring lines seen from each fairlead to the radius anchors points for strainment to the seabed floor.

12.3 Prototype II calm base buoy

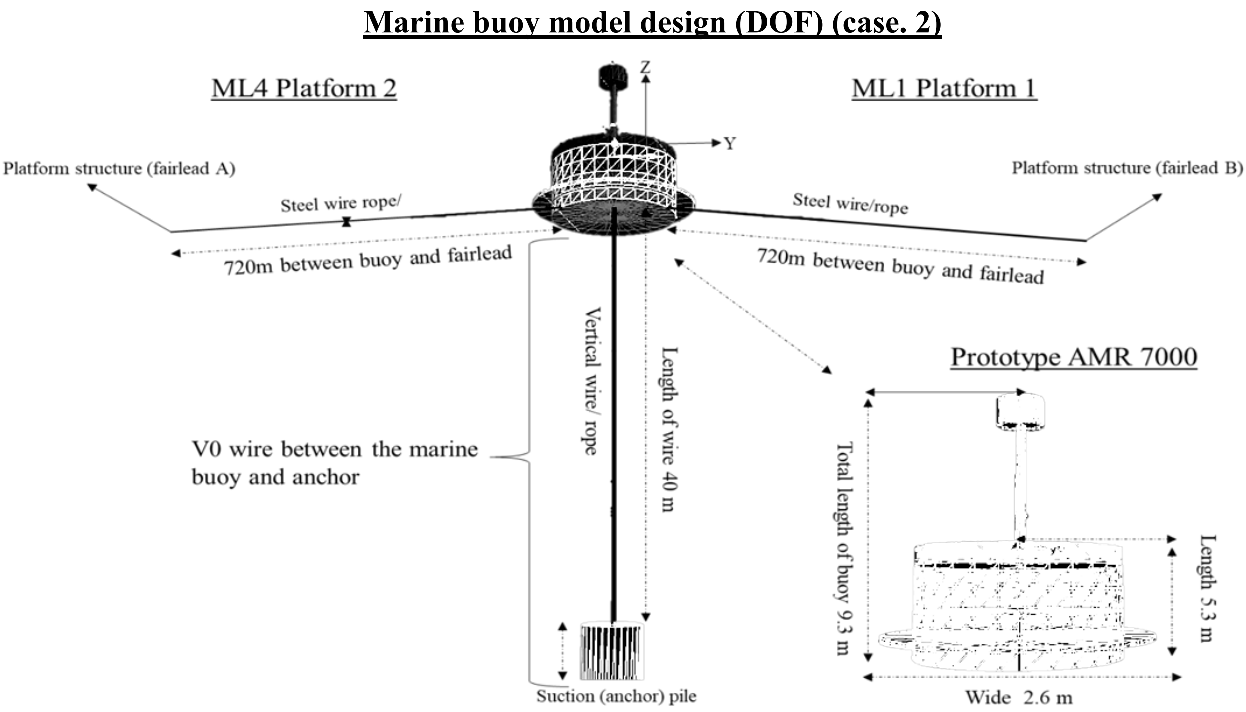

Figure 50 *Example simulation mooring buoy model 3 in configuration design case 2. (reference) Plane-sketch designed by the author LJBT.*

The calm base buoy is the chosen prototype for the prototype II and is added form an example file developed by Ocarina Ltd (Orcina Ltd, 2023, ss. 1-7). The corresponding vertical anchor is centered vertical onto the buoy with a 70 m meters vertical line in between. The morning buoy is lowered 20 meters below Sea-level (WSL). The purpose as identified is that the mooring buoy needs to be below sea level due to strong drift forces caused by the wave loads (see chapter 9.6). The placement of coordinates of the vertical anchor and mooring lines is provided in table 24. The software file could be seen in (Orcina Ltd, 2023, ss. 1-7).

Table 24 *Placement of the marine buoy*

NR.	Prototype II Coordinates mooring buoy	Coordinates marine buoy attachments			Total length	Line type
		X (m)	Y (m)	Z (m)	(m)	-
*	**Marine buoy**	0.0	5	-1	-	-
1	Calm base buoy tension vertical wire below MWL (V0)	0.0	0.0	0.0	40	100 mm steel wire

2	Fairlead upstretched (ML1) A	0.0	0.0	-14	720	100 mm steel wire
3	Fairlead upstretched (ML4) B	0.0	0.0	-14	720	100 mm steel wire
	Anchor VLP	-720	-8	0.0		

13 Case study

Introduction

Economical part (50%) and simulation part (50%)

In the economical part 1, the reference turbine RWT-15MW and CSC-semi; Umain Volturnus 15 MW are used for both the cost model (CBS) and the simulation test. In relation to the economical part, the cost model and is referred to the life cycle cost (LCC) and will be defined in chapter 16 in relation to the method. Based on the numerical cost data, which are added form other works, will be properly defined with reference to the authors. For calculation traditional Excel are used chap.16. The chosen farm location is south North Sea II (SNII) and the cost calculation will be assumed in relation to the reference location, turbine, and platform. The calculation will therefore be estimate of the total cost with a fixed rate of 8% in connection to author (Martinez, 2021, s. 7) this in relation to one 15MW wind farm of a complete assembly. Secondly, an assumption of 100MW windfarm will also be assumed in the region of SNII. The total numbers of turbines for 100MW windfarm would result to 17 units of turbines. The simulation test of dynamic reasons will be based on assumption for random significant wave heights and significant periods. The test is meant to evaluate the maximum tension in response to random sea state of Jonswap and average wind speed at North Sea conditions.

Assumptions of case study

In this case study, the South North Sea II is the choose location and is because of the high recourse of wind energy and the large farm area. However, the long distances and time travelling makes this site challenging and costly due to time traveling in relation to vessels. However, the region is interesting to investigate because it is in the category of shallow water. Moreover, using state-of-the-art technology for installation of OFWT in shallow waters. Since the condition of wind resources are high, could possibly make the floating SSP profitable and investible for the location as SNII. Therefore, the economic result will possibly provide some result based on assumptions. Moreover, the concept and idea by using floating wind turbines (FWTs) instead of bottom- fixed- turbines in region for shallow waters.

13.1 Geographic location South North Sea II (SNII)

South North Sea II (SNII) is the largest area in Norway for offshore windfarm development. The geophysical data of the prospect area is measured to 2598km^2 with a measured wind resources capacity of 1500 MW (sn2offshorewind, 2023). The farm location has a total distance of 140 Km to the nearest cost of Norway (Are Opestad Sæbø, Kristin Guldbrandsen, 2023, s. 21) seen in fig.52. Additionally, the nearest assumed harbor is in Kristiansand, in the community of Lista Agder. The assumed harbor in Lista has a measured distance of 168 Km and is the nearest of the three assumed harbors to the farm location (Are Opestad Sæbø, Kristin Guldbrandsen, 2023, s. 21). The geological area in the region is defined as sandy and in shallow waters, with an estimated average water depth is 70 meters. Based on the wind resource, the average wind speed is measured to 10.5 m/s. Nevertheless, the shallow waters and the geological ground formation could both store bottom fixed as to floating wind turbines. The geophysical data over South North Sea II consists of an area of 605km^2 which in term corresponds to an area efficiency of 5MW/km^2. The fig,52, and table. 25 provides some more information to the wind farms potential .

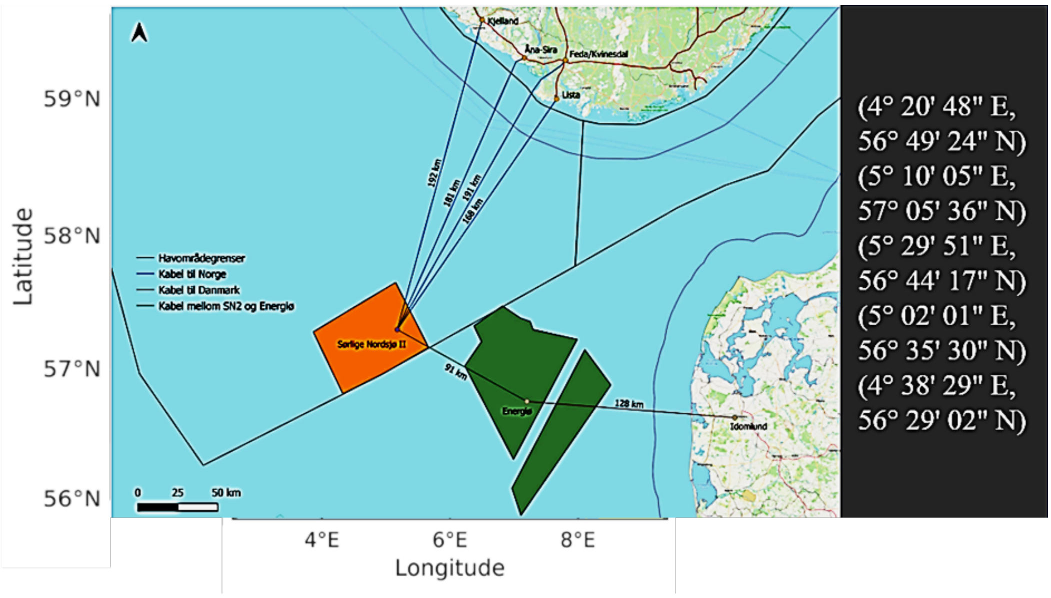

Figure 51 illustrates the location of the area and is defined in orange and identifies the SNII and the distance between the four main harbors (Are Optad Sæbø,Kristin Gulbrandsen, 2020, s. 21) the coordinates over the locations Norwigan Gov. (Tina Bru, 12, ss. 6-7)

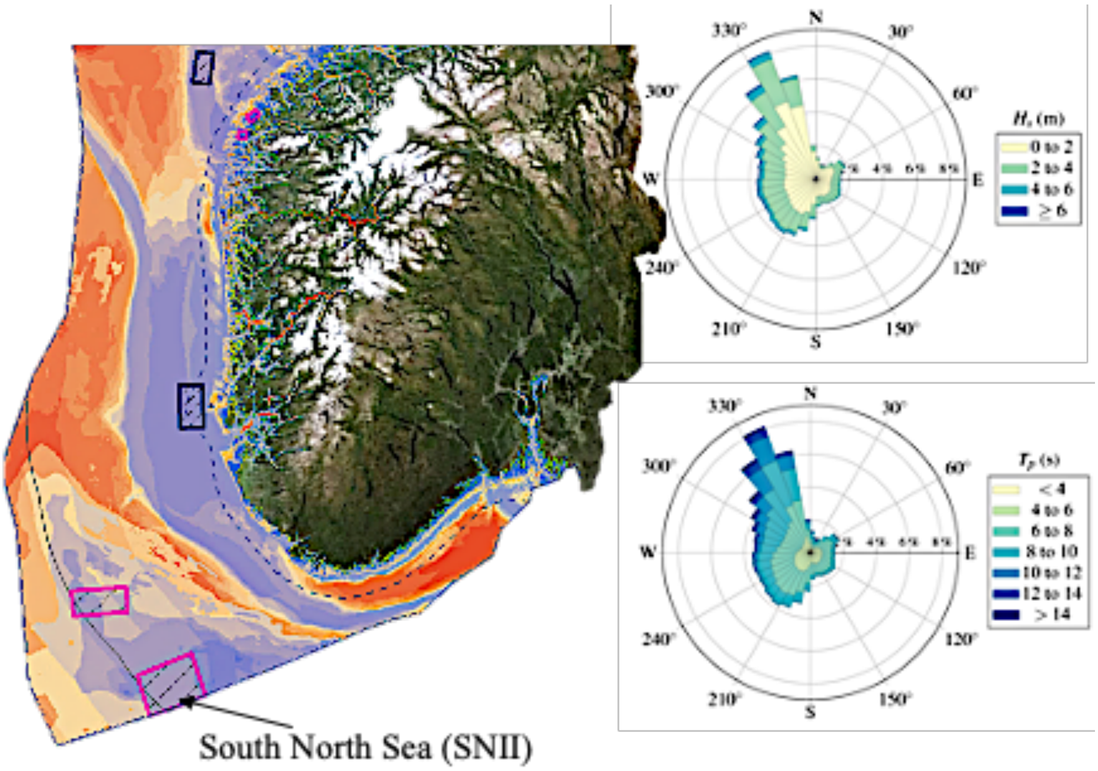

***Figure 52** illustrates the wind farm location at South North Sea (I and II). The Black arrow marks the site SNII collected through NVE* (NVE, 2023) *and meat ocean map based on at SNII* (Lin Li et al, 2023, s. 12)

***Table 25**Provides the parameters of the Soyh North Sea II*

Marine data of location	**South North Sea II**	**Units**
Soil condition	Transitional, shallow, Sandy	-
Total area	2598	Km^2
Energy capacity	1000-2000	MW
Distance to shore	140	Km
Distance to nearest harbor Lista	168	Km
Average wind speed	10,5	m/s
50-year wind speed	36,5	m/s
Significant 50-year waves height	12,9	m
Neto capacity factor of 1000 MW development	51	%
Neto capacity factor of 2000 MW development	49	%
Mean year energy production of 1000 MW development	4510	GWh
Mean yearly energy production of 2000 MW development	8920	GWh
Water depth	50–70	m
Average depth (m)	70	m
Structure type (SSP), Bottom fixed structures	Floating and bottom fixed	-

13.2 Properties of the mooring line materials to be simulated.

The mooring configuration properties

The tables below represent the chosen parameters of mooring materials used for both simulations of prototype I and II. However, for prototype I will only be tested with chain catenary mooring lines. For prototype II will be performed with calm bas buoy, chain, steel wires and synthetic fiber ropes of polyester. The parameters are given table 26,

---

The table 26 provides the key properties for various materials, dimensions, nominal diameters of mooring lines for the test. The materials are chain graded R4 185 mm, 100 mm steel wire and 268 mm polyester rope.. The tables also provide the minimum breaking (MBL) load and axial stiffness for each mooring lines. These mooring properties needs to be in line with recruitment of standard according to DNVGL-OS-E301 (DNVGL AS, 2018, s. 75). Based on the given input values, the measured tension in KN must not exceed the minimum and maximums tension in relation to recruitment DNV standard DNVGL-OS-E301in the simulation test. The purpose her is to simulate three separate nominal diameters of mooring lines to be tested for ultimate strength.

Table 26 *Provides various dimension of mooring properties.*

Mooring line parameters	**Nominal diameter (m)**	**Minimum breaking load (MBL)**	**Axial stiffness MN**
Configuration design model 1, Case 1			
Chain Studdles- link graded(R4)	0.185 m	6333.58 KN	404KN
Configuration design model 2, Case 2			
Steel wire rope (6x19- strands)	0.100 m	6333,5 KN	404KN
Steel wire rope (6x19-strands)	0.150 m		
Fiber Polyester rope (8 -strands)	0.268 m	12,24 MN	78,29e^3KN

13.3 Sea state conditions (Jonswap).

The table below corresponds to the properties which will be simulation over one hour of duration (3600 sec +200sec). The 200s corresponds to a better estimation in relation to the time series in relation the output values. The wave load direction is set to 180° towards the prototype I and II arrangements. The significant wave heights (H_s) is chosen with random significant wave heights and significant periods (T_p), and wind speed (V_{speed} = 10,5m/s. The table. 27 provides the parameters of sea state conditions. The wind drag coefficient is in the software is 1.2 and the wavelength corresponds to the (Jonswap) sea state condition in North Sea and is provided by the simulation software Orcaflex (Orcina. Ltd, 2023, s. 1)

Table 27** assumption of design load case of random variable of wave height in **SNII.

Sea state condition	***Significant Wave heights (Hs)***	***Mean zero-crossing of Wave periods. (Tp)***	***Wave direction***	***Wavelength JONSWAP***	***Average Wind Speed (m/s)***	***Simulation duration (s)***
Sea state conditions						
Simulation *Prototype I *Prototype II	2m	4s	180°	Variable values (See Appendix)	10,.5m/s	3800s
Simulation .2 *Prototype I *Prototype II	4m	6s	180°	Variable values (See Appendix)	10.5m/s	3800s
Simulation .3 *Prototype I *Prototype II	6m	8s	180°	Variable values (See Appendix)	10.5m/s	3800s
Extreme condition						
Simulation 4 *Prototype I *Prototype II	10,5m	14,2s	180°	Variable values (See Appendix)	9,2m/s	3800s
Estimated duration	-	-	-	-	-	15200s

In addition to the given input values in relation to table. 27 above provides the input value and the output value is provided below in fig. 54 of the spectral density curves. The four spectral density curves represent the significant wave heights (H_s) of 2m-, 4m-, and 6- meters and significant wave periods (T_p) 4s, 6s and 8s. The four curves illustrate the spectrum view to be simulated three times total. The spectrum curves represent the density curves in (mm^2/Hz) in y-axial direction over the given frequency in (Hz) in x-axial directions.

<u>(Jonswap) spectral density curves.</u>

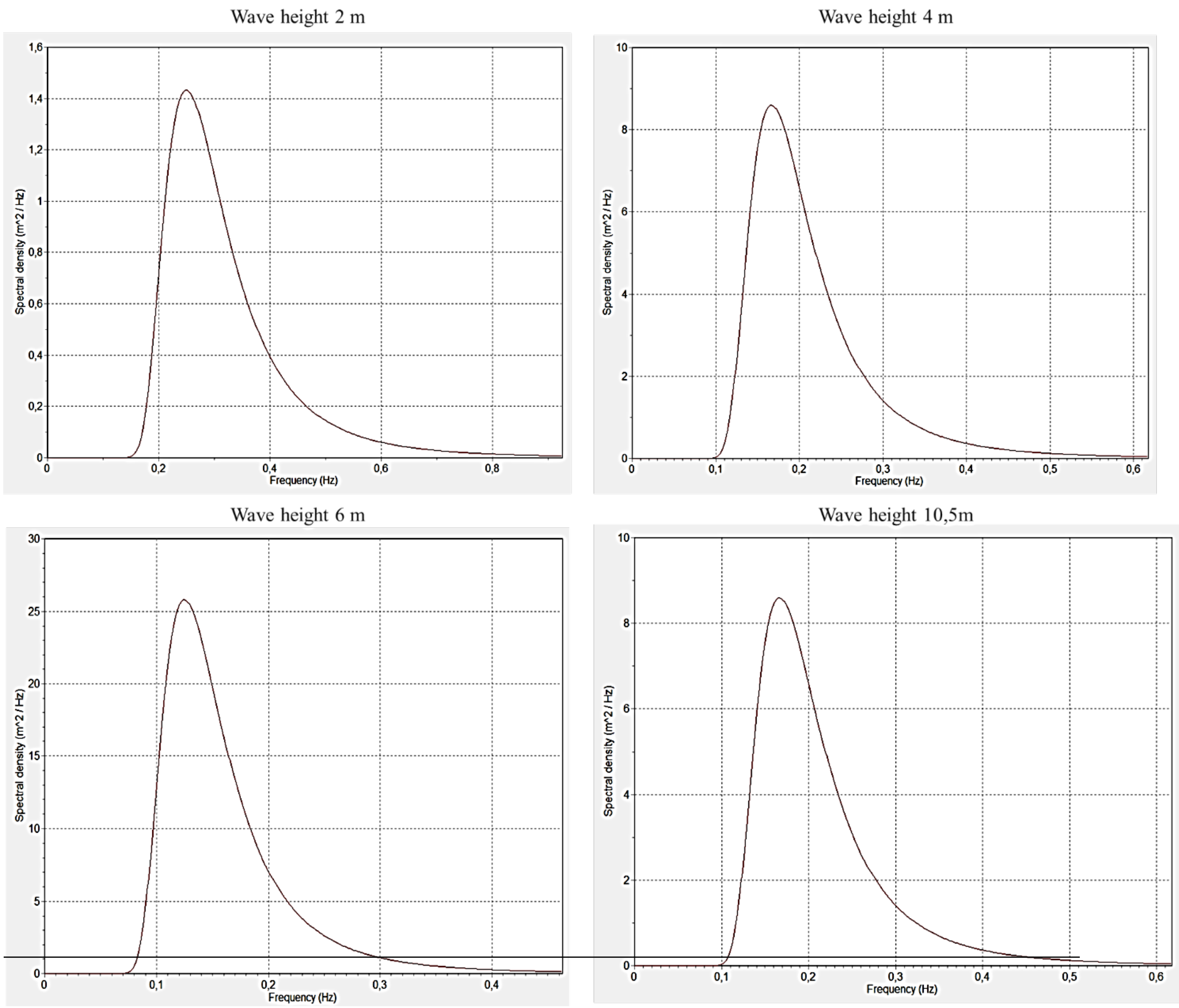

Figure 53 *The wave spectrum for irregular waves shows the separate density curves y-axial and the period (Hz) x-axial direction of random chosen wave heights of 2m, 4m, and 6m. Added from oraflex.*

14 A collection of numerical cost data for the cost result.

This table represents the numerical cost data collected through varios master thesis, articles and reports and defined in table 28. The purpose is to clarify where the data is collected from in relation to other works and to the authors. The collection of cost data will therefore be used in this thesis for calculating the LCC estimates for the six cost drivers defined in chapter 6 for this thesis and for solving the investigated research question defined in chapter 2.6. For estimating the cost estimates traditional Excel is used (see appendix). Some of this cost is collected trough (thecrownstate, 2019, s. 18)

Table 28 provides a collection of numerous cost which includes vessel,

Parameters	Abbrev	Units	Cost price	Today's inflation value	Ref. Sources (thecrownstate, 2019, s. 18). (thecrownstate, 2019, s. 18).
(thecrownstate, 2019, s. 18)			Euro	Doller	
Consenting and development			1.800.000pound	1.848.248.02	(thecrownstate, 2019, s. 18)
Environmental survey			60.000pound		(thecrownstate, 2019, s. 18)
Onshore survey			8.250pound		(thecrownstate, 2019, s. 18)
Resource and meta ocean assment			60.000pound		(thecrownstate, 2019, s. 18)
Meta mast and platform			75:000pound		(thecrownstate, 2019, s. 18)
Structure			45.000Pounds		(thecrownstate, 2019, s. 18)
Maintenance service			4500punds		(thecrownstate, 2019, s. 18)
Geological survey			120000Pounds		(thecrownstate, 2019, s. 18)
Geophysical survey			120000Pounds		(thecrownstate, 2019, s. 18)
Geotechnical survey			90000Pounds		(thecrownstate, 2019, s. 18)
Hydrographic survey			12000Pounds		(thecrownstate, 2019, s. 18)
Engineering and consulting			60000Pounds		(thecrownstate, 2019, s. 18)
					(thecrownstate, 2019, s. 18)
Wind turbine			150.000Pounds		(thecrownstate, 2019, s. 18)
Vessels	C_{Transp}		Euro	Doller	
Tug	C_{cost}	$/ day.	1000-5000	1318.12 - 6590.93	Santos 2013
Tug	C_{cost}	$/ day.	1000-4500	1095.04-	(Rahul Chitteth Ramachandran et al, 2021, s. 18)
Crane barge	C_{cost}	$/ day.	20000-50000	150.00 - 250.000$	(Ågotnes, 2013, s. 51)
Cargo vessel (transport)	C_{cost}	$/ day.	75.000	98863.997	(Jorge Altuzarra et al, 2022)
AHTS	C_{cost}	$/ day.	40.000	43802.053	(Jorge Altuzarra et al, 2022)

AHTS	C_{cost}	$/ day.		22175.99$ - 55439.98$	(Ågotnes, 2013, s. 51)
SUV	C_{cost}	$/ day.		3.000-36.000$	(Ågotnes, 2013, s. 51)
Cable vessel	C_{cost}	$/ day.	100.000	140.1900.50	(Axelsson, 2008, s. 9)
Cable vessel	C_{cost}	$/ day.	70000-115000	84242.287-138398.04	(Rahul Chitteth Ramachandran et al, 2021, s. 18)
DP-vessel	C_{cost}	$/ day.	50000-200000	60173.06-240692.2	(Rahul Chitteth Ramachandran et al, 2021, s. 18)
Crew vessel	C_{cost}	$/ day.	1750	2106.06	(Rahul Chitteth Ramachandran et al, 2021, s. 18)
SOV service operation vessl(large)	C_{cost}	$/ day.	52000	62579.985	(Rahul Chitteth Ramachandran et al, 2021, s. 18)
SOV service operation vessl (Small)	C_{cost}	$/ day.	35000	42121.144	(Rahul Chitteth Ramachandran et al, 2021, s. 18)
Semi- submersible crane vessel	C_{cost}	$/ day.	200000-360000	240692.25-433246.05	(Rahul Chitteth Ramachandran et al, 2021, s. 18)
Barge	C_{cost}	$/ day.	80000-180000	96276.90-216623.02	(Rahul Chitteth Ramachandran et al, 2021, s. 18)
FSV vessel	C_{cost}	$/ day.			
Maintenance and operations					
Helicopter	C_{cost}	$/ day.	6000	7412.93	(Castellà, 2020, s. 35)
Operation					
Fuel costs (AHTS)	C_{cost}	$/ liter.	8000	8760.41	(Jorge Altuzarra et al, 2022)
Fuel cost (tug)	C_{cost}	$/ liter	4000	4380.20	(Jorge Altuzarra et al, 2022)
Standby					
Fual cost AHTS	C_{cost}	$/ liter.	2000	2190.10	(Jorge Altuzarra et al, 2022)
Fuel cost Tug	C_{cost}	$/ liter	10000	10950.513	(Jorge Altuzarra et al, 2022)
Repair cost (minor)	C_{cost}	$	1000	1095.04	(Castellà, 2020, s. 23)
Repair cost (Major)	C_{cost}	$.	1000-10000	1095.04-10950.513	(Castellà, 2020, s. 23)
Repair cost (removal)	C_{cost}	$	100000	10950.5	(Castellà, 2020, s. 23)
Dismantling					
Cleaning	C_{cost}	$	200.000	263637.32	(Costra-Santos, 2013, s. 270)
Disposal scrap metal	C_{cost}	$	213.239	281088.8	(Costra-Santos, 2013, s. 270)

Part 1, Economical result

15 The result for economical part

Economical Result

15.1 Net annual energy produced (AEP).

In relation to estimate Capex, Opex and Decom (defined in chapter 12) the average energy produced must be estimated. Therefore, in this assumption it will be based on two cases, the first case is to find the total amount of turbines and the average energy produced (AEP). The capacity factor (Cp) for a wind turbines are defined as 40% (see chapter 8.2). Therefore, in this situation it will be assume that the renewable wind park should produce 15MW. Secondly, it will be assumed that a wind farm should produce 100MW. The estimation of Net average energy produced (AEP) is provided in table.31 below.

To provide a 15MW renewable windfarm at SNII, it needs to find the total number of turbines needed. In this situation 3 are needed for the site (see appendix). The net average energy produced (AEP) is therefore 131GWh. Regarding the other assumption to provide a 100MW wind farm it would require 17 units of wind turbines. The net average energy produced (AEP) would become 876 GWh, see table. 31. The estimated calculation is provided in appendix.

Table 29 Benchmark assumption of the net average energy produced of a wind farm.

Technical data **Concept of 15MWwind farm**	**MW**	**Number**	**AEP** **(MWh)**
Case 1			
Turbine rate	15		
Capacity factor		0.4	
Total nameplate turbines	37.5		
Number of turbines		3	
Net average energy produced (AEP)			131.400 MWh
Case 2			
Concept for 100 MW wind farm	100		
Total nameplate turbines	250		
Number of turbines		17	
Net average energy produced (AEP)			876.000 MWh

16 The result of the cost model (life cycle cost) - LCC.

This section provides the total estimation of LCC in relation to the Capex, Opex and Decom. The calculation is developed in relation to the cost model defined by (L. Castro-Santos et al, 2013). The cost estimation is divided into two cases 1 for a 15MW wind farm followed by case 2 of 100 MW wind farm this in relation to (chapter 13). For the cost estimates a fixed rate is assumed to be 8% also used according to (Martinez, 2021, s. 7)

16.1 Development and consenting cost.

In relation to the development and consenting the cost is estimated for one turbine of 15MW. The assumption used is in relation to (thecrownstate, 2019, s. 18) they had estimated the cost of respectively 50 £ Million for 1 GWh. Therefore, this estimation has been divided for one 15MW turbine and converted into today's value and inflation currency dollar (thecrownstate, 2019, s. 18).

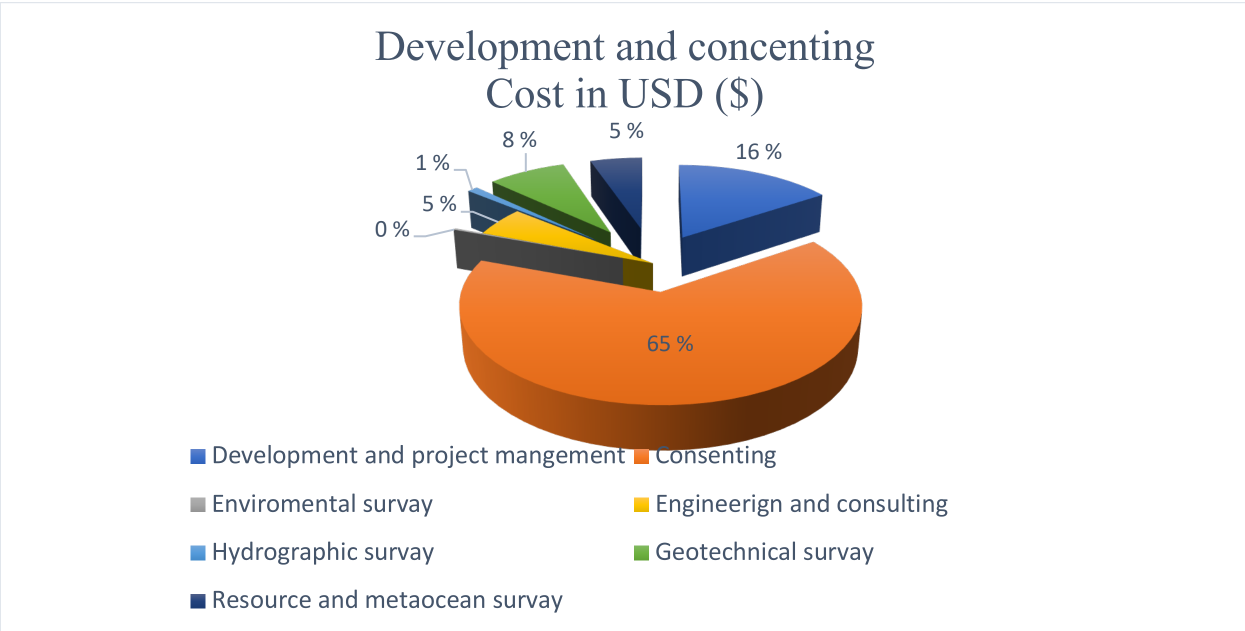

Table 30 provides the development consenting cost.

Development and consenting	Cost in USD ($)	
Case 1		
Total cost	USD 1.848.248.02	(thecrownstate, 2019, s. 18).
Case 2		
Total cost	USD 31.420.828.36	

16.2 Manufacturing cost.

Turbine manufacturing cost

The manufacturing cost for the reference platform structure U Main is based entirely on the material cost evaluated by the weight in ton. The three-cost post based on the turbine includes the rotor house (1), nacelle (2) and tower (3). Moreover, the other value in a turbine is also provided and is assumed form the cost according to (thecrownstate, 2019, s. 18). However, it is also based on other material such as cobber, fiberglass, electrical system, generator, and turbine blades. The unit price of construction steel is in metric ton 1084 $/ton in relation to the market value (Steelbenchmarker, 2023, s. 2). Sine many of the turbine components is not defined in the NREL report. A different report was found mentioned by (thecrownstate, 2019, s. 18) in relation to this will be used for making a complete cost estimate over the RWT-15MW turbine.

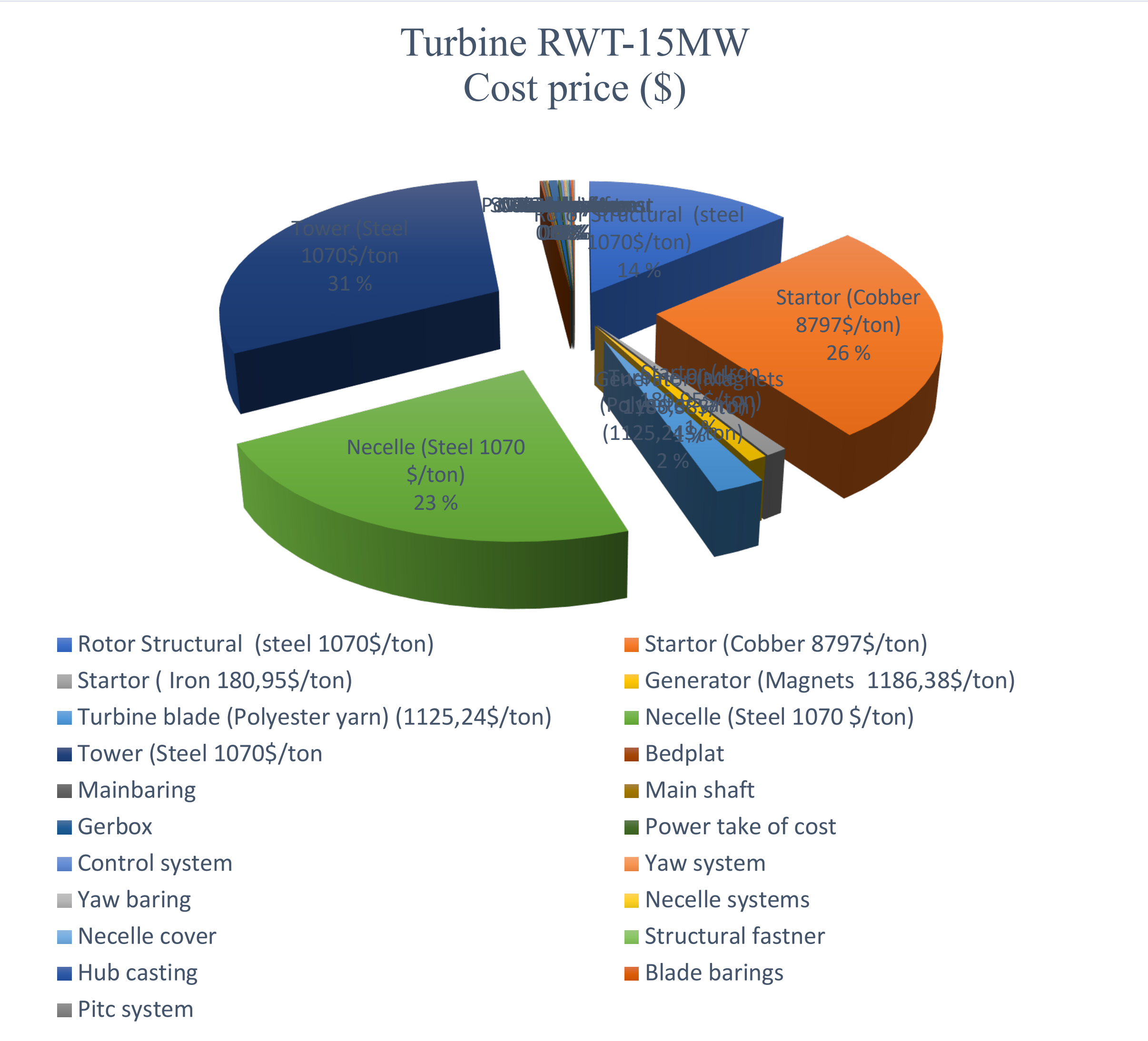

Table 31 Provides the cost of turbine for case 1 and 2.

1 Turbine RWT-15MW (15MW)	Mass (ton)	Cost in USD ($)	(%) of material
Case 1			
Rotor structural (steel 1070$/ton)	385	USD 1.103.676,43	14.0%
Stator (Cobber 8797$/ton)	9,01	USD 792.618,71	27%
Stator (Iron180,95$/ton)	180,95	USD 32.742,90	1,1%
Generator (magnets 1186,38$/ton)	24,2	USD 28.710,40	1.0%
Turbine blade (Polyester yarn) (1125,24$/ton)	65,1	USD 73.253,12	2,5%
Nacelle (Steel 1070 $/ton)	632	USD 676.240	23,0%
Tower (steel 1070$/ton)	860	USD 920.200	31,3%
Bade plate		USD 4798.80	0.16%
Main baring		USD 4798.80	0.16%
Main shaft		USD 4798.80	0.16%
Gearbox		USD 16800.75	0.56%
Power take cost		USD 4794.72	0.16%
Control system		USD 4794.72	0.16%
Yaw system		USD 1679.95	0.06%
Yaw baring		USD 1679.95	0.06%
Nacelle system		USD 1679.95	0.06%
Nacelle cover		USD 2399.38	0.08%
Structural fastener		USD 1679.85	0.06%
Hub casting		USD 3599.07	0.12%
Blade Barings		USD 4798.80	0.16%
Pitch system		USD 2399.38	0.08%
Total cost for one 15MW turbine	1877	USD 2.996.418,15	100%
Case 2			
17 Turbines RWT-15MW (100MW)			
Total cost for 17 turbines for a 100MW wind farm	31909	USD 50.939.108,56	100%

Platform manufacturing cost

The platform structure has a total weight 20206 ton, and the ballast seawater corresponds to 56%, construction steel 19,37%, concrete 12,44%, tower interface 0,5% and finally 11,7% other materials. The properties and dimensions of weight are specified in table 32. However, the market value of steel 1084 $/ton and concrete 444,4 $/ cubic of the total cost of platform structure. In relation to labor cost, it is not evaluated or included in the estimation. The total cost of UMain volunturn 15MW is estimated to 7.013.850 $/ton for one platform additionally for 17 turbines is given in table 32.

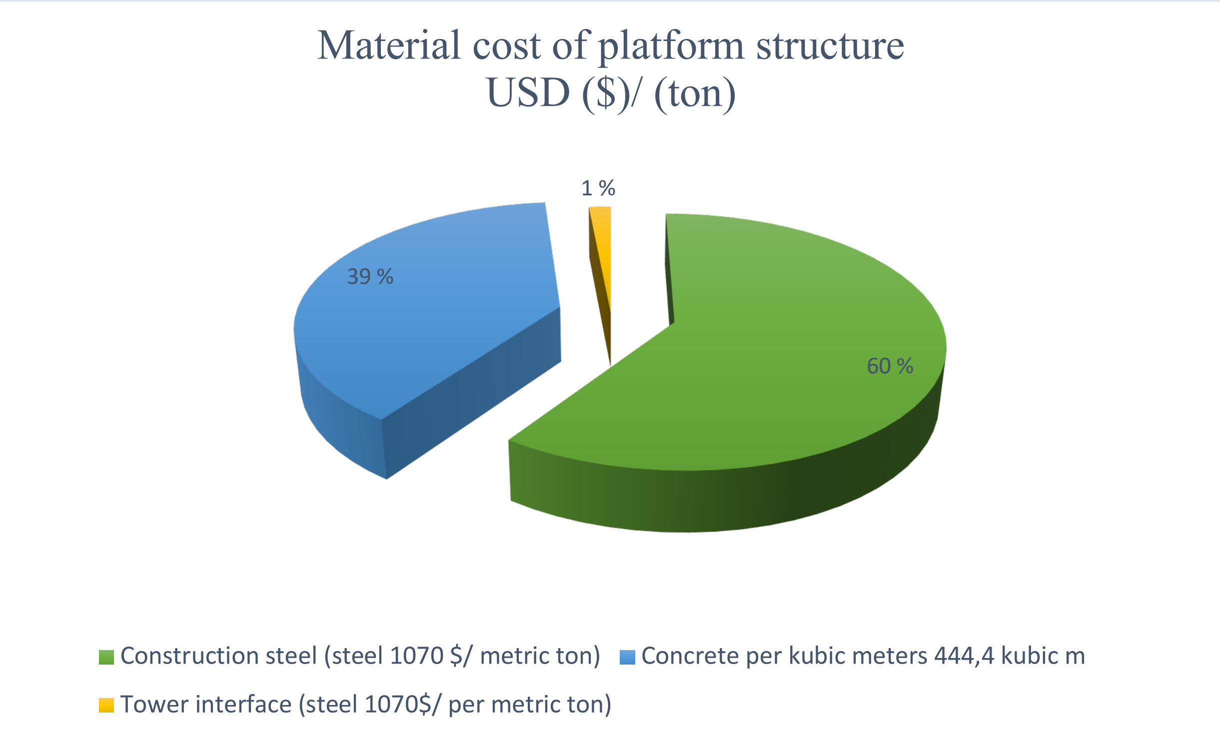

Table 32 *provides the cost of the platform UMain Voluntturn 15MW.*

1 Platform UMain Voluntrn 15MW	Mass (ton)	Cost in USD ($)	(%) of materials
Case 1			
Construction steel (steel 1070 $/ metric ton)	3914	USD 4.187.980	60%
Concrete per cubic meters 444,4 cubic m	2541	USD 2.718.870	39%
Tower interface (steel 1070$/ per metric ton)	100	USD 107.000	2%
Total material cost	6555	USD 7.013.850	100%
Case 2			
Total material cost	6555	USD 119.235.459	100%

Mooring cost and cable manufacturing cost

The manufacturing cost of mooring hardware is based on mooring lines, anchors, power cables and mooring buoy. The cost is also based on the labor cost of fabrication. Since the labor cost is hard to assume it will be left out of the estimation. However, this labor cost is quite severe cost. Since it's hard to find it will be left out of the estimates.

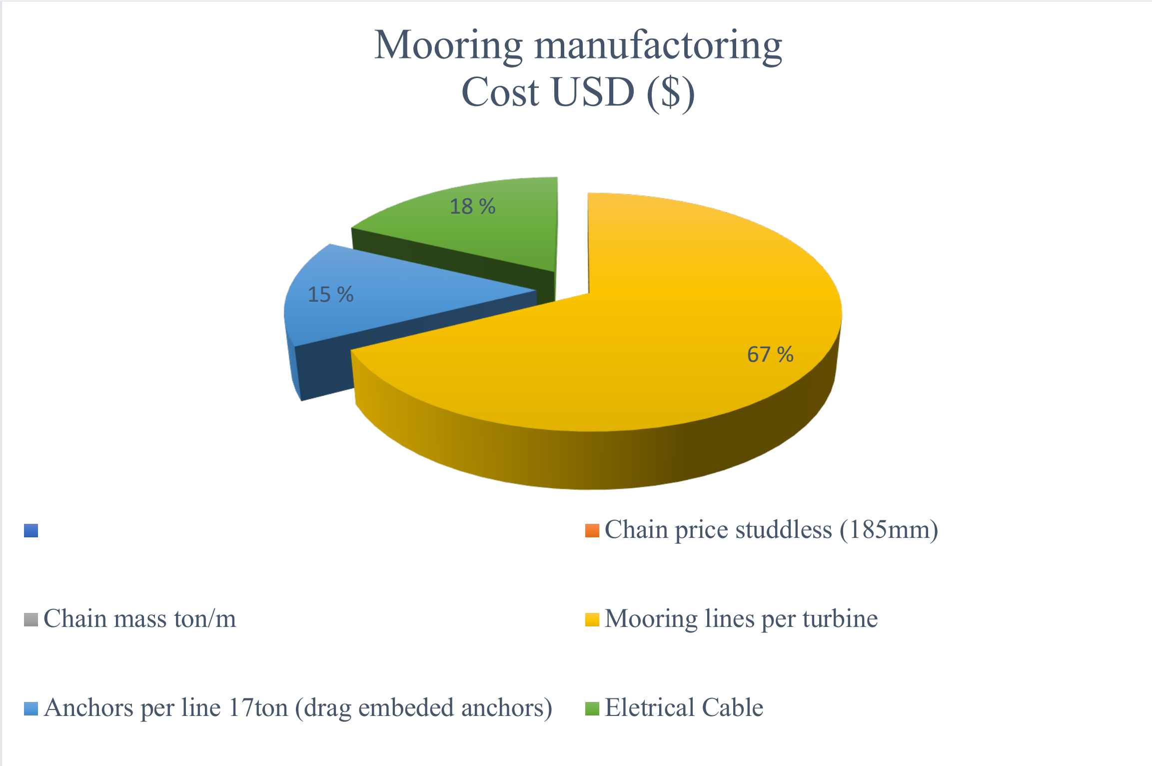

Table 33 manufacturing cost of the mooring lines, anchors, dynamic power cables.

Mooring material cost for 1 turbine	Length (m)	Mass (ton)	Cost per ($/ton)	Cost USD ($)	(%)
Case 1					
Numbers of chain 185mm	3				
Mooring line per turbine (3)	3960m	0.68108	USD1070	USD 2.697.076,8	
Drag embedded anchor per line 17ton		3x17t	USD207.488,5	USD 622.465,5	
Dynamic Power cables	610m	296,28$/m	USD766.075,70	USD 766.075,7	
Total cost				USD 4.274.413,3	100%
Case 2					
Total cost				USD 14.490.941,7	100%

16.3 Installation and transportation cost.

Addition to the installation cost for a complete assembly in the farm location is based on various vessels to be used, the installation of platforms, mooring lines, and anchors. The cost is dependent on the duration time for distance traveling, cost of vessel rate per day, the numbers of vessels and labor cost. Therefore, the estimated duration time for towing a complete platform with a speed limit of 3 knots (5,556 Km/hours) would take 11,34 hours for the total distance of 168Km. Furthermore, it is assumed the nearest harbor is Lista in Kristiansand (defined in chapter 13.1). According to (Jorge Altuzarra et al, 2022) the pre-installation of mooring lines and anchors is done before the platform SSP arrives to the fam site. Nevertheless, the vessel that is required per mooring lines and anchors are two. This means that two vessels are required per installation according to (Jorge Altuzarra et al, 2022).

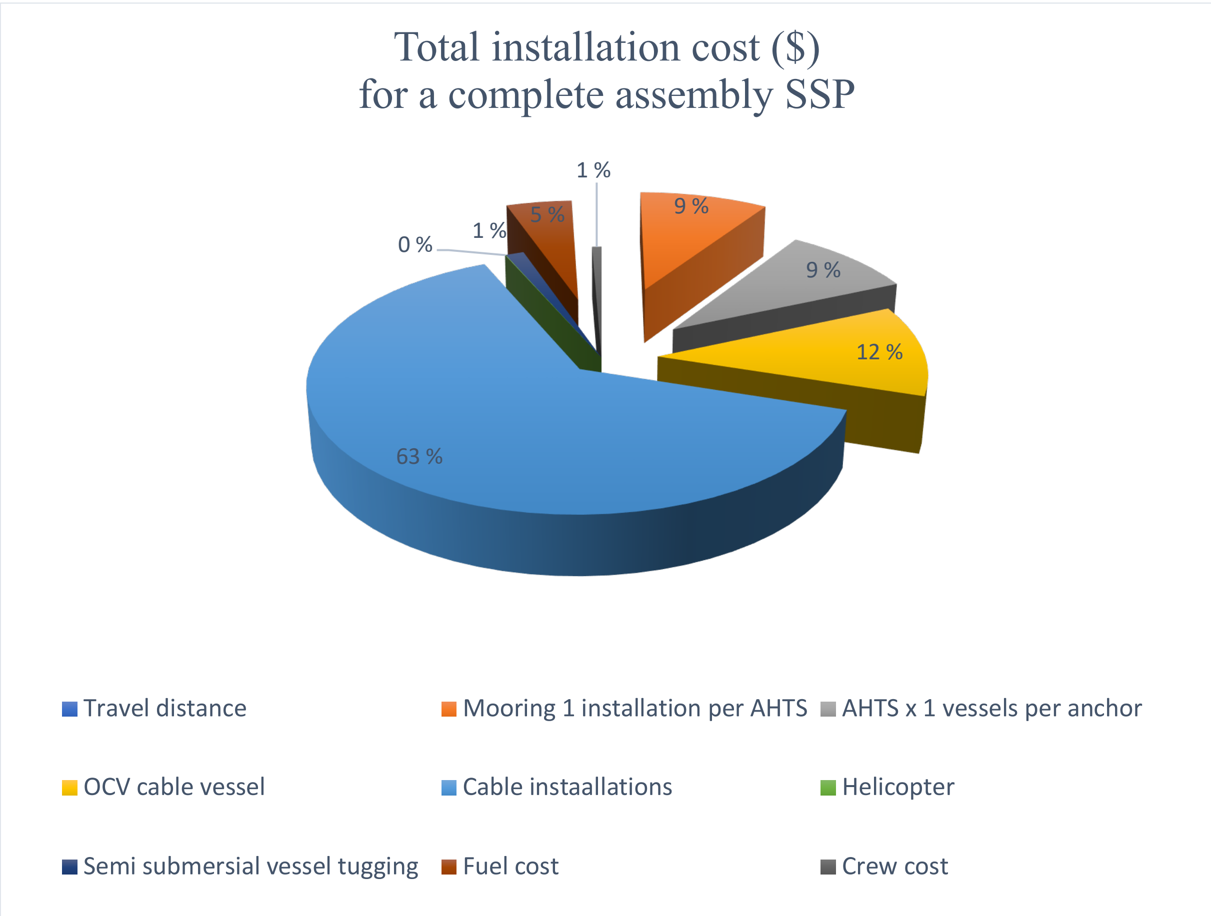

Assumed three steps in the Installation phase.

1) Using two AHTS vessel in the installation. The estimates time to South North Sea II is calculated to a round 7 hours with a speed limit of 23Km/hrs. Moreover, 10 hours for pr- installation of mooring lines according to (Jorge Altuzarra et al, 2022). Therefore, the total duration of mooring installation is respectively 17 hours for one AHTS. The cost of one 43802$x2 (times x2)=87.604$
2) The pre -installation of drag embedded anchors is three per turbine. The duration hours for pre-installation are 10 hours. Further the transportation to the location is 7 hours. Therefore, the total estimated time is 17 hours of anchors installation for one of the AHTS. The cost of one 43802$x2 = 87.604 $
3) Finally, the towing of a complete platform assembly to the destination is assumed of three towing vessels. The duration hours to the destination are estimated to 43 hours with a speed limit of 3 knots. The cost of one tug vessels is 5000$ x three=15.000 $ Therefore, the complete installation for south North Sea is provided in table below:

Table 34 Provides the cost for the installation in the region of south North Sea II.

Installation and transportation cost 1 turbine	**Installation duration time**	**Traveling duration to SNII**	**Vessel Numbers Needed**	**Cost day rate ($)**	**Total cost ($) per day**
Case 1					
Traveling distance	11.34hrs				
Vessel per mooring line AHTS	10hrs	7.0hrs	1		USD 110.879,96
Vessel per anchors AHTS	10Hrs	7.0hrs	1		USD 110.879,96
Cable installation	10hrs	7hrs	1		USD 140.191,27
OCV cable installation					USD 766075.70
Helicopter					USD 555.5
Semi-submersal tugboat		43hrs	3	5000	USD 15000
Fuel cost			l/hr	8000	USD 56.000
Crew cost			127,5$/hrs		USD 165.608
Total installation cost					USD 1.207.202,59
Case 2					
Total cost					USD 16.900.836,26

16.4 Operation and maintenance.

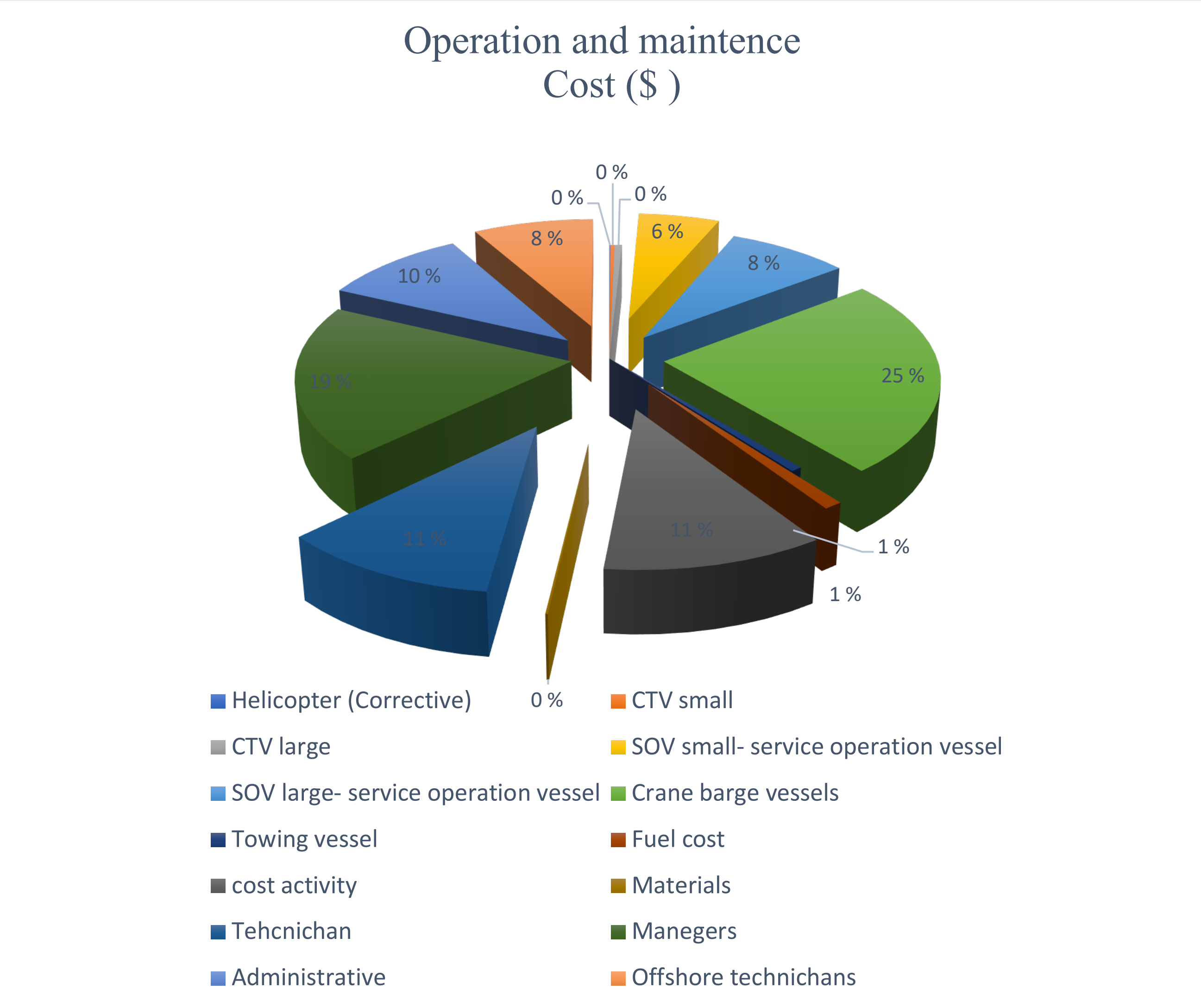

The operation and maintenance O&M service is a variable cost which includes repairs, inspection, removal, vessels, and labor cost. According to (Offshore Renewable Energy Catapult, 2019) the cost for O&M is a round 300.000 (Pound) for one year and with 2-4 inspection days on a regular basis over its lifetime of 25- year. Therefore, in these cases its assumed that the cost is estimated for one year, meaning 12 months (L. Castro-Santos et al, 2013). Since the cost assumption will be based for one turbine model. The first attempt is to estimation the cost based for one turbine, then a second attempt for 17 turbines of a 100MWwind farm. The table provides the cost measure.

Table 35 provides a cost assumption of the platform US main Volturnus.

Operation and maintenance (O&M)	**Speed of boats**	**Day Traveling SNII**	**hours**	**Cost day rate ($)**	**Total cost ($) per day**
Case 1					
Helicopter	296,32			555,35	USD 555
CTV small	46,3		1	2353	USD 110.879,96
CTV-large	46,3		1	38.23,61	USD 110.879,96
SOV small-service operational vessel	23,7Km/hrs		1	45.000	USD 180.730,80
SOV large-service operational vessel	23		1	67.000	USD 626.262,4
Crane barge			3	199.583,92	USD 2532,99
Towing vessel			l/hr	5000	USD 3823,61
Helicopter			1	555	USD 555
Other					
Fuel cost				8000	USD 8000
Cost activity				90.365	USD 90.365
Materials				1000	USD 1000
Labor					
Technician				89.061	USD 5.343.690,6
Managers				156.849,13	USD 313.698,26
Administrative				79753,73	USD 239.261.34
Offshore technicians				66.461,50	USD 398.769
Total cost					USD 7.144.233,15
1 Month					USD 103.410
12 Month					USD 1.103.676
Case 2					
1 month					USD 10.458.794
12 Month					USD 10.458.794,74

16.5 Dismantling cost

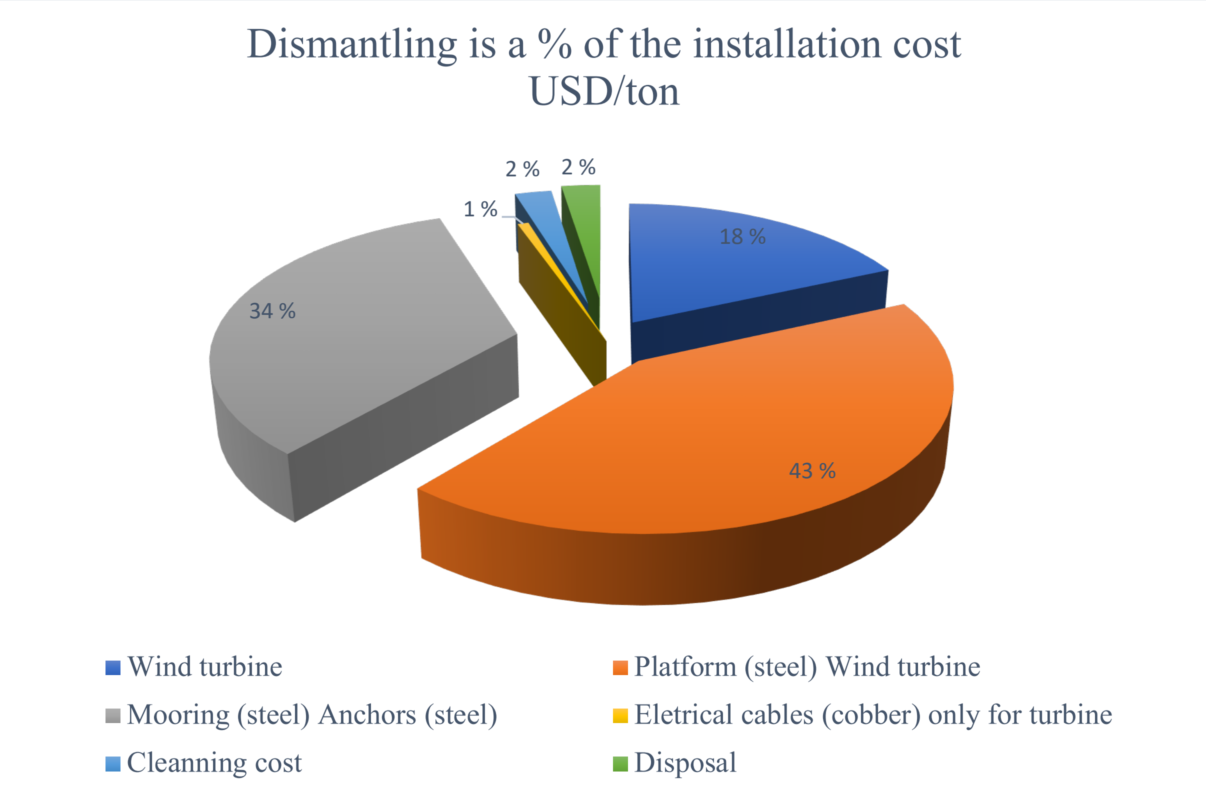

The distempering cost is dependent on the scrap value and the weight of recycled materials, cleaning of area and disposal. However, according to (Martinez, 2021, s. 7) the dismantling cost is the reverse process of the installation phase. Therefore, the percentage is used for estimating this cost. In this sense, the estimated dismantling cost is given in the table below.

Table 36 Illustrates the estimates of the dismantling cost.

Dismantling cost	**Installation cost ($)**	**(%) of installation**	**USD ($)**
Case 1			
Wind turbine (steel scrap value)	2.996.418.	70	USD 2.097.492
Platform (steel scarp value)	7.013.850	70	USD 4.909.695
Mooring (steel sharp value) Anchors (steel scrap value)	4.274.413	90	USD 3.846.972

Power cables (cobber scrap value)	766.075	10	USD 76.607
Cleaning	-262.199		USD -262.199
Disposal of materials	-279.248		USD -279.248
Total cost			USD 10.939.767
Case 2			
Total cost			USD 185.976.039

16.6 Total life cycle cost

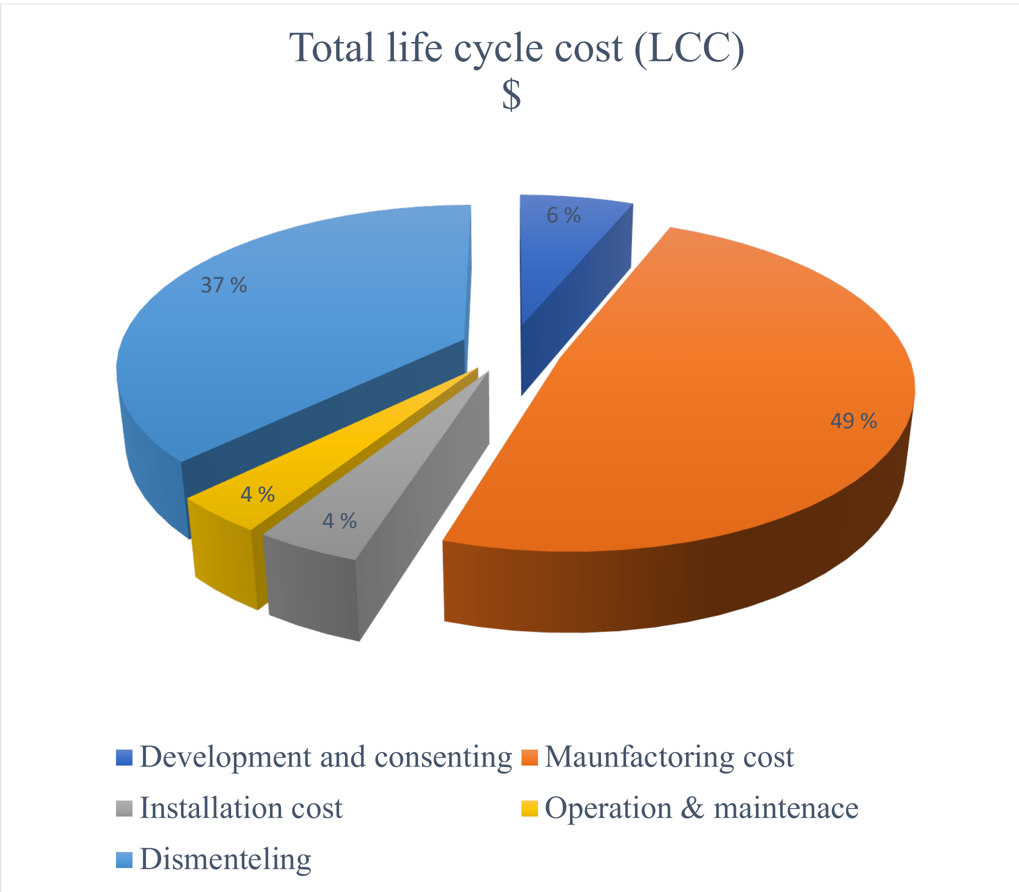

Table 37 provides the cost drivers with fixed rate of 8%

Cost drivers (post)	**Installation cost ($)**	**(%) of installation**	**USD ($)**
Case 1			
Consenting			**USD1.848.284**
Manufacturing			
Wind turbine			**USD2.996.418.**
Platform			**USD7.013.850**
Mooring			**USD4.274.413**
Installation			
Installation/ transportation			**USD1.207.202**
Maintenance service			
Operation and maintenance	12 months	89.712 per year	**USD1.076.546**
Dismantling			
Dismantling			**USD10.930.767**
Case 2			
Consenting			USD31.420.828
Manufacturing			
Wind turbine			USD50.939.106
Platform			USD119.235.450
Mooring			USD72.665.021
Installation			
Installation/ transportation			USD20.522.434
Maintenance service			
Operation and maintenance			USD10.458.791
Dismantling			
Dismantling			USD185.823.039

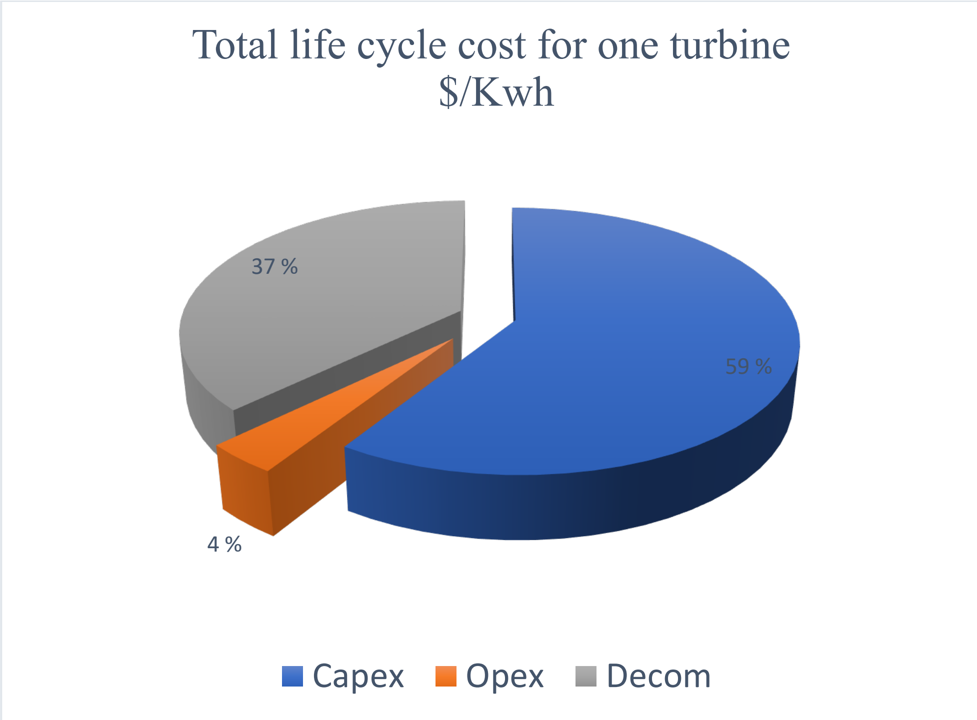

Table 38 Provides the total life cycle cost for case 1 and 2.

Total life cycle cost LCC	$/KWh/ AEP*1000	Internal rate 8%	0.08*$/Kwh/ AEP*1000	(%) of installation
Case1				
CAPEX	131.96	USD1387	10.55	59%
OPEX	8.19	USD86	0.6552	4%
DECOM	83.19	USD874	6.6552	37%
Total LCC 3 turbines.	223.34	USD2347	17.8672	100%
Case 2				
CAPEX	172.66	USD23582	13.81	59%
OPEX	20.89	USD1464	1.6712	4%
DECOM	212.13	USD14865	16.9704	37%
Total LCC for 17 turbines.	223.34	USD2347	32.4544	100%

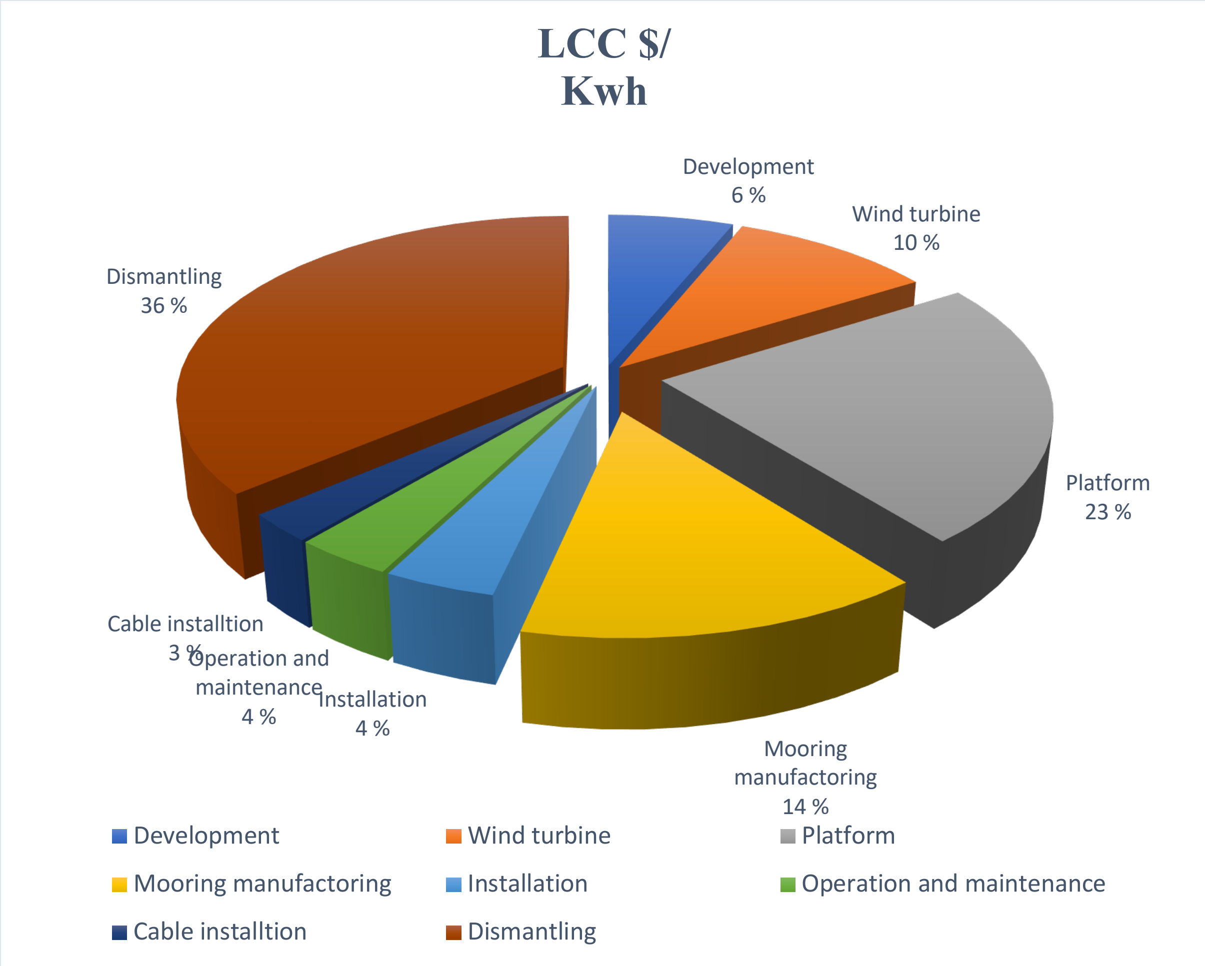

Finally, the total value of each cost components in the life cycle cost for a 15MW and 100MW wind farm is given in $/KWh in table below.

Table 39 *Illustrates the LCC in $ /KWh for a wind farm 15MW and 100MW.*

Result of the LCC	*$/ kwh*	*$/ kwh*
LCC		
Wind farm produce Cp (40%)	***15MW***	***100MW***
Wind turbine	*$/kwh 0.02280*	*$/kwh0.38766*
Platform	*$/Kwh 0,0533*	*$/kwh0.90742*
Mooring manufacturing	*$/kwh 0,0325*	*$/kwh0.90742*
Installation	*$/kwh 0,00918*	*$/kwh0.55301*
Operation and maintenance	*$/kwh 0,00819*	*$/kwh0.15618*
Dismantling	*$/kwh 0,053*	*$/kwh0.1392*

Part 2, dynamic response result

17 Response analysis of maximum tension load for significant wave height prototype I and II.

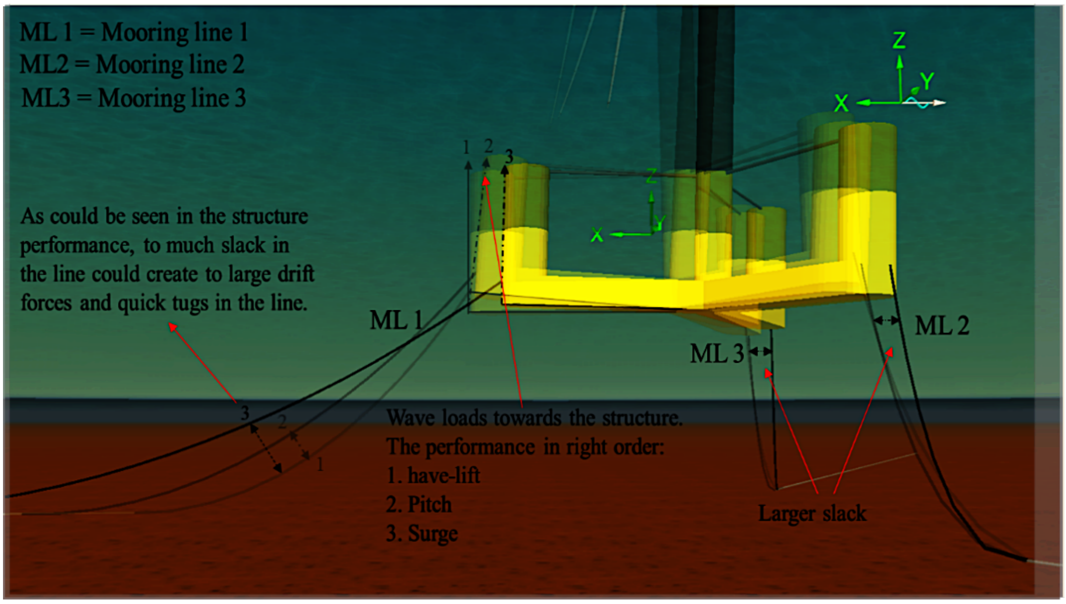

Figure 54 gives a representation of the extension in the mooring line from position 1- 3 in relation to the fairlead caused by drift motions based on have-lift, pitch and surge as a result.

The illustration of observation shows a time representation of the performing structure in response to the wave forces. The wave forces cause a larger off-balance in structure form its original steady- state positions. The mooring line ML1 in axial – position develops the highest tensile force compared two mooring line ML2 and ML3 and is becouse of the wave direction acting in this direction.

Response result of the time series

(Jonswap) sea state condition:

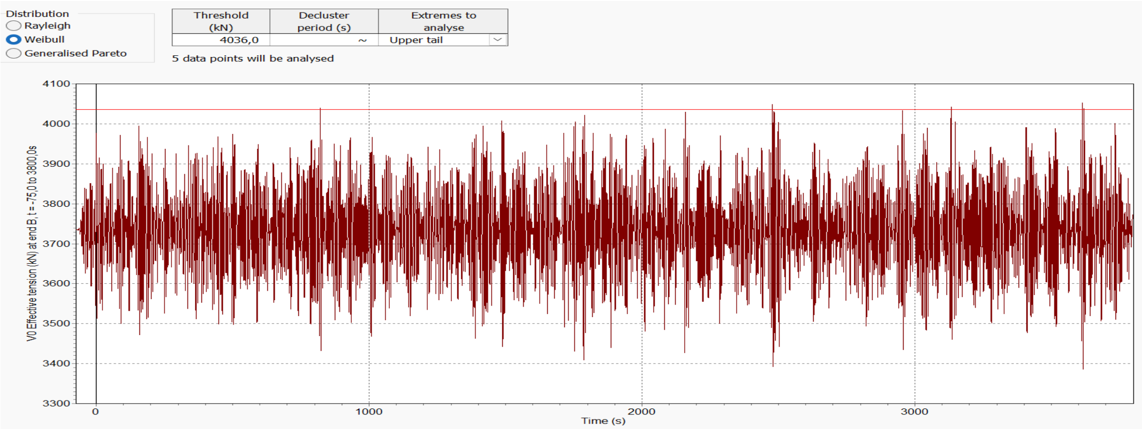

Figure 55 *Prototype I steel chain 185mm.*

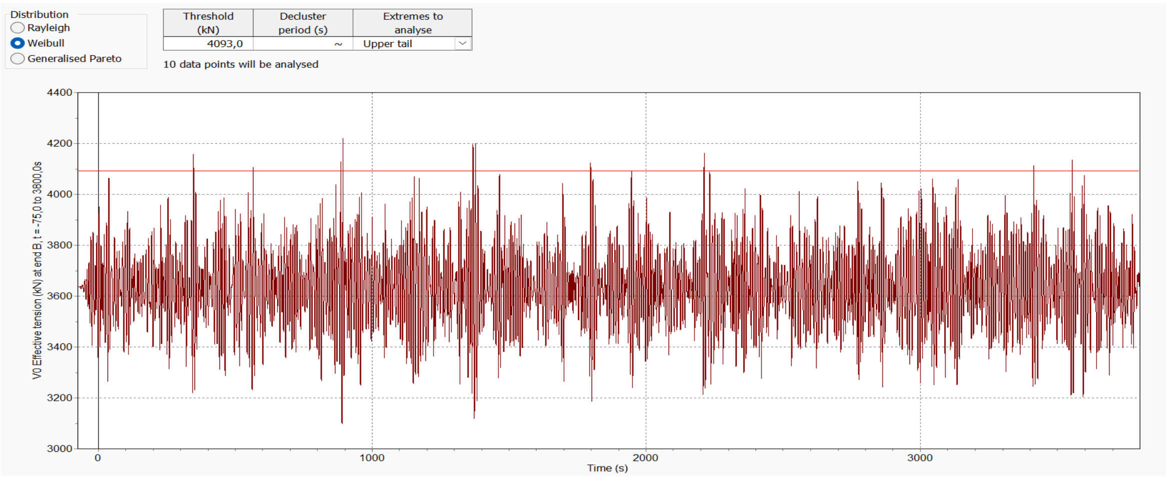

Figure 56 *Prototype II 100mm steel wire*

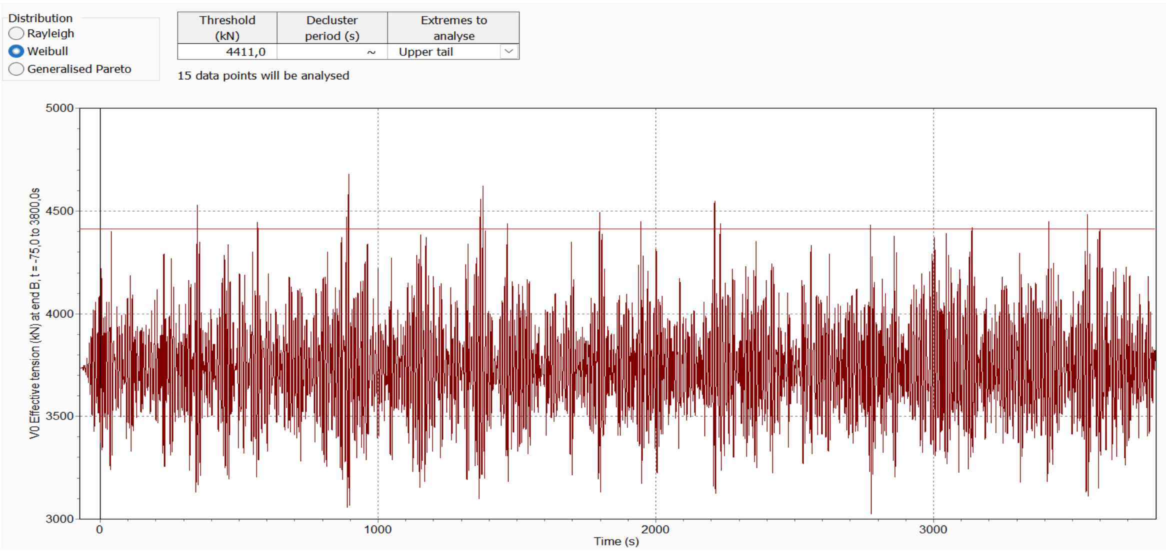

Figure 57 *Prototype II polyester rope 268mm*

Description of the result in the time domain series

The time domain of the spectral density curve (PSD) is a measured over a time of 3800 seconds. As illustrated in the time series the peak values respond to a wave direction of 180° for the vertical steel wire of 185 mm, 100 mm, and polyester rope 268 mm.

The time series that are presented has relatively equal behavior seen from 0s -3800s. From a statistical point of view the mean value shows a rather equal tension between each 1000 of a second. However, the values are very high between the outer and mean values. Nevertheless, it could also be seen that the values have very small iterations (compressed amplitudes) and fast cycles of high frequency. This could be based on when the wave loads create a drift force towards the platform and marine buoy the mooring wires creates a tension and slack (elongation and compression) However, there are 6 measurements which are above 3500 KN and are based in the region between 0-1000s and are quite large compared to the series between 1000-2000 and 2000-3800s. The simulation test could also provide errors and is based on the longitude coefficient in the software is set to low 1.2 based on the input values of the test, and therefore could provide some given errors.

17.1 Result of the mooring tension for prototype I.

The statistic response result of each dynamic tension load evaluated at 3800s for each simulation.

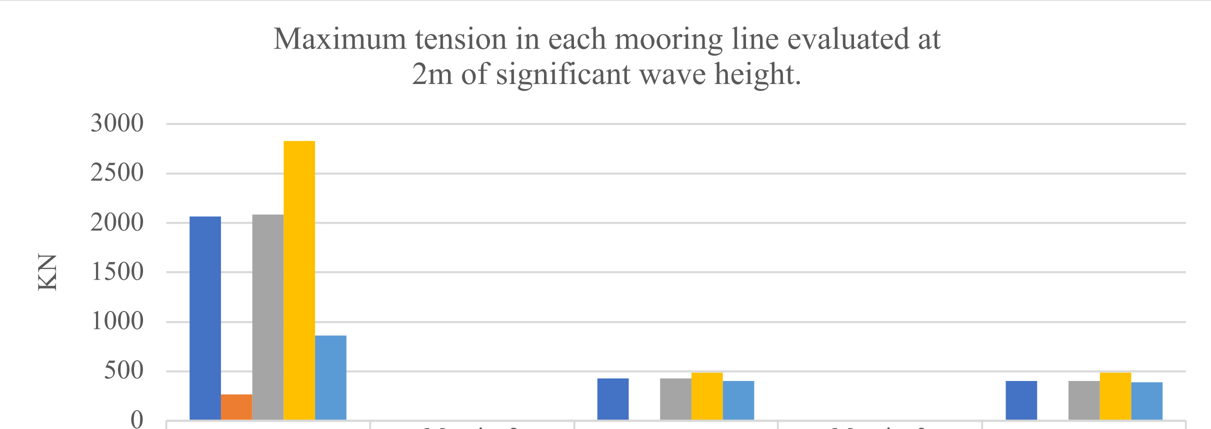

		Mooring2		Mooring3	
Mean	2064,31165	0	430,736565	0	403,6327241
Std. Dev.	266,7665008	0	9,574413234	0	9,534483301
RMS	2081,477109	0	430,8429619	0	403,7453187
max	2827,833427	0	484,0797669	0	484,1790736
min	859,3022123	0	399,9299669	0	387,9475812

***Graphs 3** Significant wave heights $H_s = 2m$, significant periods $T_P = 4$, wind speed$U_w = 10.5m/s$ 185mm Studdles link chain.*

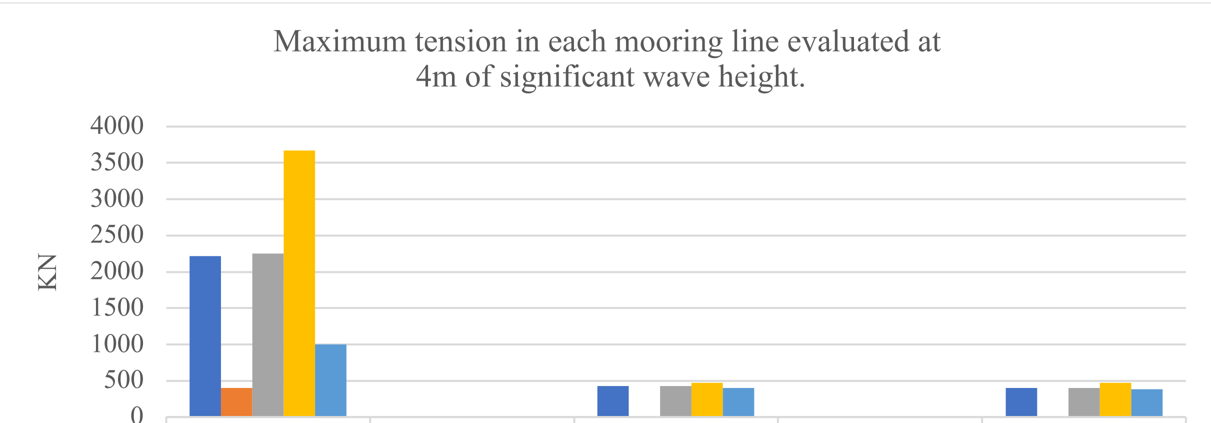

		Mooring2		Mooring3	
Mean	2216,785476	0	426,9035426	0	401,6929409
Std. Dev.	399,1295448	0	9,564746115	0	9,075047379
RMS	2252,430297	0	427,0106779	0	401,7954395
max	3667,354468	0	472,5003435	0	472,7674023
min	1000,425897	0	399,8681324	0	384,3840669

***Graphs** 4 Significant wave heights $H_s = 4m$, significant periods $T_P = 6$, wind speed$U_w = 10.5m/s$ 185 mm studdles link chain.*

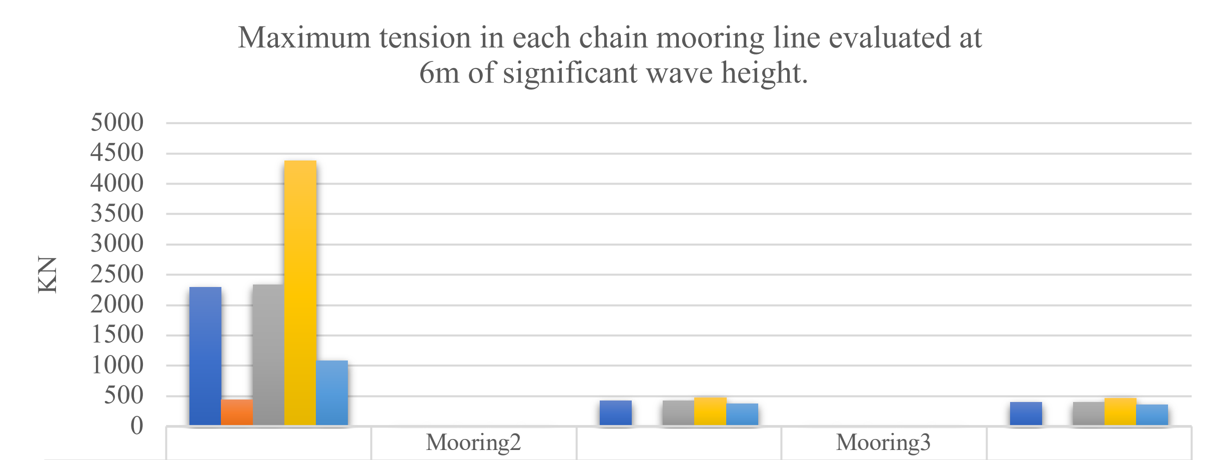

		Mooring2		Mooring3	
Mean	2293,453442	0	425,8427707	0	401,8570828
Std. Dev.	445,169223	0	11,01251043	0	10,25989985
RMS	2336,258617	0	425,9851414	0	401,9880354
max	4376,265238	0	478,3742888	0	469,2525334
min	1085,392035	0	377,7928694	0	360,4979641

***Graphs 5** Significant wave heights $H_s = 6m$, significant periods $T_P = 8$, wind speed$U_w = 10.5m/s$ 185 mm studdles link chain.*

17.2 Result of the mooring tension for prototype II

The statistic response result of each dynamic tension load evaluated at 3800s for each simulation.

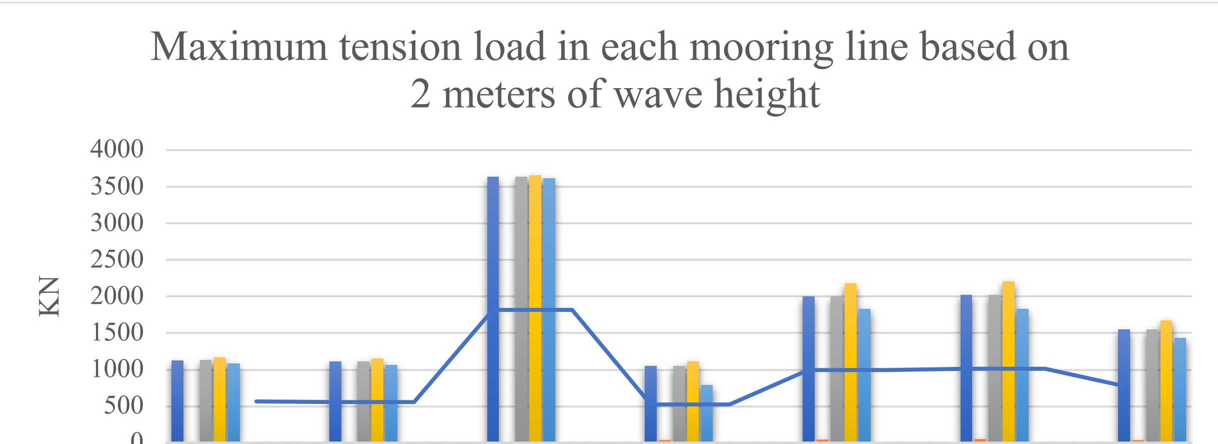

		ML4		V0		ML3		ML2		ML6		ML5	
Mean	1127,5	0	1110,3	0	3634,8	0	1050,1	0	1997,2	0	2021,9	0	1546,4
Std. Dev.	15,59	0	15,517	0	4,8933	0	45,586	0	49,947	0	57,23	0	38,016
RMS	1127,6	0	1110,4	0	3634,9	0	1051	0	1997,8	0	2022,7	0	1546,8
max	1167,9	0	1155,1	0	3654,2	0	1115,3	0	2178	0	2205,8	0	1674,1
min	1084,1	0	1062,5	0	3615,7	0	794,64	0	1829,2	0	1826,1	0	1435,2

***Graphs 6** Significant wave heights $H_s = 2m$, significant periods $T_P = 4$, wind speed$U_w = 10.5m/s$ 100mm (6X19 strands steel wire)*

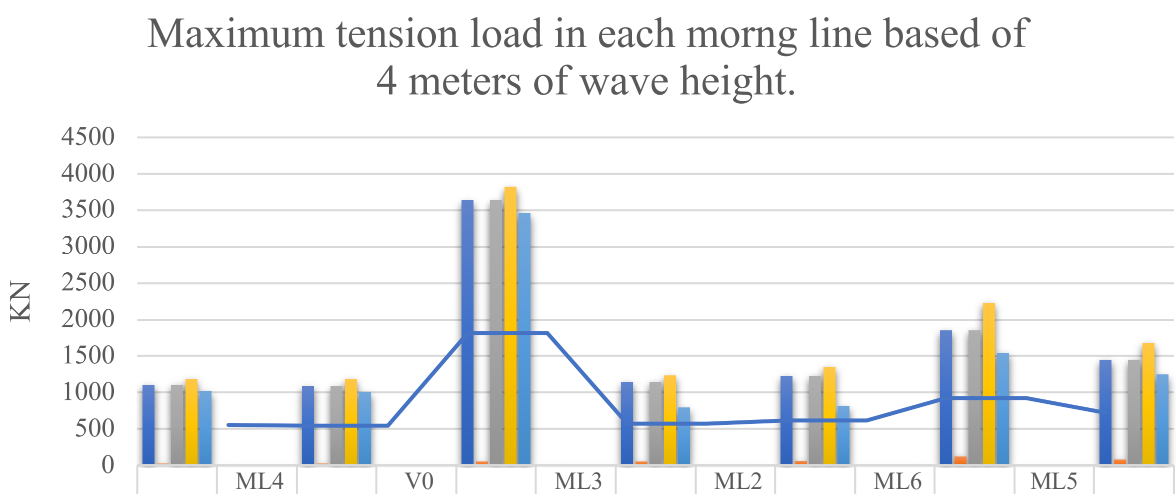

		ML4		V0		ML3		ML2		ML6		ML5	
Mean	1105,4	0	1087,8	0	3633,6	0	1144,4	0	1225,6	0	1847,5	0	1444,9
Std. Dev.	31,024	0	32,514	0	56,446	0	57,651	0	61,549	0	126,14	0	82,016
RMS	1105,8	0	1088,3	0	3634	0	1145,9	0	1227,1	0	1851,8	0	1447,2
max	1186,1	0	1184,3	0	3818,5	0	1232,3	0	1348,3	0	2229,5	0	1680,7
min	1019	0	1003,2	0	3453,8	0	790,34	0	811,63	0	1542,8	0	1243,5

***Graphs** 7 Significant wave heights $H_s = 4m$, significant periods $T_P = 6$, wind speed$U_w = 10.5m/s$ 100mm (6X19 strands steel wire)*

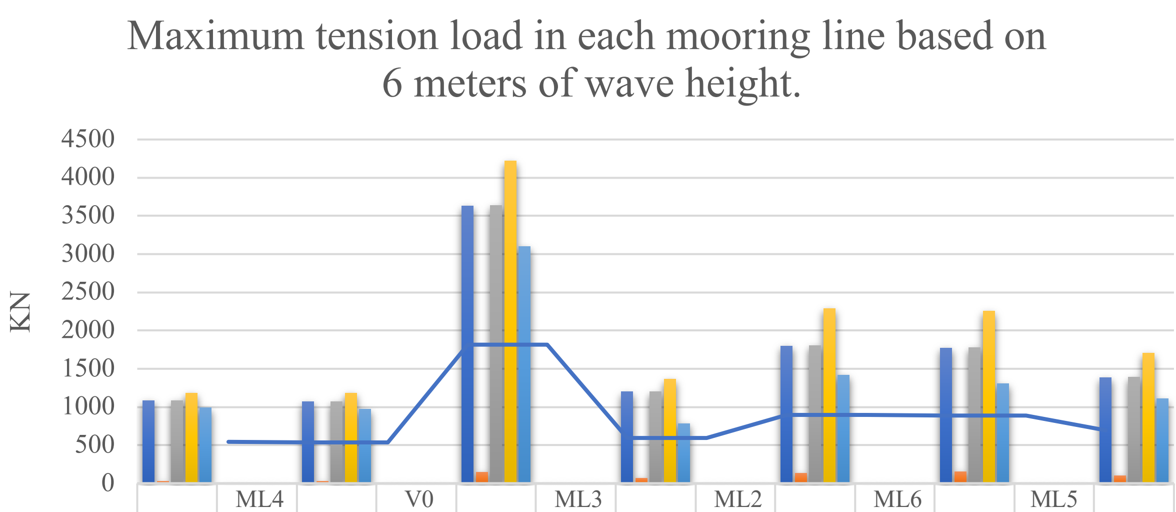

		ML4		V0		ML3		ML2		ML6		ML5	
Mean	1087,6	0	1073,9	0	3631,6	0	1198,1	0	1800,1	0	1771,9	0	1385,3
Std. Dev.	32,395	0	32,469	0	153,67	0	73,381	0	137,74	0	159,09	0	104,58
RMS	1088,1	0	1074,4	0	3634,8	0	1200,4	0	1805,4	0	1779,1	0	1389,2
max	1182,7	0	1184,8	0	4220,8	0	1363	0	2291	0	2253,1	0	1706,5
min	992,85	0	972,49	0	3098,2	0	786,65	0	1419,1	0	1304,7	0	1109,5

***Graphs 8** Significant wave heights $H_s = 6m$, significant periods $T_P = 8$, wind speed $U_w = 10.5m/s$ 100mm (6X19 strands steel wire)*

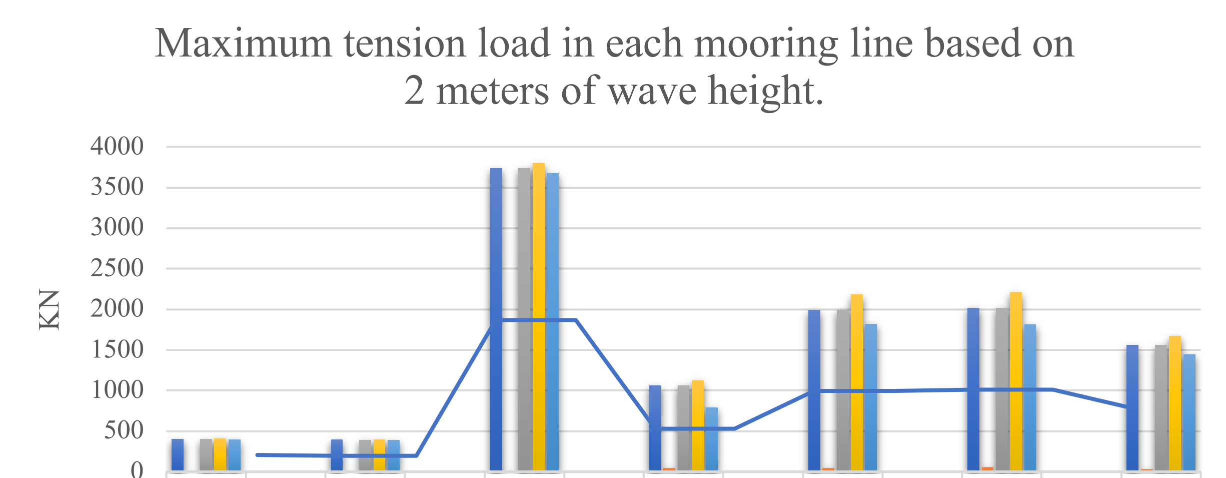

		ML4		V0		ML3		ML2		ML6		ML5	
Mean	404,46	0	390,85	0	3734,5	0	1059,4	0	1989,4	0	2015,7	0	1556,1
Std. Dev.	2,8166	0	2,0647	0	16,143	0	49,392	0	49,965	0	59,486	0	34,649
RMS	404,47	0	390,86	0	3734,6	0	1060,5	0	1990	0	2016,5	0	1556,5
max	412,75	0	396,39	0	3796,5	0	1122,4	0	2179,2	0	2208	0	1670,4
min	396,11	0	384,73	0	3673	0	792,59	0	1819,3	0	1809,8	0	1445

Graphs 9 *Significant wave heights* $H_s = 2\ m$*, significant periods* $T_P = 8\ s$*, wind speed* $U_w = 10.5\ m/s$*, 268mm polyester rope*

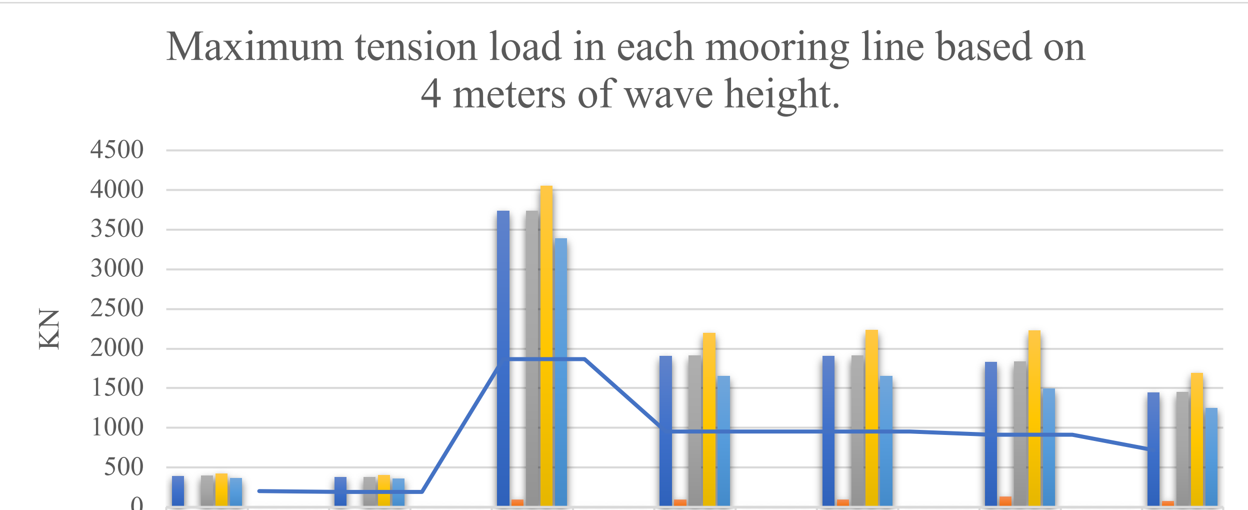

		ML4		V0		ML3		ML2		ML6		ML5	
Mean	398,15	0	384,27	0	3734,2	0	1906,9	0	1906,1	0	1828,7	0	1446,8
Std. Dev.	9,1662	0	6,5366	0	100,68	0	100,32	0	101,98	0	135,13	0	80,506
RMS	398,25	0	384,33	0	3735,6	0	1909,5	0	1908,8	0	1833,6	0	1449,1
max	427,7	0	407,93	0	4053,1	0	2197,2	0	2231,9	0	2227,4	0	1692,3
min	371,32	0	363,76	0	3386,4	0	1652,9	0	1651,6	0	1497,1	0	1253,1

Graphs 10 *Significant wave heights* $H_s = 4\ m$*, significant periods* $T_P = 6\ s$*, wind speed* $U_w = 10.5\ m/s$*, 268mm polyester rope*

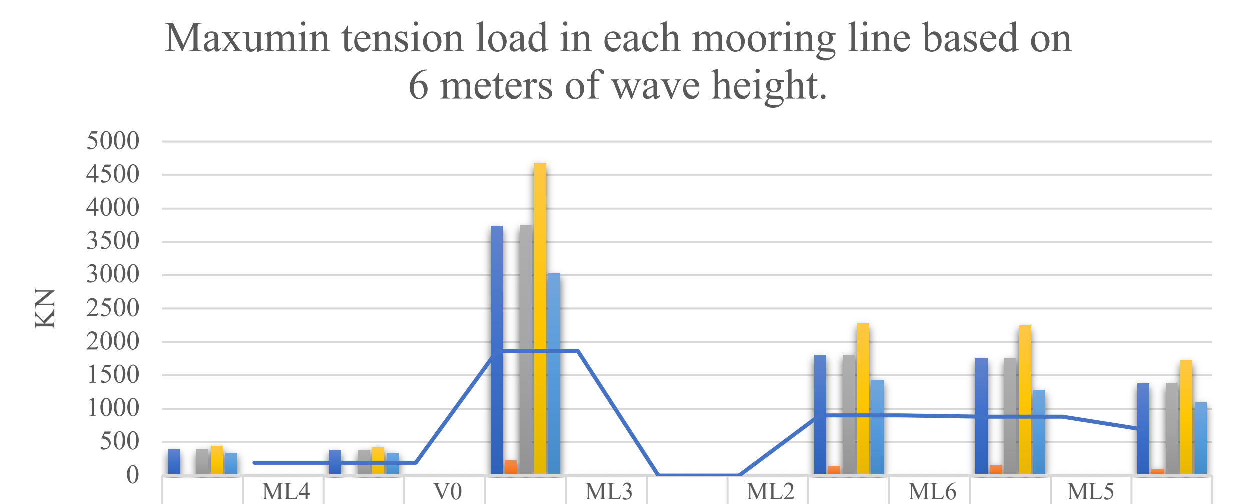

		ML4		V0		ML3		ML2		ML6		ML5	
Mean	392,95	0	382,01	0	3733,4	0	0	0	1802,4	0	1755,1	0	1380,6
Std. Dev.	15,718	0	11,783	0	225,94	0	0	0	133,92	0	166,53	0	105,03
RMS	393,27	0	382,19	0	3740,2	0	0	0	1807,4	0	1763	0	1384,6
max	445,69	0	435,69	0	4678	0	0	0	2276,9	0	2247	0	1720
min	342,42	0	346,89	0	3025,8	0	0	0	1430,6	0	1282,2	0	1096,5

Graphs 11 *Significant wave heights* $H_s = 6\ m$*, significant periods* $T_P = 8\ s$*, wind speed* $U_w = 10.5\ m/s$*, 268mm polyester rope*

Extreme condition (Jonswap) sea state conditions.

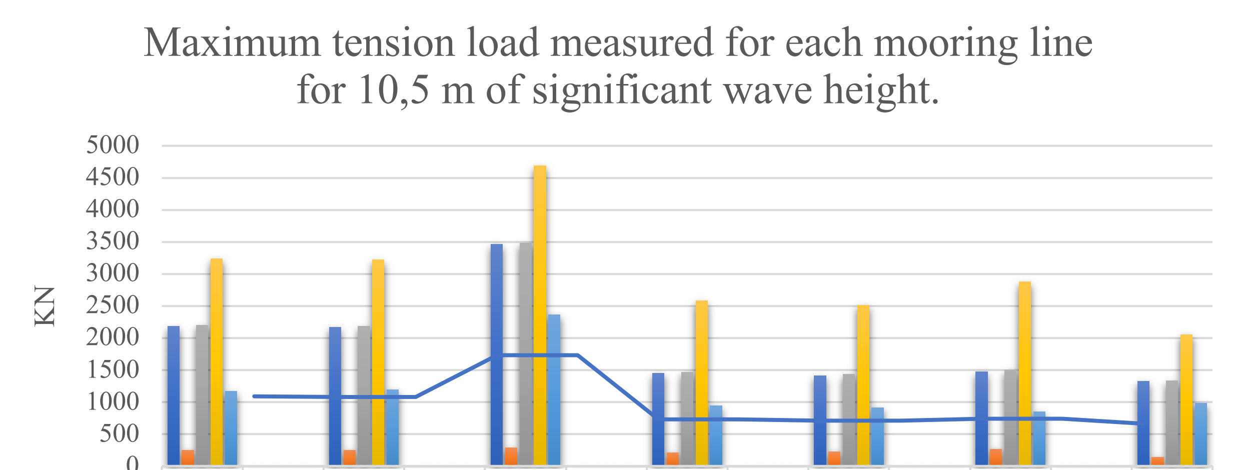

		ML4		V0		ML3		ML2		ML6		ML5	
Mean	2183,2	0	2167,7	0	3464,2	0	1451,8	0	1416,3	0	1475,7	0	1326,7
Std. Dev.	257,98	0	258,85	0	292,18	0	216,76	0	229,63	0	275,28	0	148,55
RMS	2198,4	0	2183,1	0	3476,5	0	1467,9	0	1434,8	0	1501,2	0	1335
max	3234,8	0	3220,2	0	4687,3	0	2585,2	0	2512,6	0	2876,1	0	2054,7
min	1172,9	0	1193,3	0	2366,8	0	945,26	0	915,02	0	852,29	0	982,69

Graphs 12 *Significant wave heights* $H_s = 10{,}5\ m$*, significant periods* $T_P = 14.5\ s$*, wind speed* $U_w = 9.2\ m/s$*, 150mm steel wire with fiber core*

The table below provides the measurements of the simulation test defined for both prototypes I and II. Maximum tension results.

***Table 40** provides the test result of the measures of the tension in the mooring lines.*

Result of the load cases	***Nominal diameters mm***	***2m* (KN)**	**4m (KN)**	**6m (KN)**
Prototype I				
Mean ML1	*185mm*	***2046.31***	**430.73**	**403.63**
Mean ML2	*185mm*	***2226.78***	**426.90**	**401.69**
Mean ML3	*185mm*	***2293.45***	**425.84**	**401.85**
Maximum ML1	*185mm*	***2827.83***	**3667.35**	**4376.26**
Maximum ML2	*185mm*	***484.079***	**472.50**	**478.37**
Maximum ML3	*185mm*	***484.17***	**472.76**	**469.25**
Stv.Dt ML1	*185mm*	***266.76***	**399.12**	**445.169**
Stv.Dt ML2	*185mm*	***9.57***	**9.56**	**11.012**
Stv.dt ML3	*185mm*	***9.53***	**9.075**	**10.259**
Prototype II				
Mean ML2	*185mm*	***1997.2***	**1225.6**	**1800.1**
Mean ML3	*185mm*	***1050.1***	**1144.4**	**1198.1**
Mean ML5	*185mm*	***1546.4***	**14444.9**	**1385.3**
Mean ML6	*185mm*	***2021.9***	**1847.5**	**1771.9**
Maximum ML2	*185mm*	***2178***	**1348.3**	**2291**
Maximum ML3	*185mm*	***1115.3***	**1232.3**	**1363**
Maximum ML5	*185mm*	***1674.1***	**1680.7**	**1706.5**
Maximum ML6	*185mm*	***2205.8***	**2229.5**	**2253.1**
Std. Dev ML2	*185mm*	***49.947***	**61.549**	**137.74**
Std. Dev ML3	*185mm*	***45.586***	**57.651**	**73.381**
Std. Dev ML5	*185mm*	***38.016***	**82.016**	**104.58**

STd.Dev ML6	*185mm*	***57.23***	**126.14**	**159.09**
Prototype II				
Mean V0	*100mm*	***3634.8***	**3633.6**	**3631.6**
Mean ML1	*100mm*	***1127.5***	**1105.4**	**1087.6**
Mean ML4	*100mm*	***1103.3***	**1087.8**	**1073.9**
Maximum V0	*100mm*	***3654.2***	**3818.5**	**4220.8**
Maximum ML1	*100mm*	***1167.9***	**1186.1**	**1182.7**
Maximum ML4	*100mm*	***1155.1***	**1184.3**	**1184.8**
Std.Dv V0	*100mm*	***4.89***	**56.446**	**153.67**
Std.Dv ML1	*100mm*	***15.59***	**31.024**	**32.395**
Std.Dv ML4	*100mm*	***15.517***	**32.514**	**32.469**
Mean V0	*268mm*	***3734.5***	**3734.2**	**3733.4**
Mean ML1	*268mm*	***404.46***	**398.15**	**398.95**
Mean ML4	*268mm*	***390.85***	**384.27**	**382.01**
Maximum V0	*268mm*	***3796.5***	**4053.1**	**4678**
Maximum ML1	*268mm*	***412.75***	**427.7**	**445.69**
Maximum ML4	*268mm*	***396.39***	**407.93**	**435.69**
Std.Dv V0	*268mm*	***16.143***	**100.68**	**225.94**
Std.Dv ML1	*268mm*	***2.8166***	**9.1662**	**15.718**
Std.Dv ML4	*268mm*	***2.0647***	**6.5366**	**11.783**

Evaluation of the maximum tension compared between a single offshore turbine Vs two shared solution. From this it is showed from numerical data that polyester rope creates larger tension compared to steel wires 100mm. For comparing highest mooring tension for a single OFWT with the shared mooring arrangement it could be seen that 4376>4220KN.

18 Discussion of the comparison of the reasons result.

For random significant wave heights for 2, 4 and 6 meters:

Steel wire with fiber core 100mm, explanation of maximum tension for ML1, ML4 and V0 on the marine buoy.

The result of the maximum mooring line tension was estimated with various wave loads onto the configuration system for prototype 2, with 100mm steel wires. From this test results there was some interesting founding's in relation to the maximum tension load for ML1 and ML4, connected to the buoy; in case where the steel wires were performed, the indication showed that for larger significant wave heights, and shorter significant periods, created the highest mooring tension seen for the result graphs. This is also mentioned by (Chai-Cheng Huang et al, 2018, s. 110), that the longest waves and shorter wave periods creates the higher tension in the mooring lines. This could also be explained since the velocity speed is higher for shallow waters and would causes larger tension in the mooring lines (Chai-Cheng Huang et al, 2018, s. 110) Moreover, shallow waters increases the tension and becomes proportional to the mean tension.

These compared for steel wire ML1 for 6-2meters and 4-2meters of significant wave height and corresponded to the founding's by (Chai-Cheng Huang et al, 2018, s. 110) However, when comparing mooring line ML1, with the significant wave heights of 4 m and 6 m, the tension load was slightly higher for 4 meters (1186.1 KN) in contrast to 6 meters (1182 KN), In response to the vertical mooring line V0 between the buoy and suction anchor, the tension indicates the highest peak tension for wave height of 6m (4220.8KN), thus, shorter steep periods, and followed by 4m (3818.48KN) and 2m (3654.2KN). Since the line tension for all value on the vertical wire are very high in connection to the calm base buoy would be because the buoy is set 30 meters below the water level and is affected only by current forces. The relation is mentioned by (Chai-Cheng Huang et al, 2018, s. 110) that the drag force acting on the buoy in water would be a proportional factor to the velocity of the fluid. This is because the buoy is in water which transmit the large tension forces from the current forces to the mooring lines (Chai-Cheng Huang et al, 2018, s. 110)

Explanation of maximum tension for Polyester rope 268mm for ML1, ML4 and V0 on the marine buoy.

In case for polyester rope 268 mm the maximum mooring tension indicated smaller values compared to steel wires for mooring line ML1 and ML4. However, the vertical polyester rope (V0) indicated a higher values 4678KN for all given values than the vertical steel wire. The test for comparing the same mooring line ML1 between various significant wave height of 2m, 4m and 6 m, the highest tension load was caused for 6 meters of significant wave heights and followed by 4meters and 2 meters. In this case, it corresponds very similar to the founding's mentioned by (Chai-Cheng Huang et al, 2018, s. 110) regarding a fish net. The indication on the vertical polyester rope is more in the same manner as the wire rope. This could be explained because of higher velocity speed for shallow waters causes larger tension in the mooring lines (Chai-Cheng Huang et al, 2018, s. 110) and the drag force acting on the buoy becomes a proportional factor to the velocity of the fluid, thus, the buoy is 30 meters below water level. Therefore, the buoy transmits large current forces acting towards the buoy and creates very high-tension values in the mooring lines (Chai-Cheng Huang et al, 2018, s. 110)

20 Conclusion

The Objective of this study was to estimate the cost driver in relation to the cost life cycle LCC of the OFWTs based on methods defined in chapter 2.2. The methods of the chosen model were referred to IEC international standard. The result showed that capital expenditure (CAPEX) indicated a 10.55 $/Kwh for a 15MW wind farm with a fixed rate of 8%. The following cost drivers, such as operation and maintenance (OPEX) were respectively 0.655 $/KWh and decommissioning (DECOM) 6.665 $/KWh. However, the operation and maintenance were based on a one-year periods, meaning 12 months., The estimated cost for development and consenting was USD 1.848.284, platform USD 7.013.85, Turbine USD 2.996.418, Mooring USD 4.274.413, Installation USD 1.207.202, Operation & maintenance USD 1.076.546. Based on this the cost of mooring installation in this thesis was higher compared to (Ågortnes, 2013, s. 67) estimates for the Platform and mooring configuration Wind Float (defined in chapter 10.1, graph. 1 on page. 48.)

The simulation test was to investigate the maximum mooring tension based on each mooring line of significant wave heights of 2, 4 and 6 meters and the responding cycle periods. The result of the maximum mooring tension was estimated with various wave loads onto the configuration system for prototype II. The largest tension was developed in the vertical tensioned line V0(polyester 268 mm) 4678KN for mooring material polyester compared toV0100mm steel wire. However, this was not the case when evaluating the sidelines with polyester rope ML1 and ML4. The steel wires for ML1 and ML4 had higher tension than for polyester. The indication showed that for larger significant wave heights, and shorter significant wave periods, creates the highest mooring tension in the mooring lines based on the graphs. Moreover, mentioned by (Chai-Cheng Huang et al, 2018, s. 110) that the buoy in water would be a proportional factor to the velocity of the fluid and the forces on the calm base buoy would transmit all the current forces to the mooring lines. Therefore, the mooring buoy is very effected by the period of wave-, current forces, and the wave direction onto the platform structure and the submerged marine buoy in water.

21 Future work

Future work that could be a possible investigation is to use 9.5 Hexagonal farm layout arrangement to evaluate the cost of life cycle. Moreover, to make a response analyze based on three 15 MW CSC-semi turbines with a buoy to evaluate the mooring tension on the buoy. This in relation to several sea states.

22 Reference list:

abc-mooring.weebly. (2023, May 13). *abc-mooring.weebly.com*. Retrieved from http://abc-moorings.weebly.com: http://abc-moorings.weebly.com/mooring-systems.html

Abc-moorings. (2023, April 27). *abc-moorings*. Retrieved from abc-moorings: http://abc-moorings.weebly.com/mooring-systems.html

Aceton . (2023, May 5). *www.globalunderwaterhub,com.* Retrieved from globalunderwaterhub: https://www.globalunderwaterhub.com/documents/presentations/lloyd%20inglis%20-%20subsea%20technologies%20for%20offshore%20renewables.pdf

Ala' K. Abu-Rumman et al. (2017, October (Accepted) 29). Cycle Costing of Wind Generation System. *Jourenal of Applied reseach on indutial Engineering. Vol. 4, No. 3 (2017)185–191*, pp. 185-191.

al, Jens N. Sørensen et. (2018, August 6). Towards the North Sea wind power revolution. *Wind Energ. Sci. Discuss., https://doi.org/10.5194/wes-2018-53*, pp. 1-27.

Alberto Ghigo et al. (2020, October (Published) 23). Platform Optimization and Cost Analysis in a Floating Offshore Wind Farm. *Journal of Marine Science and Engineering*, pp. 1-26.

Alibaba.com. (2023, April 3). *Alibaba.com*. Retrieved from Alibaba: https://www.alibaba.com/product-detail/Factory-price-cylindrical-mooring-steel-buoy_1600468434706.html

Alibaba.com. (2023, May 1). *www.alibaba.com.* Retrieved from alibaba: https://www.alibaba.com/product-detail/High-Buoyancy-IALA-Cross-Type-Steel_60779829232.html?spm=a2700.shop_plfe.41413.16.569e7365c6QnUJ

American Bureau of Shipping (ABS). (2017). *GUIDE FOR THE CERTIFICATION OF OFFSHORE MOORING CHAIN.* American Bureau of Shipping Incorporated by Act of Legislature of the State of New York 1862: American Bureau of Shipping (ABS).

Are Opestad Sæbø, Kristin Guldbrandsen. (2023, April 23). *https://api.greenstat.no.* Retrieved from https://api.greenstat.no: https://api.greenstat.no/uploads/optimal_utnyttelse_av_energi_fra_havvind_i_sorlige_nordsjo_ii_hr_1a34742514.pdf?updated_at=2022-10-06T14:26:18.575Z

Are Opstad sæbø et al. (2021). *Greenstate making green happen.* Bergen (Not spesified): Greenstate, Høgskulen på Vestland, University of Bergen m.m.

Are Optad Sæbø,Kristin Gulbrandsen. (2020, April 23). *https://api.greenstat.no.* Retrieved from https://api.greenstat.no: https://api.greenstat.no/uploads/optimal_utnyttelse_av_energi_fra_havvind_i_sorlige_nordsjo_ii_hr_1a34742514.pdf?updated_at=2022-10-06T14:26:18.575Z

Axelsson, T. (2008, Not spesified Not spesified). *cdn.b12.io.* Retrieved from cdn.b12.io: https://cdn.b12.io/client_media/n8KzZTRM/b0590e9e-d2e8-11eb-be12-0242ac110002-Energy_Ocean_08_3U_Technologies_080619.pdf

Ågortnes, C. B. (2013). *Levelized costs of energy for offshore floating wind turbine concepts.* Ås: Norwigian University of life sciences: department of mathematical sciences and technology.

Ågotnes, C. B. (2013). *Levelized costs of energy for offshore floating wind turbine concepts.* Ås: Norwigan University of life sciences.

Bureau of ocean energy management, Boem. (2011, October (slide publised) 11). *boem.gov*. Retrieved from www.boem.gov: https://www.boem.gov/sites/default/files/documents/renewable-energy/state-activities/RWF_Project_construction_and_cable_laying_508.pdf

Castellà, X. T. (2020). *OPERATIONS AND MAINTENANCE COSTS FOR OFFSHORE WIND FARM.* Not spesified: UNIVERSITAT POLITÈCNICA DE CATALUNYA.

C.D. O'Loughlin et al. (2015, May 4-7). Novel Anchoring Solutions for FLNG - Opportunities Driven by Scale. *Offshore Technology Conference held in Houston, Texas, USA, 4–7 May 2015.*, pp. 1-29.

CDIP mobile. (2023, April (added) 20). *ucsd.edu.* Retrieved from Cdip: http://cdip.ucsd.edu/m/documents/_downloads/5abe5c75d20e4047af274588ee993d11/buoy_watch_circle.pdf

Chai-Cheng Huang et al. (2018, January (accepted) 7). Effects of waves and currents on gravety-type cages in the open sea. *Sicencedirect acualtural engineering 38 (2008) 105-116*, pp. 105-116.

Christopher Allen et al. (2020). *Definition of the UMaine VolturnUS-S Reference Platform Developed for the IEA Wind 15- Megawatt Offshore Reference Wind Turbine.* National Renewable Energy Laboratory 15013 Denver West Parkway Golden, CO 80401: NREL is a national laboratory of the U.S. Department of Energy Office of Energy Efficiency & Renewable Energy Operated by the Alliance for Sustainable Energy, LLC.

Christopher Allen et al. (2020). *IEA Wind TCP Task 37 Definition of the UMaine VolturnUS-S Reference Platform Developed for the IEA Wind 15- Megawatt Offshore Reference Wind Turbine Technical Report.* National Renewable Energy Laboratory 15013 Denver West Parkway Golden, CO 80401: University of Main, National renewabe energy laboratory.

Costra-Santos, L. (2013, March 20). Methodology to calculate mooring and anchoring costs of floating offshore wind devices. *Researhgate*, pp. 268-272.

Costro-Santos, L. (2016). *Life-cycle cost of a floating offshore wind farm.* A Coruna Ferrol 15403, Spain: Universidade da Coruna.

CRP subsea. (2023, Mai 1). *Crp subsea an Ais company.* Retrieved from CRP subsea: https://www.crpsubsea.com/products/product-families/buoyancy-floats/installation-buoyancy/modular-buoy/

Det Norske Veritas. (2013, October Not spesified). *https://dokumen.tips/download/link/dnv-os-e302-offshore-mooring-chain.html.* Retrieved from https://dokumen.tips: https://dokumen.tips/download/link/dnv-os-e302-offshore-mooring-chain.html

Dimitrios Loukidis et al. (2014, June, April (Uploaded) 22). Limit lateral resistance of vertical piles in plane strain. *Researchgate DOI: 10.1201/b17017-122*, pp. 681-685.

DNV. (2021, June Not specified). *https://brandcentral.dnv.com.* Retrieved from brandcentral.dnv.com: https://brandcentral.dnv.com/fr/gallery/10651/others/09cdc0a1a0d54a58a698f9f51ff625d2_hi.pdf?_ga=2.193175213.1611469586.1684082821-2034977491.1684082821

DNVGL AS. (2018, July Not specified). *Position mooring.* Retrieved from https://dokumen.tips/download/link/dnvgl-os-e301-position-general-updates-based-on-experience-and-feedback-ch2-sec4.html: https://dokumen.tips/documents/dnvgl-os-e301-position-general-updates-based-on-experience-and-feedback-ch2-sec4.html

Espen Oland et al. (2017, Not spesified Not spesified). Condition Monitoring Technologies for Synthetic Fiber Ropes - a Review . *International Journal of Prognostics and Health Management, ISSN2153-2648, 2017 014*, pp. 1-14. Retrieved from phmsociety.org: https://www.google.no/url?sa=i&rct=j&q=&esrc=s&source=web&cd=&ved=0CAIQw7AJahcKEwjg2uyX3_7-AhUAAAAAHQAAAAAQAg&url=https%3A%2F%2Fpapers.phmsociety.org%2Findex.php%2Fijphm%2Farticle%2Fdownload%2F2619%2F1577&psig=AOvVaw24xiaUCz7YGJx80KTBkrpc&ust=168449483498

Evan Gaertner et al. (2020). *Definition of the IEA 15-Megawatt Offshore Reference Wind.* National Renewable Energy Laboratory 15013 Denver West Parkway Golden, CO 80401 303-275-3000: National laboratory of the U.S Department of energy office.

Even Geertner et al. (2020, March). Definition of the IEA wind 15-megawatt offshore referance wind turbine technical report. *National renewable energy laboratory*, pp. 1-44.

Evgeniy Dimkin at DNVGL noble Denton. (2019, April 4). *mcedd.com.* Retrieved from www.mcedd: https://mcedd.com/wp-content/uploads/2019/04/MCEDD-2019-Evgeniy-Dimkin.pdf

Focus-economics. (2023, April 6). *focus-economics*. Retrieved from www.focus-economics.com: https://www.focus-economics.com/commodities/base-metals/steel-usa/

Fontana, C. (2019). *A Multiline Anchor Concept for Floating Offshore Wind Turbines.* UNIVERSITY OF MASSACHUSETTS AMHERST: University of Massachusetts Amherst University of Massachusetts Amherst.

Fortress marine anchors. (2023, March 5). *fortressanchors*. Retrieved from www.fortressanchors.com: https://fortressanchors.com/product/fortress-anchor/

Fredrik von Schlanbusch & Asgeir Sorteberg. (2022). *Driving Factors for Levelized Cost of Energy in Floating Wind Farms.* Nygårdshøyden: University of Bergen.

Godfrey Boyle et al. (2012). Renewable energy power for sustainable future fourth edition. In G. B. al, *power for sustainable future fourth edition* (pp. 1-656). 198 Madison Avenue, New York, NY 10016, Unite Tates of America: United state of America by Oxsford University press.

Gofrey Boyle et al. (2012). *Renewable energy power for a sustainable future; fourth edition.* 198 Madison Avenue, New York, NY 10016, United States of America: Oxford university press.

handsmetals.co.uk. (2023, May 5). *handsmetals.co.uk*. Retrieved from www.handsmetls.co.uk: https://www.handsmetals.co.uk/scrap-metal-prices/

H Munir et al. (2021, May (conferance meeting) 28). Global analysis of floating offshore wind turbines with shared mooring system. *IOP Conf. Series: Materials Science and Engineering 1201 (2021) 012024 doi:10.1088/1757-899X/1201/1/012024*, pp. 1-13.

H Munir, MC Ong. (2021, October 9-13). Global analysis of flating wind turbines with shared mooring system. *IOP Conference series: materials science and engineering 201 (2021) 012024*, pp. 1-14.

hydrosphere.co.uk. (2014, September Not spesified). *hydrosphere.co.uk*. Retrieved from https://hydrosphere.co.uk: https://hydrosphere.co.uk/datasheets/hydrosphere_mobilis-amr_17000-5000_v_2_01_sep_14_web.pdf

Hyungjun Kim et al. (2014, June 8-13). Design of Mooring Lines of Floating Offshore Wind Turbine in Jeju Offshore Area. *Journal of the Society of Naval Architects of Korea · August 2014, DOI: 10.1115/OMAE2014-23772* , pp. 1-12.

Ibbrahim Engine Taze. (2022, Agust 31). *Master thesis : Deepwater Mooring Analysis for a 15 MW Seme-submersible FOWT located at the Morro Bay Wind Energy Area, California.* Faculté des Sciences appliquées.

Ingo Jermin et al. (2009, June 8). LIFE CYCLE COST ANALYSIS OF TRANSMISSION AND DISTRIBUTION SYSTEMS. *C I R E D 20th International Conference on Electricity Distribution Prague, 8-11 June 2009 Paper 0098*, p. 4.

Iñigo Mendikoa Alonso. (2021, July 6). *twindproject.eu*. Retrieved from https://twindproject.eu: https://twindproject.eu/wp-content/uploads/2021/07/G-KN2_Inigo.pdf

J.M.J. Journee et al. (2001). Offshore hydrodynamics first edition. In J. Journee. Delft Univesity of technology.

jinbomarine. (2023, May 7). *jinbomarine*. Retrieved from www.jinbomarine.com: https://www.jinbomarine.com/ws-vertical-loaded-ancor-vla-anchor-modu.html

john F. Flory et al. (2004, May 6). Defining, Measuring, and Calculating the Properties of Fiber Rope Deepwater Mooring Lines. *Offshore Technology Conference, https://www.researchgate.net/publication/254518629*, pp. 1-15.

Jorge Altuzarra et al. (2022, September (published) 22). Mooring System Transport and Installation Logistics for a Floating Offshore Wind Farm in Lannion, France. *Journal of marine science and engineering. 2022, 10(10), 1354;*.

Jump, E. (2021, July 10). *Catapult offshore renewable energy.* Retrieved from ORE.CATAPULT.ORG.UK: https://ore.catapult.org.uk/wp-content/uploads/2021/12/PN000413-RPT-003-Rev-2-Mooring-and-Anchoring-Market-Projections_Formatted.pdf

Jump, E. (2021). *MOORING AND ANCHORING SYSTEMS - MARKET PROJECTIONS FLOATING OFFSHORE WIND CENTRE OF EXCELLENCE.* Inovo 121 George Street Glasgow G1 1RD: Catapult offshore renewable energy.

Junho Lee et al. (2021, July (uploaded) 6). Installability of a Multiline Ring Anchor System in a Seabed under Severe Environmental Conditions. *Researchgate DOI: 10.23919/OCEANS44145.2021.9705679*, pp. 1-9.

Kabir Sadeghi et al. (2019, March Not specified). SEMISUBMERSIBLE PLATFORMS: DESIGN AND FABRICATION: AN OVERVIEW. *Academic Research International Vol. 10(1) March 2019*, pp. 28-38.

Karsten M et al. (2020, July 24). Aerodynamic characterization of barge and spar type floating offshore wind turbines at different sea states. *Wind EnergyVolume 23, Issue 11 p. 2087-2112*, pp. 2087-2112.

Kaasen, K. E. (2017). *Balance wave energy converter decribtion with comments.* TorgardenNO-7465 Trondheim, Norway: Sintef.

L. Castro-Santos et al. (2013, March 20). Methodology to calculate mooring and anchoring costs of floating offshore wind devices. *Researchgate*, pp. 286-272.

Lin Li et al. (2023, March 9). *https://www.gceocean.no.* Retrieved from https://www.gceocean.no: https://www.gceocean.no/media/4558/221025-offshore-wind-conference_science-meets-industry_etienne-cheynet-uib.pdf

Liu Jinsong et al. (2018). Alternative mooring systems for a very large offshore wind turbine supported by a semisubmersible floating platform. *Journal of solar energy engineering*, p. 1.

Luvside. (2020, April 1). *Luvside*. Retrieved from www.luvside.de: https://www.luvside.de/en/capacity-factor-wind-turbine/

Made-in-China. (2022, October 22). *made-in-china.* Retrieved from https://www.made-in-china.com: https://shundehai.en.made-in-china.com/product/gNtmedwVyohC/China-100mm-Jiangsu-Aohai-Mooring-Anchor-Chain-with-ABS-Nk-Dnv-Certificate.html

Made-in-china. (2023, May 1). *made-in-china.com.* Retrieved from marinefender.en.made-in-china.com: https://marinefender.en.made-in-china.com/product/GODTfJKbYRWM/China-Marine-Mooring-Anchor-Pendant-Foam-Filled-Buoys.html

Maria Ikhennicheu et al. (2020). *D3.1 Review of the state of the art of dynamic cable system design.* Not pessified: European union`s horizontal 2020 research and innovation NO 815083.

Martinez, A. I. (2021, November 17). Mapping of the levelised cost of energy for floating offshore wind in the European Atlantic. *Renewable and Sustainable Energy Reviews · February 2022 DOI: 10.1016/j.rser.2021.111889, researchgate* , pp. 1-29.

Matthew Hall & Patrick connolly. (2018, June Not specified). Coupled Dynamics Modelling of a Floating Wind Farm With Shared Mooring Lines. *Researchgate DOI:10.1115/OMAE2018-78489*.

Maximiano, A. (2021, May 31). PivotBuoy An Advanced System for Cost-effective and Reliable Mooring, Connection, Installation & Operation of Floating Wind. *Researchgate DOI: 10.13140/RG.2.2.31161.65120*, pp. 1-79.

Mert kaptan et al. (2021, November (Accepted) 20). (http://creativecommons.org/licenses/by/4.0/).Analysis of spar and semi-submersible floating wind concepts with respect to human exposure to motion during maintenance operations. *MArine structures 83 (2022) 103145*, p. 8.

Mohammad Barooni et al. (2022, December 14). Floating Offshore Wind Turbines: Current Status and Future Prospects. *Journal energies 2023, 16(1), 2; https://doi.org/10.3390/en16010002*, pp. 1-28.

Monfort, D. T. (2017). *Design optimization of the mooring system for a floating offshore wind turbine foundation.* Lisboa, Portugal: Universidade de Lisboa Instituto Superior Técnico Portugal.

Nick Cresswell et al. (2016, October Not specified). Anchor Installation for the Taut Moored Tidal Platform PLAT-O. *Researchgate*, pp. 1-8.

Nordvik, S. B. (2019). *Installation of Anchors for Mooring System of Floating Wind Turbines.* Trondheim, glasshugen: Norwigan University of science and technology.

nrel.github. (2020, January 23). *nrel.github.io*. Retrieved from nrel.github.io: https://nrel.github.io/turbine-models/IEA_15MW_240_RWT.html

NVE. (2023, fabruary 3). *temakart.nve.no*. Retrieved from temakart.nve: https://temakart.nve.no/tema/havvind

NVE. (2023). *www.NVE.no.* Retrieved from NVE: https://publikasjoner.nve.no/rapport/2023/rapport2023_04.pdf

Ocarina Ltd. (2023, March 1). *https://www.orcina.com.* Retrieved from https://www.orcina.com: https://www.orcina.com/resources/examples/?key=k

Offshore Renewable Energy Catapult. (2019, January Not specified). *thecrownestate.co.uk.* Retrieved from www.thecrownestate.co.uk: https://www.thecrownestate.co.uk/media/2861/guide-to-offshore-wind-farm-2019.pdf

Orcina Ltd. (2023, March 1). *https://www.orcina.com.* Retrieved from https://www.orcina.com: https://www.orcina.com/wp-content/uploads/examples/c/c06/C06%20CALM%20buoy.pdf

Orcina Ltd. (2023, March 1). *https://www.orcina.com.* Retrieved from https://www.orcina.com: https://www.orcina.com/wp-content/uploads/examples/k/k03/K03%2015MW%20semi-sub%20FOWT.pdf

Orcina. Ltd. (2023, March 20). *https://www.orcina.com.* Retrieved from https://www.orcina.com: https://www.orcina.com/webhelp/OrcaFlex/Content/html/Environment,DataforJONSWAPandISSCspectra.htm

Ore.catapult.org.Uk. (2021, October 7). Mooring and anchoring system-market projecttions Floating offshore wind centre of excellence. *Delivered by catapult offshore renewable energy*, pp. 1-40.

PADI International Resort Association. (1996-2005). *Mooring Buoy Planning Guide.* Published by International PADI, Inc. 30151 Tomas Street Rancho Santa Margarita, CA 92688-2125: PADI International Resort Association.

Petter andreas Berthelsen et al. (2012, July 1). CONCEPTUAL DESIGN OF A FLOATING SUPPORT STRUCTURE AND MOORING SYSTEM FOR A VERTICAL AXIS WIND TURBINE. *Proceedings of the ASME 2012 31st International Conference on Ocean, Offshore and Arctic Engineering OMAE2012 July 1–6, 2012, Rio de Janeiro, Brazil*, pp. 1-8.

Pham, H.-D. (2019). *Modeling and Service Life Monitoring of Mooring Lines of Floating Wind Turbines.* Ecole Centrale de Nantes (France): Universite Bretagne Loire.

Puglia, G. (2013). *Life cycle cost analysis on wind turbines; master of science thesis in energetic engineering.* Gotenburg, Sweden: Calmers University of technology.

Python.org. (2023, march 2). *www.python.org.* Retrieved from python.org: https://www.python.org/downloads/

Rahul Chitteth Ramachandran et al. (2021). *Floating offshore wind turbines: Installation, operation, maintenance and decommissioning challanges and opportunities.* MaREI Centre, Environmental Research Institute, University College Cork, Ireland: Wind Energy Science discussion.

Rahul Chitteth Ramachandran et al. (2021, October 25). Floating offshore wind turbines: Installation, operation, maintenance and decommissioning challenges and opportunities. *wind energy science discussions*, p. 19.

Rahul Chitteth Ramachandran et al. (2021, October 25). Floating offshore wind turbines: Installation, operation, maintenance and decommissioning challenges and opportunities. *eawe Wind energy science discussions*, pp. 1-32.

Rahul Chitteth Ramachandran et al. (2021, October (start od discussion) 25). Floating offshore wind turbines: Installation, operation, maintenance and decommissioning challenges and opportunities. *eawe wind energy science discussions*, pp. 1-32.

Reardon, M. (2023, May 2). *www.Jamestowndistribution.com.* Retrieved from jamestowndistribution: https://support.jamestowndistributors.com/hc/en-us/articles/360052013434-Mooring-Basics-How-to-install-a-permanent-mooring

Regjeringe.no. (2023, April 25). *www.regjeringen.no*. Retrieved from Regjeringen: https://www.regjeringen.no/no/tema/energi/vindkraft-til-havs/id2873850/

Ronson, K. T. (1980, May 5). *OTC ropes for deep water mooring.* Retrieved from Seilbahnen.org: https://www.google.no/url?sa=i&rct=j&q=&esrc=s&source=web&cd=&ved=0CAIQw7AJahcKEwjAy5ms3P7-AhUAAAAAHQAAAAAQAg&url=https%3A%2F%2Fwww.seilbahnen.org%2Fde%2Findex.php%3Fsection%3Ddownloads%26cmd%3D266%26download%3D12798&psig=AOvVaw0SWzs7mlFpQVpWHzBYjCQ3&ust=

Samuel Wilson et al. (2021, Not spesified Not specified). Linearized Modeling and Optimization of Shared Mooring Systems. *www.sciencedirect.com/science/article/pii/S0029801821013457*, pp. 1-19.

Shayan, H. (2017). *ECONOMIC MODELLING OF FLOATING OFFSHORE WIND POWER.* Västerås, May 2017: Mälardalen University in Västerås,Sweden.

Sintef. (2019, January 17). *www.sintef.no*. Retrieved from https://www.sintef.no: https://www.sintef.no/globalassets/project/eera-deepwind-2019/presentations/e2_yukakikuchi20190117r.pdf

Smith, L. J. (2009). *Equitable Testing and Evaluation of Marine Energy Extraction Devices in terms of Performance, Cost and Environmental Impact Grant agreement number: 213380.* University of Exeter.

sn2offshorewind. (2023, Mai 5). *sn2offshorewind.com.* Retrieved from https://sn2offshorewind.com: https://sn2offshorewind.com/infographic/

solarpontoon.wixsite. (2023, Januar 23). *https://solarpontoon.wixsite.com*. Retrieved from https://solarpontoon.wixsite.com: https://solarpontoon.wixsite.com/home/mooring-lines--anchor-systems

Steelbenchmarker. (2023, May 8). *Steelbenchmarker.* Retrieved from www.steelbenchmarker.com: http://steelbenchmarker.com/history.pdf

Subseadesign. (2023, March 12). *https://subseadesign.com*. Retrieved from https://subseadesign.com: https://subseadesign.com/products-services/suction-anchors/

Taze, I. E. (2022). *Deepwater Mooring Analysis for a 15 MW Seme-submersible FOWT located at the Morro Bay Wind Energy Area, California.* 90034 Los Angeles, USA: University of California.

T.T.Bakker et al. (2006, Not spesified Not specified). *www.Yumpu.com.* Retrieved from Yumpu: https://www.yumpu.com/en/document/read/5218610/theory-of-a-vertically-loaded-suction-pile-in-clay-offshore-moorings

thecrownstate. (2019, January Not specified). *thecrownstate.* Retrieved from www.thecrownstate.co.uk: https://www.thecrownestate.co.uk/media/2861/guide-to-offshore-wind-farm-2019.pdf

Tina Bru. (12, June 2020). *regjeringen.no.* Retrieved from www.regjeringen.no: https://www.regjeringen.no/contentassets/aaac5c76aec242f09112ffdceabd6c64/royal-decree-opening-of-areas-june-2020.pdf

Torbjørn Herberg Roksvaag et al. (2021). *Mooring of Floating Offshore Wind Turbines.* Trondheim, Glasshaugen: Norwegian University of Science and Technology Faculty of Engineering Department of Ocean Operations and Civil Engineering.

Twind offshore wind energy. (2021, July 9). *twindproject.eu*. Retrieved from https://twindproject.eu: https://twindproject.eu/wp-content/uploads/2021/07/D-SP3_Manuel.pdf

Tyler stehly et al. (2019). *2019 cost of wind energy review.* National Renewable Energy Laboratory 15013 Denver West Parkway Golden, CO 80401 303-275-3000: National renewable energy laboratory(NREL).

Ubc eooas. (2019, March Not specified). *eoas.ubc.ca.* Retrieved from www.eoas.ubc.ca: https://www.eoas.ubc.ca/courses/atsc113/sailing/met_concepts/08-met-waves/8b-wave-characteristics/index.html

Vryhof anchor . (2005). *Vryhof anchor manual 2005.* Vryhof anchors p.o. box 105, 2920 AC krimpen ad yssel, the netherlands: Vryhof.

Vryhof manual. (2015, January Not spesified). *plaisance-prtique.* Retrieved from www.plaisance-prtique.com: https://www.plaisance-pratique.com/IMG/pdf/Vryhof_Anchor_Manual2015.pdf

Vryof anchors. (2005, Not specified Not specified). *Ocw.tudelft.nl.* Retrieved from Ocw.tudelft.nl: https://ocw.tudelft.nl/wp-content/uploads/AM2000.pdf

Walter Musial et al. (2020). *Cost of Floating Offshore Wind Energy Using New England Aqua Ventus Concrete Semisubmersible Technology.* University of maine, National laborratory of the U.S.

Wei-Hua Huang et al. (2021, April 12). Water Depth Variation Influence on the Mooring Line Design for FOWT within Shallow Water Region. *Journal of Marine Science and Engineering. 2021, 9, 409.*, pp. 1-20.

Weiwei Zhou et al. (2023, January 11). Experimental Study on Vortex-Induced Vibration of Tension Leg and Riser for Full Depth Mooring Tension Leg Platform. *J. Mar. Sci. Eng. 2023, 11(1), 180; https://doi.org/10.3390/jmse11010180*, pp. 1-12.

Wentzell, K. (2023, April 28). *www.rbritchielist.com*. Retrieved from rbritchielist: https://www.ritchielist.com/consumer-items/marine-equipment-anchor/other-vryhof-anchor-stevpris-stevshark/012465f8-6940-4715-87a7-3f2f4dee4776.html

Xinkuan Yan et al. (2023, March 13). Numerical investigations on nonlinear effects of catenary mooring systems for a 10-MW FOWT in shallow water. *Ocean engineering volume 276, 15 May 2023, 114207*, p. 276.

Xu, K. (2015). *Design and anaysis of mooring system for semi-submersial floating wind turbines in shallow water.* Trondheim: NTNU-Norwigan University of science and technology.

Yang, W.-H. H.-Y. (2021, April (Published) 12). Water Depth Variation Influence on the Mooring Line Design for FOWT within Shallow Water Region. *J. Mar. Sci. Eng. 2021, 9(4), 409; https://doi.org/10.3390/jmse9040409*, p. 409.

Zhi-Ming Yuan et al. (2019, April Not specified). Numerical study on a hybrid mooring system with clump weights and buoys. *researchgate*, pp. 1-11.

23 Appendix

Cost comparison of 5MW, 10MW, 15Mw

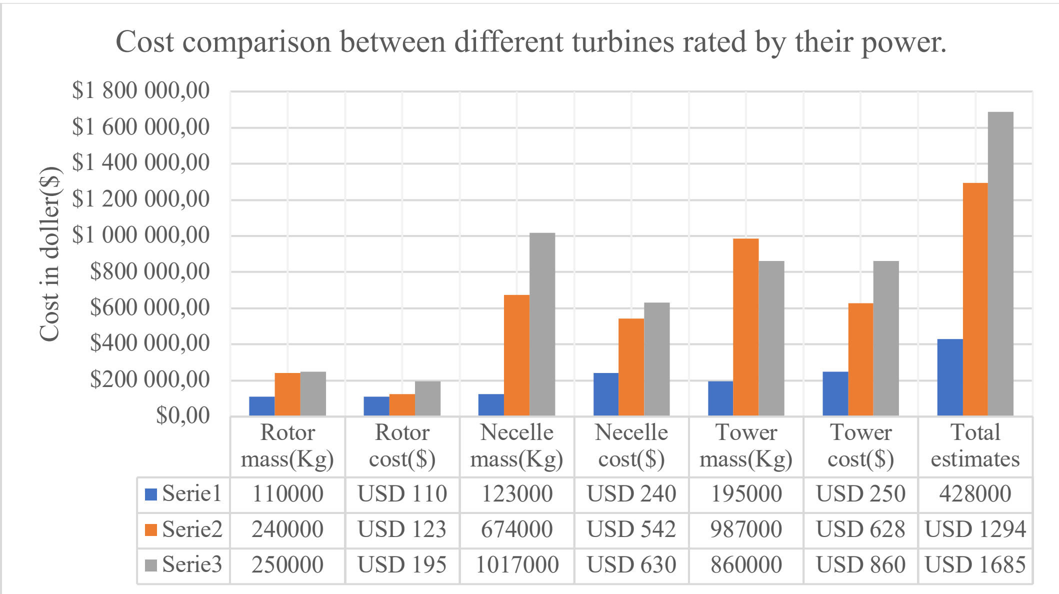

	Rotor	Necelle
5MW	USD 110 000,00	USD
Cost	USD 117 700 000 000,00	USD 000,00
10MW	USD 123 000,00	USD
Cost	USD 131 610 000 000,00	USD 000,00
15MW	USD 195 000,00	USD
Cost	USD 208 650 000 000,00	USD 000,00
Total cost of each turbine	USD 457 960 000 000,00	USD 000,00

Rotor mass(Kg)	110000	
Rotor cost($)	USD 110 000,00	USD
Necelle mass(Kg)	123000	
Necelle cost($)	USD 240 000,00	USD

Tower mass(Kg)	195000	
Tower cost($)	USD 250 000,00	USD
Total estimates	428000	USD

Labor cost

Labour crew cost	Units	Cost ($)
Amninistration cost		
Hourly labour rate Capex	USD $/h	30
Technican daily cost maintenace	USD $/day	221

Turbine properties

Turbine properties RWT-15 MW

	Value	**Units**
Turbine class	IEC Class 1B	
Power rating	15	MW
Specific rating	332	
Rotor orientating	Upwind	
Number of blades	3	
Cut-in wind speed	3	m/s
Related wind speed	10,59	m/s
Cu-out wind speed	25	m/s
Design tip-speed ratio	9	
Min rotor speed	5	rpm
Max rotor speed	7,56	rpm
Max tip speed	95	m/s
Power coefficient (Cp)	0,489	-
Dimension properties		
Airfoil series	FFA-W3	
Rotor diameter	240	m
Hub height	150	m

Hub diameter	7,94	m
Hub overhang	11,35	m
Rotor precone angle	-4,0	deg
Blade prband	4	m
Blade mass	65	m
Drivetrain	Direction drive	
Shaft tilt angle	6	deg
Rotor nacelle assembly mass	1,027	ton

Transition piece height	15	m
Tower base diameter	10	m
Tower mass	860	ton

Single mooring platform

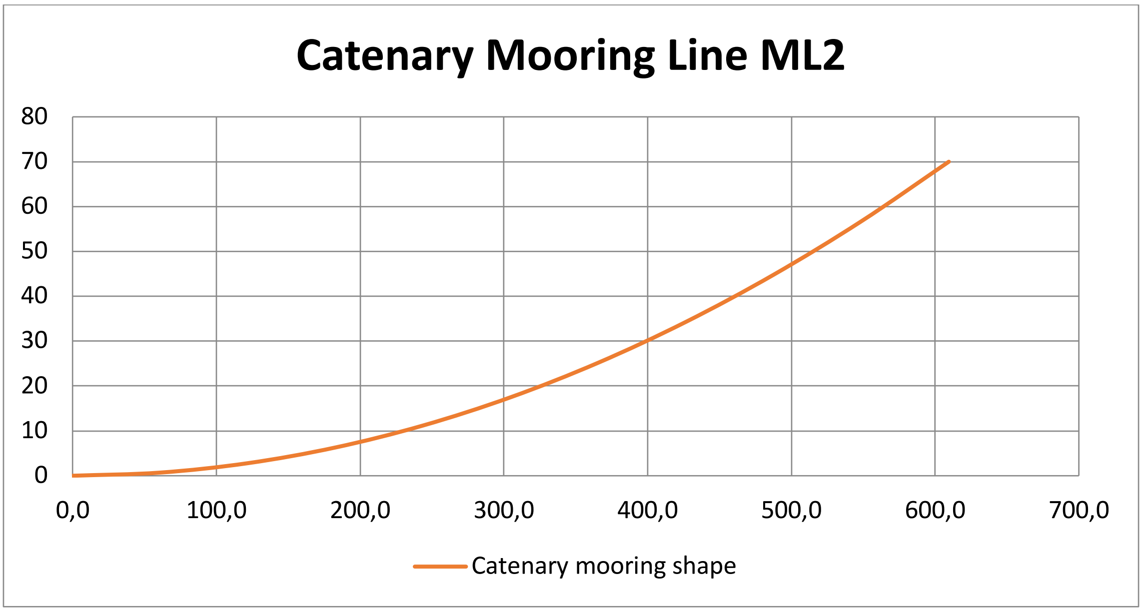

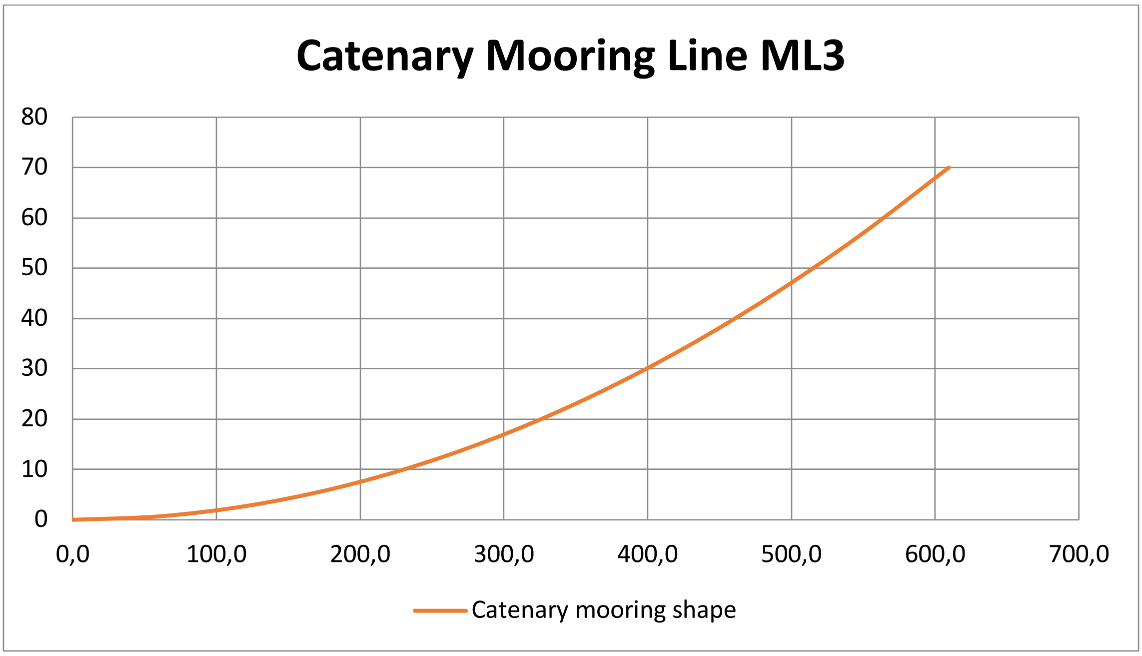

Net annual energy produced - AEP

Net average energy produced AEP

Case 1

15MW= total nameplate capacity *capacity factor (0.40)

Total nameplate capacity=$\frac{15MW}{0.40} = 37.5\ MW$

Number of turbines=$\frac{37.5}{15MW} = 2.5 = 3\ turbines\ needed$

Expected energy production (net annual energy production)

AEP= 37.5 MW* 8760 hours*0.40 (capacity factor) = 131400MWh

Case 2

15MW= total nameplate capacity *capacity factor (0.40)

Total nameplate capacity = $(\frac{100MW}{0.40}) = 250\ MW$

Number of turbines=$\frac{250MW}{15MW} = 16{,}67 = 17\ turbines\ needed\ for\ SNII$

Expected energy production (Net annual energy production)

AEP = 250 MW *8760 hours *0.40 (capacity factor) = 876000MWh

100MW = the total energy capacity* capacity factor 0.489

$$Total\ turbiens\ capacity\ factor = \frac{100MW}{0.40} = 250MW$$

$$The\ numbers\ of\ turbines\ needed = \frac{250MW}{15MW} = 17\ units$$

The net energy produced (AEP) in the wind farm.

250MW*(24hr*365$\frac{hr}{hr}$)*0.4 (capacity factor) = 876000 Mwh

Result economical.

Development and consenting	Cost in USD ($)	%
Development and project mangement	$ 288 074,74	15,59 %
Consenting	$ 1 199 992,88	64,92 %
Enviromental survay	$ 4 799,91	0,26 %
Engineerign and consulting	$ 95 996,60	5,19 %
Hydrographic survay	$ 19 214,50	1,04 %
Geotechnical survay	$ 144 118,14	7,80 %
Resource and metaocean survay	$ 96 087,25	5,20 %
Total cost	$ 1 848 284,02	100 %

Turbine RWT- 15MW	Mass (ton)	Cost price ($) /ton
Rotor Structural (steel 1070$/ton)	385	$ 411 950,00
Startor (Cobber 8797$/ton)	9,01	$ 792 618,71
Startor (Iron 180,95$/ton)	180,95	$ 32 742,90
Generator (Magnets 1186,38$/ton)	24,2	$ 28 710,40

Turbine blade (Polyester yarn) (1125,24$/ton)	65,1	$ 73 253,12
Necelle (Steel 1070 $/ton)	632	$ 676 240,00
Tower (Steel 1070$/ton	860	$ 920 200,00
Bedplat		$ 4 798,80
Mainbaring		$ 4 798,80
Main shaft		$ 4 798,80
Gerbox		$ 16 800,75
Power take of cost		$ 4 794,72
Control system		$ 4 794,72
Yaw system		$ 1 679,95
Yaw baring		$ 1 679,95
Necelle systems		$ 1 679,95
Necelle cover		$ 2 399,38
Structural fastner		$ 1 679,95
Hub casting		$ 3 599,07
Blade barings		$ 4 798,80
Pitc system		$ 2 399,38
Total cost 1 turbine	1975,31	USD 996 418,15

Platform structure USmain	Mass (Ton)	Cost USD ($) / ton
Construction steel (steel 1070 $/ metric ton)	3914	USD 187 980,00
Concrete per kubic meters 444,4 kubic m	2541	USD 718 870,00
Tower interface (steel 1070$/ per metric ton)	100	USD 107 000,00
Total cost	6555	USD 013 850,00

one turbine

Mooring manufactoring cost	Number	Length(m)
	3	
Chain price studdless (185mm)		
Chain mass ton/m		
Mooring lines per turbine	3	
Anchors per line 17ton (drag embeded anchors)	3	
Eletrical Cable	1	
Total cost		

100MW 14 turbines

Mooring manufactoring cost	Number	Length(m)
Number of lines	14	
fiber rope (268mm polyester rope)	1	
Mooring bouy	1	
Chain price studdless (185mm)		
Chain mass ton/m		
Mooring lines per turbine	3	
Anchors per line 17ton (drag embeded anchors)	3	
Eletrical Cable	1	
Total cost		

Transportation and Installation cost	Installation time (Hr)	Day used
Travel distance	11,34	
Mooring 1 installation per AHTS	10 hours inst. (vessel per mooring line)	37hours (traveling time and inst
AHTS x 1 vessels per anchor	10	37 hours (traveling time and ins
OCV cable vessel		1
Cable instaallations		
Helicopter		1
Semi submersial vessel tugging	43	43 hours
Fuel cost Crew cost		
Total cost		117

Transportation and Installation cost	Installation time (Hr)	Day used
Travel distance	11,34	
Mooring 1 installation per AHTS	10 hours inst. (vessel per mooring line)	37hours (traveling time and inst
AHTS x 1 vessels per anchor	10	37 hours (traveling time and ins
OCV cable vessel		1
Cable instaallations		
Helicopter		1
Semi submersial vessel tugging	43	43 hours
Fuel cost Crew cost		
Total cost		117

Opeartion and maintenace	Speed max	South North Sea
Helicopter (Corrective)	296.32Km/hr	168Km
CTV small	46.3Km/hr	168Km
CTV large	46.3Km/hr	168Km
SOV small- service operation vessel	23.70Km/hr	168Km
SOV large- service operation vessel	23.70Km/hr	168Km
Crane barge vessels	23.15Km/hr	168Km
Towing vessel		
Fuel cost		
cost activity		
Materials		
Tehcnichan		
Manegers		
Administrative		
Offshore technichans		
Offshore logestics Turbine		
Total cost		

Bjerkseter

Dismanteling	Installation Cost ($)	% of installation cost
Wind turbine	USD 2 996 418,15	70 %
Platform (steel) Wind turbine	USD 7 013 850,00	70 %
Mooring (steel) Anchors (steel)	USD 4 274 413,38	90 %
Eletrical cables (cobber) only for turbine	USD 766 075,70	10 %
Cleanning cost	USD 262 199,10	

Disposal	USD 279 248,65	
Total cost	USD 14 509 309,48	

LCC	Total Cost$	% of installation
Development and consenting	USD 1 848 284,02	0,17
Maunfactoring cost	USD 14 284 681,53	1,31
Installation cost	USD 1 207 202,59	0,11
Operation & maintenace	USD 1 076 546,66	0,10
Dismenteling	USD 10 930 767,31	1,00

One turbine

Capex	USD 17 340 168,14	59 %
Opex	USD 1 076 546,66	4 %
Decom	USD 10 930 767,31	37 %
Total LCC for one OFWT	USD 29 347 482,11	100 %

17 Turbine		
Capex	USD 151 249 693,48	
Opex	USD 18 301 293,22	
DecmX	USD 185 823 044,33	
Total LCC one OFWT	USD 355 374 031,04	$/Kwh

LOCE	USD 0,22	MUSD/MWh MUSD/MWh

LOCE	USD 193,55	MUSD/MWh

USD 294 USD
782,86 23 582,63
USD 18 USD
301,29 1 464,10
USD 185 USD
823,04 14 865,84
USD 498 USD
907,20 39 912,58

USD
17 340,17
USD
1 076,55
USD
10 930,77

LCC	One	1 Turbine
Development	USD 1 848 284,02	USD 0,01
Wind turbine	USD 2 996 418,15	USD 0,02280
Platform	USD 7 013 850,00	USD 0,05338
Mooring manufactoring	USD 4 274 413,38	USD 0,03253
Installation	USD 1 207 202,59	USD 0,00919
Operation and maintenance	USD 1 076 546,66	USD 0,00819
Cable installtion	USD 766 075,70	USD 0,01
Dismantling	USD 10 930 767,31	USD 0,08319

Mooring material cost for 14 turbines.	Cost ($)
Numbers of chain 185mm	14
Numbers of fiber ropes	7

Mooring buoy		7
Mooring line per turbine (3)	USD	6.223.572,8
fiber rope	USD	9997747,2
Drag embedded anchor per line 17ton	USD	2.904.839
Dynamic Power cables	USD	5.362.529,90
Total cost	USD	14.490.941,7

Mooring materials

CHAIN PROPERTIES

[per unit length]

Weight: 6,67909kN/m

Buoyancy: 0,87543kN/m

Submerged weight: 5,80366kN/m

Mass: 0,68108te/m

Displaced mass: 0,08927te/m

Submerged mass: 0,59181te/m

Diameter to submerged weight ratio: 0,05738m/(kN/m)

Diameter to submerged mass ratio: 0,56268m/(te/m)

USED IN

ML3

ML2

ML6

ML5

Min breaking loads

Grade2: 13,69e3kN

Grade3: 19,59e3kN

ORQ: 21,09e3kN

R4: 27,38e3kN

Minimum breaking loads are for guidance only.

Values are based on formulae given in

manufacturer's catalogues (see help for details).

Studless

Wire

ROPE/WIRE PROPERTIES			
[per unit length]			
Weight: 0,39126kN/m			
Buoyancy: 0,05053kN/m			
Submerged weight: 0,34073kN/m			
Mass: 0,0399te/m			
Displaced mass: 0,00515te/m			
Submerged mass: 0,03474te/m			
Diameter to submerged weight ratio: 0,23479m/(kN/m)			
Diameter to submerged mass ratio: 2,3025m/(te/m)			
USED IN			
ML1		100mm	
ML4			
V0			
Min breaking load: 6333,58kN			
Minimum breaking loads are for guidance only.			
Values are based on a best fit to catalogue data			

#NAVN?			

ROPE/WIRE PROPERTIES			
[per unit length]			
Weight: 0,56193kN/m			
Buoyancy: 0,41937kN/m			
Submerged weight: 0,14256kN/m			
Mass: 0,0573te/m			
Displaced mass: 0,04276te/m			
Submerged mass: 0,01454te/m			
Diameter to submerged weight ratio: 1,61673m/(kN/m)			
Diameter to submerged mass ratio: 15,8547m/(te/m)			
USED IN			
ML1			
ML4			
V0			
Min breaking load: 12,24e3kN			
Minimum breaking loads are for guidance only.			
Values are based on a best fit to catalogue data			
and may underestimate the strength of smaller			

ropes. See help for further details.			

Simulation occaflex

Steel wire 100mm

Linked statistics: ML1

OrcaFlex 11.3d: 2.sim (modified 20:15 on 13.04.2023 by OrcaFlex 11.3d)
Period: Whole simulation

	Time (s)	Effective tension (kN) at end B
Mean		1087,64571
Std. Dev.		32,3949211
RMS		1088,12804
Mean up-crossing period Tz (s)		14,3352713
Mean crest period Tc (s)		7,19814126
m0		1049,43092
m2		5,10671969
m4		0,09856013
Bandwidth (ε)		0,86479331
max	351,3	1182,73057
min	3599,2	992,849047

Linked statistics: ML4

OrcaFlex 11.3d: 2.sim (modified 20:15 on 13.04.2023 by OrcaFlex 11.3d)
Period: Whole simulation

	Time (s)	Effective tension (kN) at end A
Mean		1073,89324
Std. Dev.		32,4692139
RMS		1074,38399
Mean up-crossing period Tz (s)		12,8986301
Mean crest period Tc (s)		5,91083969
m0		1054,24985
m2		6,3366011
m4		0,18136689
Bandwidth (ε)		0,88882165
max	232,7	1184,753
min	2775,4	972,492947

Linked statistics: V0

OrcaFlex 11.3d: 2.sim (modified 20:15 on 13.04.2023 by OrcaFlex 11.3d)
Period: Whole simulation

	Time (s)	Effective tension (kN) at end B
Mean		3631,5673
Std. Dev.		153,673362
RMS		3634,81727
Mean up-crossing period Tz (s)		8,04551148
Mean crest period Tc (s)		7,60569745
m0		2,36E+04
m2		364,829432
m4		6,30683946
Bandwidth (ε)		0,32610303
max	892,9	4220,81529
min	889,3	3098,23184

Linked statistics: ML3

OrcaFlex 11.3d: 2.sim (modified 20:15 on 13.04.2023 by OrcaFlex 11.3d)
Period: Whole simulation

	Time (s)	Effective tension (kN) at end B
Mean		1198,14862
Std. Dev.		73,3807542
RMS		1200,39363
Mean up-crossing period Tz (s)		9,86646707
Mean crest period Tc (s)		0,58680703
m0		5384,73509
m2		55,314756
m4		160,638777
Bandwidth (ε)		0,9982298
max	2799,8	1363,01762
min	-74,2	786,654849

Linked statistics: ML2

OrcaFlex 11.3d: 2.sim (modified 20:15 on 13.04.2023 by OrcaFlex 11.3d)
Period: Whole simulation

	Time (s)	Effective tension (kN) at end A
Mean		1800,13248
Std. Dev.		137,739058
RMS		1805,39442
Mean up-crossing period Tz (s)		10,047027
Mean crest period Tc (s)		0,9818712
m0		1,90E+04
m2		187,948591
m4		194,95305
Bandwidth (ε)		0,99521321
max	2781,5	2291,01519
min	2836,4	1419,08526

Linked statistics: ML6

OrcaFlex 11.3d: 2.sim (modified 20:15 on 13.04.2023 by OrcaFlex 11.3d)

Period: Whole simulation

	Time (s)	Effective tension (kN) at end A
Mean		1771,92836
Std. Dev.		159,086197
RMS		1779,05551
Mean up-crossing period Tz (s)		11,1399381
Mean crest period Tc (s)		0,90785647
m0		2,53E+04
m2		203,938605
m4		247,437236
Bandwidth (ε)		0,9966737
max	481,5	2253,13554
min	2782,1	1304,7209

268mm

Zm 8m

Summary results for ML1 at time 3800,0s

OrcaFlex 11.3d: K03 15MW semi-sub conditions 1440m(six times the rotor) 3 polyester 268mm.dat (modified 12:59 on 12.04.2023 by OrcaFlex 11.3d)

End A	
Total force (kN	397,1514744
End tension (k	397,1508969
End shear forc	0,677322598
Total momen	0
End bend mo	0
End torque (k	0
End curvatur	0
End Ez-angle (	49,52531777
End force azim	270,6032332
End force dec	97,9817548
End force Ez-a	49,42853447
End force Exy	167,0090062

d A components

Summary results for ML1 at time 3800,0s

Load	magnitude	Ex	Ey	Ez	GX	GY	GZ
					Global axes		
Force (kN)	397,1514744	-293,9531663	67,81576877	258,305732	4,140787665	-393,28221	-55,14756175
Moment (kN.	0	0	0	0	0	0	0

End B	
Total force (kN	395,3957472
End tension (k	395,3951399
End shear forc	0,693010632
Total momen	0
End bend mo	0
End torque (k	0
End curvatur	0
End Ez-angle (	89,89121803
End force azim	270,8368439
End force dec	84,59020605
End force Ez-a	89,89379872
End force Exy	264,5059045

End B components

Load	magnitude	Ex	Ey	Ez	GX	GY	GZ
		End axes			Global axes		
Force (kN)	395,3957472	-37,85637858	-393,5786508	0,732890106	5,749096809	-393,59262	37,27731402
Moment (kN.	0	0	0	0	0	0	0

Node positions and orientations; * indicates seabed contact

Node	Arc length (m)	X (m)	Y (m)	Z (m)	Azimuth (deg)	eclination (de	Gamma (deg)
A	0	-8,768880207	-53,26663337	-13,9286871	270,6018828	97,8840487	5,843837431
2	10	-8,664298978	-63,2217988	-15,30733172	270,6016729	97,7860156	5,84380882
3	20	-8,559742003	-73,18160041	-16,65189667	270,6021597	97,5894376	5,843873171
4	30	-8,45489511	-83,14594222	-17,96218841	270,6042601	97,3916269	5,844146391
5	40	-8,3495128	-93,11473642	-19,23794081	270,6076478	97,1922165	5,844575885
6	50	-8,243393639	-103,0878998	-20,47883283	270,6121259	96,991037	5,845128299
7	60	-8,136360117	-113,0653466	-21,68453946	270,617555	96,7882267	5,845779194
8	70	-8,02825897	-123,0469819	-22,85478786	270,6237867	96,584219	5,846504454
9	80	-7,918964351	-133,0326968	-23,98940428	270,6306634	96,379638	5,847280507
10	90	-7,808377978	-143,0223682	-25,08833381	270,6380604	96,1751111	5,848089094
11	100	-7,696417542	-153,0158618	-26,15162222	270,6459103	95,9711185	5,848919395
12	110	-7,583008389	-163,0130369	-27,17938303	270,6541256	95,7679877	5,849759366
13	120	-7,468098837	-173,0137498	-28,17177742	270,6624324	95,5659786	5,850579667
14	130	-7,351709829	-183,0178553	-29,12901089	270,6703687	95,3652225	5,85133583
15	140	-7,233951232	-193,0252113	-30,05129173	270,6775683	95,1655358	5,851996887
16	150	-7,114971983	-203,0356842	-30,93876252	270,6839875	94,9664245	5,852564018
17	160	-6,994897422	-213,0491508	-31,79146016	270,6897076	94,7672704	5,853049613
18	170	-6,873848098	-223,0654975	-32,60931207	270,6945189	94,5675986	5,853441622
19	180	-6,752022795	-233,0846153	-33,39218987	270,6978678	94,3672484	5,85370326
20	190	-6,629736064	-243,1063952	-34,13996551	270,6992355	94,1662549	5,853805965
21	200	-6,507368673	-253,1307273	-34,8525235	270,6985617	93,964659	5,853759034
22	210	-6,385256848	-263,1574994	-35,52975082	270,6963713	93,762483	5,853611932
23	220	-6,263598207	-273,1865964	-36,17154046	270,6936194	93,5597205	5,853436207
24	230	-6,142394945	-283,2179002	-36,77777789	270,6913707	93,3563995	5,853300122
25	240	-6,021471944	-293,2512884	-37,34836663	270,6904033	93,1526053	5,853244515
26	250	-5,900558761	-303,2866356	-37,88322281	270,6910694	92,9483666	5,853279197
27	260	-5,779356696	-313,3238157	-38,38226079	270,6934652	92,7436955	5,85339738
28	270	-5,657561225	-323,3627011	-38,84540173	270,6975934	92,5385708	5,853586844
29	280	-5,534872479	-333,4031641	-39,27255339	270,703346	92,3329047	5,85383064
30	290	-5,411023565	-343,4450769	-39,663607	270,7105664	92,1265113	5,854110939
31	300	-5,285769256	-353,4883126	-40,01840597	270,7192	91,9191534	5,854415062
32	310	-5,158861742	-363,5327437	-40,33675913	270,7290826	91,7108628	5,854727597
33	320	-5,030113315	-373,5782397	-40,61852195	270,7397121	91,5019988	5,855025402
34	330	-4,899452294	-383,6246683	-40,86363002	270,7504845	91,2930165	5,855288182
35	340	-4,766903014	-393,671896	-41,07209935	270,7612135	91,0842216	5,855510717
36	350	-4,632459201	-403,7197885	-41,24397372	270,7724492	90,8755417	5,85570242
37	360	-4,495952483	-413,7682108	-41,37924468	270,7851301	90,6665784	5,855872208
38	370	-4,357047389	-423,817026	-41,47781725	270,7997537	90,4570221	5,856014717
39	380	-4,215401256	-433,866096	-41,53957531	270,8156486	90,2470959	5,856112121
40	390	-4,070914216	-443,9152846	-41,56450306	270,8311251	90,0375564	5,856151184
41	400	-3,923836553	-453,9644605	-41,55275082	270,8445004	89,8292297	5,856136856
42	410	-3,774658918	-464,0134983	-41,50459356	270,854906	89,622515	5,856088456
43	420	-3,623936302	-474,0622773	-41,4203226	270,8622313	89,417371	5,856028403
44	430	-3,472198123	-484,1106791	-41,30019926	270,8667146	89,213619	5,85597602
45	440	-3,319915775	-494,1585871	-41,14445313	270,8688088	89,0111676	5,8559445
46	450	-3,167459609	-504,2058855	-40,95331422	270,8691757	88,8100348	5,855938117
47	460	-3,015068783	-514,2524592	-40,72701927	270,868619	88,6100226	5,855950867
48	470	-2,86283166	-524,2981913	-40,46572959	270,8679011	88,4105704	5,855969455
49	480	-2,710719953	-534,3429611	-40,16948609	270,8674579	88,2110115	5,855982357
50	490	-2,558669324	-544,3866442	-39,83821713	270,8673688	88,0108464	5,855985147
51	500	-2,406623675	-554,4291132	-39,47178927	270,8674976	87,8098864	5,855980406
52	510	-2,254566598	-564,4702397	-39,07006569	270,8676018	87,6082329	5,855976308
53	520	-2,102527001	-574,5098963	-38,63294939	270,8675038	87,4061077	5,85598068
54	530	-1,950550705	-584,5479566	-38,16038231	270,867224	87,2037759	5,85599389
55	540	-1,798659423	-594,5842958	-37,65236123	270,8668864	87,0015524	5,856010953
56	550	-1,646855348	-604,6187919	-37,10893934	270,8665487	86,7996691	5,856029211
57	560	-1,495139956	-614,6513248	-36,53019551	270,8661504	86,5980928	5,856052205
58	570	-1,343536631	-624,6817734	-35,91617211	270,8655022	86,3966282	5,856091967
59	580	-1,192113069	-634,7100154	-35,26688042	270,8643302	86,1952533	5,856167975
60	590	-1,040988518	-644,735931	-34,58235592	270,8624365	85,9941179	5,856297293
61	600	-0,890299739	-654,7594032	-33,86266314	270,8598482	85,7932664	5,856482907
62	610	-0,740156236	-664,7803141	-33,10785398	270,8567417	85,592597	5,85671639
63	620	-0,590632859	-674,7985439	-32,31795802	270,8532977	85,3920632	5,856987174
64	630	-0,441775797	-684,8139733	-31,49301179	270,8496206	85,1916809	5,857289086
65	640	-0,293623256	-694,8264828	-30,63305122	270,8457108	84,9913531	5,857623738
66	650	-0,146221186	-704,8359508	-29,73807972	270,8414859	84,7908892	5,858000118
B	660	3,63E-04	-714,8422525	-28,80806746	270,8392793	84,6905992	5,858202382

Segment positions and orientations; * indicates seabed contact

Segment	Arc length (m)	X (m)	Y (m)	Z (m)	Azimuth (deg)	eclination (de	Gamma (deg)
1	5	-8,716589592	-58,24421609	-14,61800941	270,6018828	97,8840487	5,843837431
2	15	-8,612020491	-68,2016996	-15,9796142	270,6014631	97,6879825	5,843780578
3	25	-8,507318557	-78,16377131	-17,30704254	270,602856	97,4908927	5,843964535
4	35	-8,402203955	-88,13033932	-18,60006461	270,6056637	97,2923611	5,844325754
5	45	-8,29645322	-98,10131811	-19,85838682	270,6096311	97,0920719	5,844822468
6	55	-8,189876878	-108,0766232	-21,08168615	270,6146195	96,8900022	5,845429633
7	65	-8,082309543	-118,0561642	-22,26966366	270,6204892	96,6864512	5,846123432
8	75	-7,97361166	-128,0398394	-23,42209607	270,6270828	96,4819868	5,846879476
9	85	-7,863671165	-138,0275325	-24,53886905	270,6342424	96,2772891	5,847675024
10	95	-7,75239776	-148,019115	-25,61997802	270,6418768	96,072933	5,848496239
11	105	-7,639712965	-158,0144493	-26,66550262	270,6499423	95,8693039	5,849335267
12	115	-7,525553613	-168,0133933	-27,67558022	270,6583073	95,6666714	5,850175956
13	125	-7,409904333	-178,0158026	-28,65039415	270,6665562	95,4652858	5,850976027
14	135	-7,29283053	-188,0215333	-29,59015131	270,67418	95,2651593	5,851688888
15	145	-7,174461607	-198,0304477	-30,49502712	270,6809556	95,0659122	5,852298923
16	155	-7,054934702	-208,0424175	-31,36511134	270,6870184	94,8669368	5,85282379
17	165	-6,93437276	-218,0573242	-32,20038612	270,6923959	94,6676041	5,85327071
18	175	-6,812935447	-228,0750564	-33,00075097	270,6966413	94,4675931	5,853608794
19	185	-6,69087943	-238,0955053	-33,76607769	270,699094	94,2669038	5,853795559
20	195	-6,568552369	-248,1185612	-34,49624451	270,699377	94,065606	5,853816119
21	205	-6,44631276	-258,1441133	-35,19113716	270,6977466	93,8637121	5,853703395
22	215	-6,324427527	-268,1720479	-35,85064564	270,6949962	93,661254	5,853522914
23	225	-6,202996576	-278,2022483	-36,47465917	270,6922428	93,4581871	5,853351953
24	235	-6,081933444	-288,2345943	-37,06307226	270,6904988	93,254612	5,853249848
25	245	-5,961015352	-298,268962	-37,61579472	270,6903079	93,0505986	5,853239353
26	255	-5,839957728	-308,3052257	-38,1327418	270,6918307	92,8461346	5,853317678
27	265	-5,71845896	-318,3432584	-38,61383126	270,6950995	92,6412564	5,853474149
28	275	-5,596216852	-328,3829326	-39,05897756	270,700087	92,4358851	5,853695056
29	285	-5,472948022	-338,4241205	-39,46808019	270,7066045	92,2299242	5,853960353
30	295	-5,348396411	-348,4666948	-39,84100648	270,7145278	92,0230984	5,854254359
31	305	-5,222315499	-358,5105282	-40,17758255	270,7238716	91,8152083	5,854567275
32	315	-5,094487528	-368,5554917	-40,47764054	270,734293	91,6065174	5,854878416
33	325	-4,964782804	-378,601454	-40,74107599	270,7451308	91,3974803	5,855162493
34	335	-4,833177654	-388,6482821	-40,96786468	270,7558377	91,1885527	5,855404102
35	345	-4,699681107	-398,6958422	-41,15803653	270,766589	90,9798905	5,855607538
36	355	-4,564205842	-408,7439997	-41,3116092	270,778309	90,7711929	5,855786626
37	365	-4,426499936	-418,7926184	-41,42853097	270,791951	90,561964	5,855945333
38	375	-4,286224323	-428,841561	-41,50869628	270,8075561	90,3520803	5,856069808
39	385	-4,143157736	-438,8906903	-41,55203918	270,8237409	90,1421114	5,856139606
40	395	-3,997375384	-448,9398726	-41,55862694	270,8385093	89,9330014	5,856149287
22	405	-3,849247735	-268,1720479	-41,52867219	270,8504915	93,661254	5,856113574
42	415	-3,69929761	-469,0378878	-41,46245808	270,8593206	89,5195721	5,856055405
43	425	-3,548067212	-479,0864782	-41,36026093	270,8651422	89,3151699	5,855996207
44	435	-3,396056949	-489,1346331	-41,2223262	270,868287	89,1120682	5,855953046
45	445	-3,243687692	-499,1822363	-41,04888368	270,8693307	88,9102671	5,855935035
46	455	-3,091264196	-509,2291723	-40,84016675	270,8690208	88,7098026	5,85594147
47	465	-2,938950221	-519,2753252	-40,59637443	270,8682172	88,5102426	5,855960964
48	475	-2,786775807	-529,3205762	-40,31760784	270,8675851	88,3108981	5,855978496
49	485	-2,634694639	-539,3648026	-40,00385161	270,8673306	88,1111249	5,85598644
50	495	-2,482646499	-549,4078787	-39,6550032	270,8674071	87,9105679	5,855983787
51	505	-2,330595137	-559,4496764	-39,27092748	270,8675882	87,709205	5,855976865
52	515	-2,1785468	-569,490068	-38,85150754	270,8676155	87,5072608	5,855975727
53	525	-2,026538853	-579,5289264	-38,39666585	270,8673922	87,3049547	5,855985831
54	535	-1,874605064	-589,5661262	-37,90637177	270,8670557	87,1025972	5,856002247
55	545	-1,722757385	-599,6015438	-37,38065029	270,8667171	86,9005076	5,856019959
56	555	-1,570997652	-609,6350584	-36,81956743	270,8663803	86,6988305	5,85603876
57	565	-1,419338293	-619,6665491	-36,22318381	270,8659203	86,4973551	5,856066056
58	575	-1,26782485	-629,6958944	-35,59152627	270,865084	86,2959014	5,856118619
59	585	-1,116550793	-639,7229732	-34,92461817	270,8635763	86,0946053	5,856218664
60	595	-0,965644128	-649,7476671	-34,22250953	270,8612964	85,8936305	5,856377935
61	605	-0,815227987	-659,7698587	-33,48525856	270,8583995	85,6929024	5,856590436
62	615	-0,665394548	-669,789429	-32,712906	270,8550834	85,4922915	5,856845273
63	625	-0,516204328	-679,8062586	-31,90548491	270,8515115	85,2918348	5,85713223
64	635	-0,367699527	-689,8202281	-31,06303151	270,8477291	85,091527	5,857449282
65	645	-0,219922221	-699,8312168	-30,18556547	270,8436918	84,8911793	5,857801764
66	655	-0,072928855	-709,8391017	-29,27307359	270,8392793	84,6905992	5,858202382

Mid-segment loads; * indicates seabed contact

Segment	Arc length (m)	Effective tension (kN)	Shear force (kN)	Bend radius (m)	Curvature (rad/m)	Bend moment (kN.m)	Wall tension (kN)	Max von Mises stress (kPa)
1	5	397,0559[illegible]	0	5844,519892	1,71E-04	0	390,9255197	[illegible]
2	15	396,868[illegible]	0	2914,649928	3,43E-04	0	390,1668047	[illegible]
3	25	396,6851983	0	2896,335023	3,45E-04	0	389,4270845	9508,00987
4	35	396,506914	0	2872,85143	3,48E-04	0	388,706541	9503,73663
5	45	396,3334765	0	2847,299048	3,51E-04	0	388,0053967	9499,57957
6	55	396,1649917	0	2824,09403	3,54E-04	0	387,3238926	9495,54122
7	65	396,0015582	0	2807,219312	3,56E-04	0	386,662253	9491,62394
8	75	395,8432521	0	2799,079616	3,57E-04	0	386,0206473	9487,82955
9	85	395,690116	0	2799,57264	3,57E-04	0	385,3991663	9484,15909
10	95	395,5421586	0	2806,664349	3,56E-04	0	384,7978205	9480,61275
11	105	395,3993628	0	2818,354647	3,55E-04	0	384,2165595	9477,19012
12	115	395,2616956	0	2833,92569	3,53E-04	0	383,6552926	9473,89043
13	125	395,1291117	0	2851,792632	3,51E-04	0	383,1138976	9470,71257
14	135	395,0015583	0	2867,435067	3,49E-04	0	382,592235	9467,65529

Polyester rope 268mm

Linked statistics: ML1

OrcaFlex 11.3d: K03 15MW semi-sub conditions 1440m(six times the rotor) 3 polyester 268mm.dat (modified 12:59 on 12.04.2023 by OrcaFlex 11.3d)
Period: Whole simulation

	Time (s)	Effective tension (kN) at end B
Mean		398,1486037
Std. Dev.		9,166247098
RMS		398,2541032
Mean up-crossing period Tz (s)		10,79545455
Mean crest period Tc (s)		5,788041854
m0		84,02008586
m2		0,72094354
m4		0,021519785
Bandwidth (ε)		0,844119261
max	504,7	427,6980644
min	2440,5	371,3228634

Linked statistics: ML4

OrcaFlex 11.3d: K03 15MW semi-sub conditions 1440m(six times the rotor) 3 polyester 268mm.dat (modified 12:59 o

Period: Whole simulation

Mean
Std. Dev.
RMS
Mean up-crossing period Tz (s)
Mean crest period Tc (s)
m0
m2
m4
Bandwidth (ε)
max
min

Linked statistics: V0

OrcaFlex 11.3d: K03 15MW semi-sub conditions 1440m(six times the rotor) 3 polyester 268mm.dat (modified 12:59 on 12.04.2023 by OrcaFlex 11.3d)
Period: Whole simulation

	Time (s)	Effective tension (kN) at end B
Mean		3734,20926
Std. Dev.		100,680319
RMS		3735,56627
Mean up-crossing period Tz (s)		6,20016051
Mean crest period Tc (s)		5,86424242
m0		1,01E+04
m2		263,683709
m4		7,66760034
Bandwidth (ε)		0,32468833
max	3615,5	4053,07541
min	3618,5	3386,36485

Linked statistics: ML3

OrcaFlex 11.3d: K03 15MW semi-sub conditions 1440m(six times the rotor) 3 polyester 268mm.dat (modified 12:59 on 12.04.2023 by OrcaFlex 11.3d)

Period: Whole simulation

	Time (s)	Effective tension (kN) at end A
Mean		1906,85977
Std. Dev.		100,321993
RMS		1909,49697
Mean up-crossing period Tz (s)		9,90391645
Mean crest period Tc (s)		1,11919075
m0		1,01E+04
m2		102,607326
m4		81,9162656
Bandwidth (ε)		0,99359443
max	276,1	2197,17009
min	2358,9	1652,89417

Linked statistics: ML2

OrcaFlex 11.3d: K03 15MW semi-sub conditions 1440m(six times the rotor) 3 polyester 268mm.dat (modified 12:59 on 12.04.2023 by OrcaFlex 11.3d)

Period: Whole simulation

	Time (s)	Effective tension (kN) at end A
Mean		1906,07066
Std. Dev.		101,976328
RMS		1908,79662
Mean up-crossing period Tz (s)		8,42700893

Mean crest period Tc (s)		1,18533823
m0		1,04E+04
m2		146,437339
m4		104,223882
Bandwidth (ε)		0,99005804
max	1535,6	2231,89305
min	2377,4	1651,61963

Linked statistics: ML6

OrcaFlex 11.3d: K03 15MW semi-sub conditions 1440m(six times the rotor) 3 polyester 268mm.dat (modified 12:59 on 12.04.2023 by OrcaFlex 11.3d)
Period: Whole simulation

	Time (s)	Effective tension (kN) at end A
Mean		1828,66148
Std. Dev.		135,130333
RMS		1833,64747
Mean up-crossing period Tz (s)		9,42635659
Mean crest period Tc (s)		1,14114353
m0		1,83E+04
m2		205,502905
m4		157,811054
Bandwidth (ε)		0,99264534
max	594,8	2227,39333
min	2640,7	1497,05161

Linked statistics: ML5

OrcaFlex 11.3d: K03 15MW semi-sub conditions 1440m(six times the rotor) 3 polyester 268mm.dat (modified 12:59 on 12.04.2023 by OrcaFlex 11.3d)
Period: Whole simulation

	Time (s)	Effective tension (kN) at end A
Mean		1446,83531
Std. Dev.		80,5061827
RMS		1449,07338
Mean up-crossing period Tz (s)		7,63726708
Mean crest period Tc (s)		0,93782082
m0		6481,24545
m2		111,117513
m4		126,340552
Bandwidth (ε)		0,99243201

max	577,6	1692,31565
min	735,9	1253,08001